

# Control of Gene Expression by Cell Size

by

**Chia-Yung Wu**

B.A. Biochemistry  
Rutgers University,  
New Brunswick, NJ  
2001

Submitted to the Department of Biology in partial fulfillment  
of the requirements for the thesis degree of

Doctor of Philosophy in Biology

at the  
Massachusetts Institute of Technology  
May, 2010

© 2010 Chia-Yung Wu. All rights reserved.

The author hereby grants to MIT permission to reproduce and to distribute publicly paper and  
electronic copies of this thesis document in whole or in part in any medium now known or  
hereafter created.

Signature of Author: \_\_\_\_\_

Department of Biology  
Date

Certified by: \_\_\_\_\_

Gerald R. Fink, Ph.D.  
Professor, Department of Biology  
Thesis Supervisor

Accepted by: \_\_\_\_\_

Stephen P. Bell, Ph.D.  
Professor, Department of Biology  
Chairman, Committee for Graduate Students

## **Table of Contents**

Abstract .....	3
Acknowledgements .....	4
Chapter 1. Introduction .....	5
Polyploidization/whole genome duplication as a mechanism of evolution ...	5
Polyploidy in diploid multi-cellular organisms during development, stress response and tumorigenesis .....	8
Ploidy and gene expression – examples from multi-cellular eukaryotes .....	12
Budding yeast as a model system to study consequences of polyploidy .....	15
Control of cell size in yeast and metazoans .....	19
Summary .....	24
References .....	25
Chapter 2. Control of gene expression by cell size	
Summary .....	29
Introduction .....	29
Results .....	32
Discussion .....	38
Materials and Methods .....	42
References .....	49
Figures .....	52
Tables .....	59
Chapter 3. Reduced binding of transcriptional activators of <i>FLO11</i> in polyploids	
Summary .....	65
Introduction .....	66
Results .....	79
Discussion .....	88
Materials and Methods .....	91
References .....	96
Figures and Table .....	101
Chapter 4. Discussion and future directions .....	109
Appendix: Growth of isogenic yeast strains of different ploidies and mating types	121

## **Abstract**

Polyploidy, increased copy number of whole chromosome sets in the genome, is a common cellular state in evolution, development and disease. Ploidy enlarges cell size and alters gene expression, producing novel phenotypes and functions. Although many polyploid cell types have been discovered, it is not clear how ploidy changes physiology. Specifically, whether the enlarged cell size of polyploids causes differential gene regulation has not been investigated. In this thesis, I present the evidence for a size-sensing mechanism that alters gene expression in yeast. My results indicate a causal relationship between cell size and gene expression. Ploidy-associated changes in the transcriptome therefore reflect transcriptional adjustment to a larger cell size. The causal and regulatory connection between cell size and transcription suggests that the physical features of a cell (such as size and shape) are a systematic factor in gene regulation. In addition, cell size homeostasis may have a critical function – maintenance of transcriptional homeostasis.

## **Acknowledgements**

I sincerely thank my thesis advisor, Dr. Gerald R. Fink, for his professional guidance and for providing an excellent research environment. I am highly appreciative of the intellectual freedom entrusted to me during my pursuit of fundamental questions in biology. In the Fink lab, one not only learns to conduct rigorous scientific research but also to become a versatile, professional creator of knowledge.

I have benefited much from the wisdom and kindness of many former and current Fink lab members in my personal and professional development. In the Fink lab, our work atmosphere is always friendly and collaborative. Our conversations are fun and intellectually stimulating. It has been a great pleasure working daily with a group of talented and well-rounded individuals.

The Biology department and Whitehead Institute are both instrumental to my successful education at MIT. Many thanks to the faculty members and the Biology headquarter for nurturing us graduate students into competent and dependable professionals. I am deeply indebted to the wholesome community at Whitehead, from whom I learned what a community is about, and without whom my experience at MIT would not have been fulfilling.

Special thanks to the following groups at MIT for their helpful discussions and generous support: Amon lab, Bell lab, Gifford lab, Hochwagen lab, Lindquist lab, Regev group, and Young lab.

Many thanks as well to members of my thesis committee: Dr. Frank Solomon and Dr. Stephen Bell for much helpful advice since the beginning of this thesis project, Dr. Angelika Amon for many insightful discussions and Dr. David Pellman for constructive feedback on this thesis.

Much appreciation to National Institute of Health, Massachusetts Institute of Technology and Whitehead Institute for Biomedical Research for funding and infrastructural support.

Last but not least, I sincerely thank my family and friends for enriching my life by making me a part of their lives with their love and friendship.

## Chapter 1. Introduction

### **Polyploidization/whole genome duplication as a mechanism of evolution**

Recent advances in genome sequencing and comparative genomics indicate that many living diploid organisms are paleopolyploids – ancient polyploids that underwent diploidization through sequence divergence between the duplicated chromosomes (Wolfe, 2001). Polyploidy is particularly common in the plant kingdom. Many diploid plants have been referred to as paleopolyploids (Blanc and Wolfe, 2004). Species that are polyploid appear to be more prevalent in colder regions, usually establishing niches different from those of their diploid progenitors (Hegarty and Hiscock, 2008; Hijmans et al., 2007). The relationship between genome duplication and evolution was pioneered by Susumu Ohno, who proposed the idea that whole genome duplication/polyploidization creates substrates for evolution (Ohno, 1970).

Ohno specifically hypothesized that two rounds (2R) of whole genome duplication shaped the evolutionary history of vertebrates. This hypothesis was largely based on his discovery of seemingly quadruplicated chromosomal segments in the human genome. A later study showed that the four large homeobox gene clusters in vertebrates arose from duplications of one ancestral cluster related to the cluster in *Drosophila* (Schughart et al., 1989). The high degree of conservation of structural organization between the vertebrate and insect clusters suggests that the duplications involved large chromosomal regions, or possibly entire chromosomes. Since duplications of individual chromosomes tend to be deleterious, whole genome duplication was proposed as a plausible mechanism.

Recently, four copies of large (>100 gene) chromosomal segments have been identified in at least 25% of the human genome, and these segments have corresponding, single-copy

paralogous regions in the primitive cordate sea squirt *Ciona* (Dehal and Boore, 2005). The conserved structural organization and the large number of such paralogous genomic segments favor whole genome duplication. Generation of these regions through a series of independent small gene amplification would be extremely unlikely at the same time. Furthermore, four-fold duplication is the dominant mode of redundancy for the paralogs in the human genome. The simplest and most likely mechanism of the large scale four-fold duplication is two rounds of whole genome duplication, a strong argument for the 2R hypothesis.

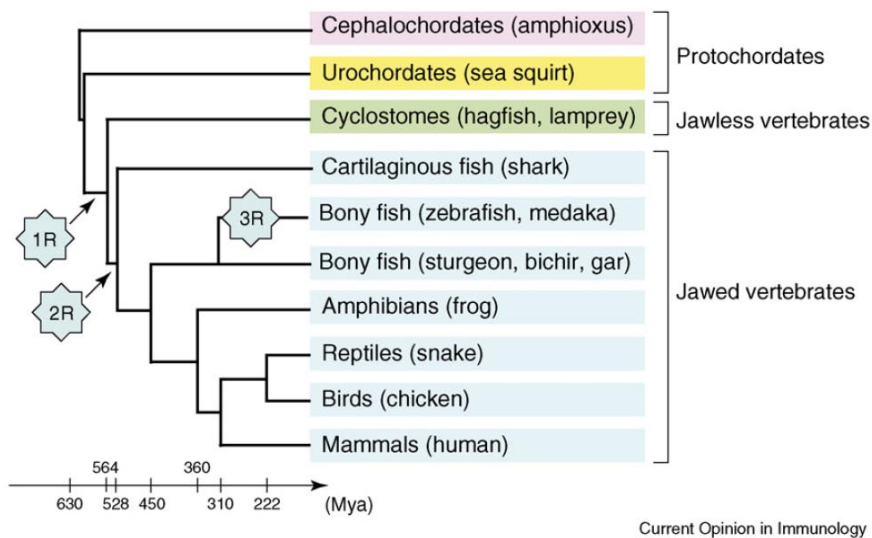


Figure 1. Probable whole genome duplication events in the evolutionary history of vertebrates based on comparative genomics (Kasahara, 2007).

More striking evidence for Ohno's hypothesis comes from the fungal kingdom. Species of the *Saccharomyces* genus appear to have evolved from a tetraploid ancestor that arose from whole genome duplication. A systematic search for sequence homology within the *Saccharomyces cerevisiae* genome led to the discovery of 55 pairs of large (longer than 50Kb on average) duplicated regions scattered throughout the genome. Within each pair of duplicated regions are homologous genes in conserved gene order and orientation with respect to the

centromeres (Wolfe and Shields, 1997). A tetraploid origin for *Saccharomyces* is thus inferred. Whole genome duplication likely gave rise to the tetraploid ancestor around 100 million years ago, after *Saccharomyces* diverged from *Kluyveromyces*. Most of the functionally redundant gene pairs in the ancient tetraploid lost one member as the organism further evolved.

The emergence of fermentative yeast species is cited as one of the best documented example for the evolutionary consequences of whole genome duplication. In *S. cerevisiae*, many of the gene pairs retained after genome duplication participate in carbohydrate metabolism and show differential expression patterns in response to glucose or oxygen availability (Wolfe and Shields, 1997). The duplicated genes escaped deletion by gaining novel functions to cope with conditions related to fermentation. Independently, comparative genomics shows systematic transcriptional network rewiring in descendents of the tetraploid ancestor. The descendent species appear to have lost a *cis*-regulatory element upstream of dozens of ORFs encoding mitochondrial ribosomal proteins, whereas the same *cis* element is retained in promoters of genes required for cytoplasmic ribosomal biogenesis (Ihmels et al., 2005). As a result, synthesis and assembly of cytoplasmic ribosomes are decoupled from mitochondrial ribosomes, enabling these organisms to thrive in low-oxygen conditions and to ferment. In contrast, species that did not evolve from the tetraploid ancestor, such as *Candida albicans*, have the *cis*-regulatory element in genes for both mitochondrial and cytoplasmic ribosome biogenesis. As expected, these species display a strong correlation between mitochondrial and cytoplasmic ribosomal biogenesis and do not grow anaerobically.

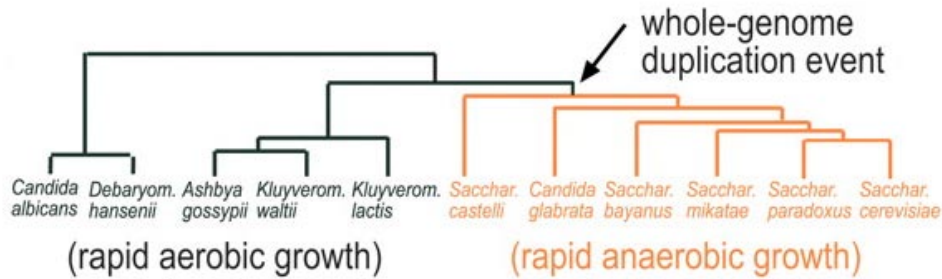


Figure 2. Phylogenetic tree of fermentative (rapid anaerobic growth) and non-fermentative (rapid aerobic growth) yeast species (Ihmels et al., 2005).

The apparent link between whole genome duplication and fermentative yeast speciation exemplifies the evolutionary potential of polyploidy. Gene duplication on the whole genome scale provides unparalleled evolutionary space, making rapid and coordinated extensive changes in fundamental cellular processes (such as metabolism) possible. It is worth noting that the whole genome duplication event occurred as fruiting angiosperms populated the earth's flora (Wolfe and Shields, 1997). The enhanced evolutionary potential of polyploidy and the increasing availability of fruits likely fostered the emergence of fermentative yeast.

### **Polyploidy in diploid multi-cellular organisms during development, stress response and tumorigenesis**

In a wide range of tissues in diploid organisms, polyploidy is achieved through endoreplication, a specialized cell cycle in which the genome content increases by DNA replication without subsequent cell division (Edgar and Orr-Weaver, 2001). Trophoblasts and megakaryocytes are well-known mammalian examples of polyploid cell types arising from endo-



replication (Edgar and Orr-Weaver, 2001; Ravid et al., 2002). Multiple tissues in *Drosophila* initiate endo-replication to become polyploid during embryogenesis, and endo-replication occurs again later in cells lining the larval gut track (Smith and Orr-Weaver, 1991). Various somatic tissues in seed plants are also known to become highly polyploid during development (Barow and Meister, 2003; Galbraith et al., 1991).

Polyploidy via endo-replication, typically associated with terminal differentiation, is considered a convenient mechanism to produce cells with high metabolic capability and specialization in mass production/storage of macromolecules (Edgar and Orr-Weaver, 2001). In *Drosophila* adult females, polyploid nurse and follicle cells are crucial for oocyte development. Specific disruption of endo-replication in these cells severely delays maturation of egg chambers and results in sterility (Maines et al., 2004). Trophoblasts in the mammalian placenta have a DNA content of  $>1000C$ . They facilitate embryo implantation and are needed to meet the high demand of molecular transport between mother and fetus (Zybina and Zybina, 2005). Differentiation of megakaryocytes requires multiple rounds of endo-replication. High ploidy (up to  $128n$ ) facilitates mass production and release of platelets (Ravid et al., 2002). During plant seed development, endo-replication correlates with rapid biosynthesis of starch and overall increase of endosperm mass (Lee et al., 2009; Schweizer et al., 1995). Seed plants capable of endo-replication in somatic tissues tend to develop, flower, and produce seeds faster than species without endo-replication in the same geographical niche. Endo-replication/polyploidy in key organs seems to boost metabolism in these species to impart an advantage in growth (Barow and Meister, 2003).

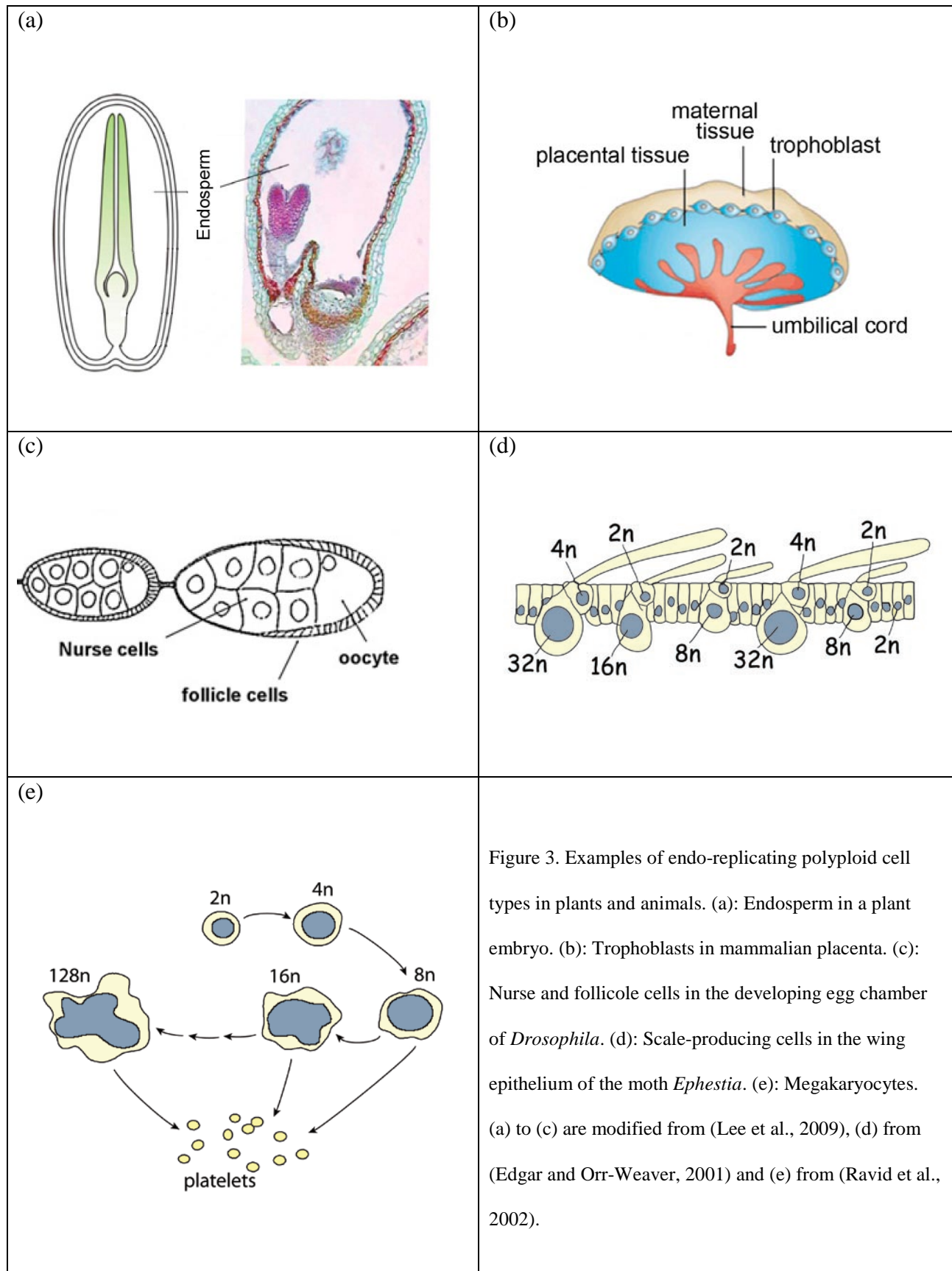


Figure 3. Examples of endo-replicating polyploid cell types in plants and animals. (a): Endosperm in a plant embryo. (b): Trophoblasts in mammalian placenta. (c): Nurse and follicle cells in the developing egg chamber of *Drosophila*. (d): Scale-producing cells in the wing epithelium of the moth *Ephesia*. (e): Megakaryocytes. (a) to (c) are modified from (Lee et al., 2009), (d) from (Edgar and Orr-Weaver, 2001) and (e) from (Ravid et al., 2002).

Polyploidization has been observed in hepatocytes and cardiomyocytes as a proliferation-independent stress response. Hepatocytes with dysfunctional telomeres do not undergo apoptosis or senescence as do mitotically active cells. When challenged by the demand to regenerate liver after partial hepatectomy, these cells perform endo-replication to become polyploids, a process that accounts for the regeneration of liver mass and function (Lazzerini Denchi et al., 2006). Polyploid cardiomyocytes are found in human hearts after myocardial infraction (Herget et al., 1997). A switch to endo-replication may be a convenient means to cope with injuries when neither cell death nor proliferation is desirable.

Polyploidy in tissues can occur not only through programmed endo-replication but also as an undesirable result of failed cytokinesis, mitotic slippage from spindle checkpoint, or pathogen-induced cell fusion (Ganem et al., 2007). The resultant polyploids exhibit greater chromosomal instability and increased tumorigenic potential. Tetraploid *p53*-null mouse mammary epithelial cells, but not the genetically matching diploid cells, produced tumors *in vitro* and *in vivo* with numerous gross chromosomal rearrangements (Fujiwara et al., 2005). A study on clinical samples of cervical tissue revealed a strong correlation between tetraploidy and near-tetraploid aneuploidy, both of which were significantly over-represented in dysplastic samples compared with normal samples. The aneuploidy is largely dependent on the presence of tetraploidy in abnormal samples, indicating that aneuploidy developed from tetraploidy during disease progression (Olaharski et al., 2006). A number of other studies also indicate that tetraploidy is an early, intermediate state in the development of cancer [summarized in (Ganem et al., 2007) and (Olaharski et al., 2006)]. Besides genome instability, dominant mutations in key oncogenes may accumulate more efficiently in polyploids and thereby raise tumorigenic potential (Otto, 2007).

## **Ploidy and gene expression – examples from multi-cellular eukaryotes**

Functional and morphological changes associated with polyploidy indicate that ploidy alters gene expression. Despite a plethora of known polyploid cell types in multi-cellular organisms, few cell types have been transcriptionally characterized. Gene expression profiling of human and mouse cardiomyocytes and hepatocytes shows that a wide range of processes in stress response are induced by polyploidy, such as inhibition of apoptosis, response to hypoxia, DNA damage repair, glycolysis and protein turnover (Anatskaya and Vinogradov, 2007). This discovery is consistent with the known injury-coping capabilities of polyploid cardiomyocytes and hepatocytes (Herget et al., 1997; Lazzerini Denchi et al., 2006). However, it is unclear to what extent the observed differential gene expression was strictly caused by polyploidy. Cells at different ploidy states could reside in distinct micro-environments in the heart and liver tissues. Differential regulation of some of the genes could reflect changes in external factors. Furthermore, it has been shown that the majority of polyploid hepatocytes in mice are binucleated (Lu et al., 2007). Such binucleated cells could represent a different physiological state from endo-replication derived polyploidy. Whether or not the binucleated cells in heart and liver tissues were excluded from the transcriptome profiling was not specified. These technical concerns reflect the greater complexity of cellular biology in the context of tissue or organ development.

Transcriptional profiling of human megakaryocytes (2n to 16n) differentiated *in vitro* revealed down-regulation of genes involved in DNA replication and repair, whereas genes important for platelet production and secretion were up-regulated (Raslova et al., 2007). Ploidy-associated induction of platelet biogenesis genes is consistent with the physiology of polyploid megakaryocytes. It is unclear why DNA replication and repair factors were repressed in the

polyploids. The authors proposed two interpretations of the results, based on the increasing expression of platelet biogenesis genes with increasing ploidy. One interpretation is that polyploidization is likely a part of the terminal differentiation program of megakaryocytes, rather than a pre-requisite of differentiation, as the platelet biogenesis genes were already induced during the polyploidization process. Alternatively, the results could reflect rising probability of terminal differentiation as ploidy increases. This study posed technical challenges that hindered a better understanding of the megakaryocyte ploidy series. Because of the low abundance of megakaryocytes in bone marrow, culturing the ploidy series *in vitro* was necessary. However the cultured megakaryocytes only could reach a much lower ploidy level and were mixed with progenitor cells. Consequently the results obtained *in vitro* may not reflect the physiology *in vivo* or the changes wholly unique to the megakaryocyte transcriptome.

Although many studies on gene expression in polyploid plants have been published, the literature is predominately based on allopolyploids, in which the “homologous” chromosome sets come from different parental species. Allopolyploidy is prominent in the plant kingdom, and many species important to agriculture and manufacture (wheat, oat, cotton, coffee, canola...etc) are allopolyploids (Osborn et al., 2003). Hybridization of different genomes, rather than polyploidization per se, is known to cause large-scale, rapid changes in allopolyploids (Albertin et al., 2006; Albertin et al., 2005; Osborn et al., 2003; Otto, 2007). Some of the altered gene expression in allopolyploids results from deletion or rearrangement in the genome upon hybridization [mechanisms reviewed in (Osborn et al., 2003)]. Besides genetic changes, transcriptional regulators encoded by the different genomes may interact in a novel or unbalanced fashion, altering their molecular function. Factors encoded in one genome may differently regulate the chromatin on the other genome. Both mechanisms would lead to many

epigenetic changes in allopolyploids, which often display novel traits and thus evolutionary opportunities when compared with their parental species (Osborn et al., 2003; Wang et al., 2004).

Autopolyploid plants, in which the homologous chromosome sets come from a single species, have attracted much fewer molecular investigations than allopolyploids. The autopolyploidy state may be more difficult to maintain. As illustrated in the genome evolution of yeast (Wolfe and Shields, 1997), duplicated homologous genes that are functionally redundant tend to face rapid elimination in the process of re-calibration of the genome to the diploid state. Nonetheless a few autopolyploid species have thrived and play important roles in agriculture, such as alfalfa, cassava and potato (Guo et al., 1996; Osborn et al., 2003).

One study compared expression levels of 18 genes in the leaves in a ploidy series of corn (Guo et al., 1996). One gene encoding a thiol protease was strongly repressed in the autopolyploids. Another gene of unknown function was significantly induced by increasing ploidy. It was concluded that with few exceptions, autopolyploidy increases gene expression on a per cell basis, and the increase is proportional to the gene dosage at the given ploidy. Proteomics of leaf and stem tissues in autopolyploid cabbage agree with this notion (Albertin et al., 2006; Albertin et al., 2005).

The model plant species *Arabidopsis thaliana* has been examined in the context of autopolyploidy. A small number of genes among the ~2300 examined in the leaf tissue showed ploidy-associated changes in expression (Wang et al., 2004). Repressed in the autotetraploid were genes encoding a cellulose synthase subunit, a NAD-dependent malate dehydrogenase, a DNA-binding protein, and a putative protein of unknown function. Induced by ploidy were genes

encoding Rad54 for DNA repair, a protein for vacuolar sorting/transport, a nuclear matrix component, and a kinesin-related protein. Why these genes were differentially regulated in the autotetraploid was not explored, since allotetraploids were the focus of the study and the autotetraploid was included as a control for ploidy. Notably, RNAi inhibition of two DNA-methylases known to modify the chromatin of *RAD54* derepressed its expression in allotetraploids. It remains to be examined whether autotetraploidy alters the expression of *RAD54* by affecting methylation of its chromatin.

In one study, polyploidy-dependent differential methylation in *A. thaliana* was observed in the transgene hydromycin phosphotransferase (HTP) (Mittelsten Scheid et al., 2003). Hydromycin resistance conferred by HTP was stably inherited in diploids but subject to progressive loss in autotetraploids. Loss of hydromycin resistance was not due to mutations in the nucleotide sequence but was correlated with cytosine methylation levels in the gene. Interestingly, presence of the methylated allele of HTP caused progressive methylation and repression of unmethylated allele. The *trans*-methylation phenomenon between epi-alleles required meiosis in tetraploids, suggesting that polyploidy alters chromosomal interactions in meiosis and enables novel *trans*-regulation between *cis*-elements.

### **Budding yeast as a model system to study consequences of polyploidy**

The unicellular *S. cerevisiae* is amenable to precise genetic engineering and can be cultured at multiple ploidy states. Recent studies have demonstrated that budding yeast is a useful model system to investigate the effects of polyploidy on cellular physiology. Similar to higher eukaryotes, yeast cells enlarge as ploidy increases (Andalis et al., 2004; Di Talia et al.,

2007; Galitski et al., 1999; Storchova et al., 2006). Besides the enlarged cell size, polyploid yeast exhibits different gene regulation and phenotypes compared to haploids and diploids.

A microarray-based study identified a small number of ploidy-regulated genes in yeast (figure 4), i.e., genes whose transcript representation is altered proportionally to ploidy (Galitski et al., 1999). Because the employed yeast strains had identical genome sequence, this study unambiguously demonstrates an effect of ploidy on gene regulation. Although the genes identified did not reveal how ploidy alters gene expression, differential regulation of some genes accounts for phenotypes unique to polyploids. For example, strong repression of the adhesin-encoding gene *FLO11* severely diminishes agar adhesion of polyploids. The strongly ploidy-induced *CTS1* encodes an endochitinase promoting mother-daughter separation at cytokinesis. Elevated expression of *CTS1* likely contributes to the much reduced cell-cell association of polyploids.

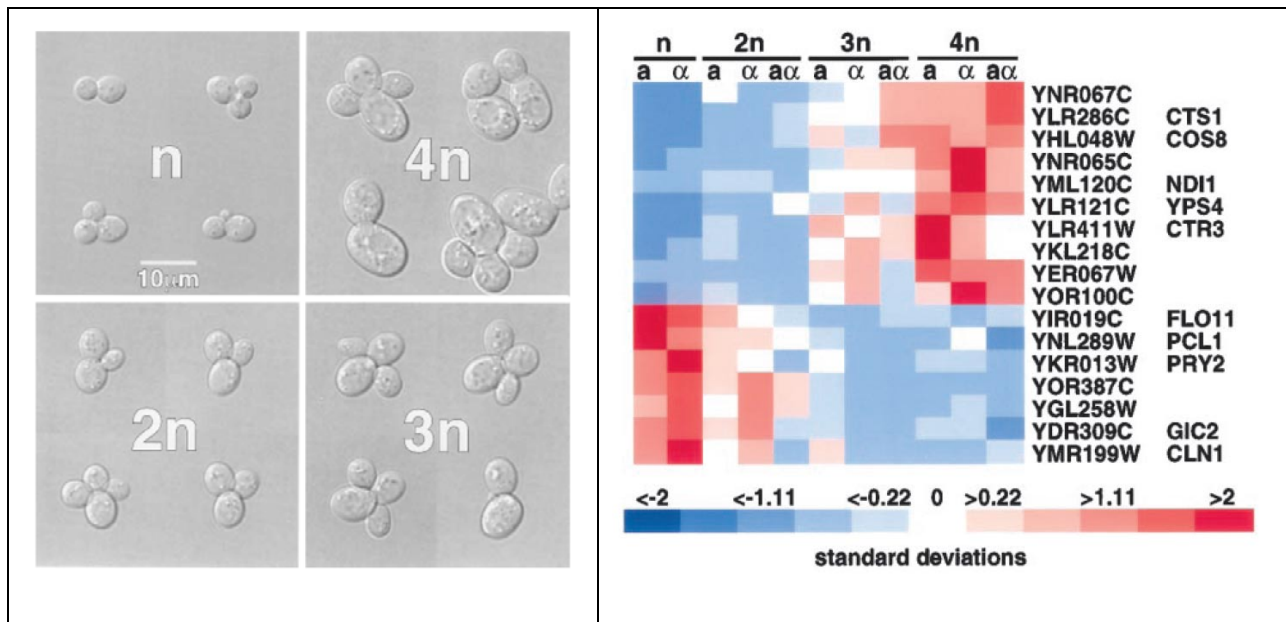


Figure 4. An isogenic ploidy series and genes differentially regulated in them (Galitski et al., 1999). **Left:**

Exponentially growing cells of an isogenic *MATα* series. Cell size increases with increasing ploidy. **Right:** Ploidy-



regulated genes identified by transcriptome profiling with microarrays. Expression levels of a gene in the ploidy series are normalized to the mean (set to 0) and the standard deviation (set to 1).

In stationary phase, polyploid but not haploid yeast cells fail to arrest their cell cycle and lose viability rapidly, although the transcriptional profile of polyploids resembled stationary phase (Andalis et al., 2004). The loss of viability is partially rescued by heterozygosity at the mating-type loci, which improves the efficiency of mitotic arrest of polyploids in stationary phase. When incubated in water instead of spent medium, post-diauxic polyploid cells arrest cell cycle and maintain viability like haploids. These observations of polyploid growth suggest abnormalities in signaling pathways transmitting nutrient availability to cell cycle regulation, so that depletion of nutrients is not sensed properly and that absolute deprivation from energy source is needed to arrest cell cycle. Consistent with this explanation, in the absence of the G1 cyclin Cln3, mitotic entry is diminished and viability is significantly restored in polyploids (figure 5). In WT haploids, Cln3 protein level is down-regulated to delay mitosis in response to nitrogen (Gallego et al., 1997) and carbon (Hall et al., 1998) depletion. Polyploids likely suffer from an inability to down-regulate *CLN3* and thus aberrantly continue cell cycle progression, regardless how unfavorable mitosis is under the growth condition. Deletion of *CLN3* could restore viability by enabling a switch from proliferation to quiescence (G0), even though *CLN3* appears to be required for optimal metabolic adaption to stationary phase (figure 5).

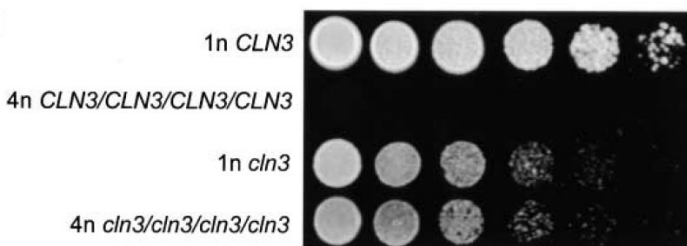


Figure 5. Deletion of *CLN3* restores survivorship of polyploids in stationary phase (Andalis et al., 2004). Cells grown in stationary phase for 12.5 days were serially diluted and spotted onto YPD to compare viability.

Polyloid yeast has also provided much insight on the origin of genome instability associated with increasing ploidy during tumorigenesis in metazoans. A systematic survey identified lethal mutations specific to tetraploids but not to haploids or diploids (Storchova et al., 2006). The mutations collectively reveal vulnerability in sister chromatid cohesion, homologous recombination and mitotic spindle function. Sensitivity to perturbations in these processes reflects the greater burden of maintaining a much larger and more complex genome. Because the probability of spontaneous DNA damage increases with increasing DNA content, polyloids endure a higher frequency of DNA lesion, rendering DNA damage repair an essential process for survival. The most pronounced genomic defect in polyloids is the much higher rate (>200x) of chromosome loss, and syntelic attachment of chromosomes (both sister chromatids are attached to the same spindle pole) occurs more frequently in polyloids. Fluorescence imaging and electron tomography show that while the spindle pole body expands its surface area proportionally to ploidy and to the number of nuclear microtubules, the length of pre-anaphase spindle remains unchanged by ploidy (figure 6). The unequal scaling between spindle pole body and spindle length could favor syntelic attachment. Defects in sister chromatid cohesion, of which the basis in polyloids is unclear, could lead to increased syntelic attachment and chromosomal loss as well.

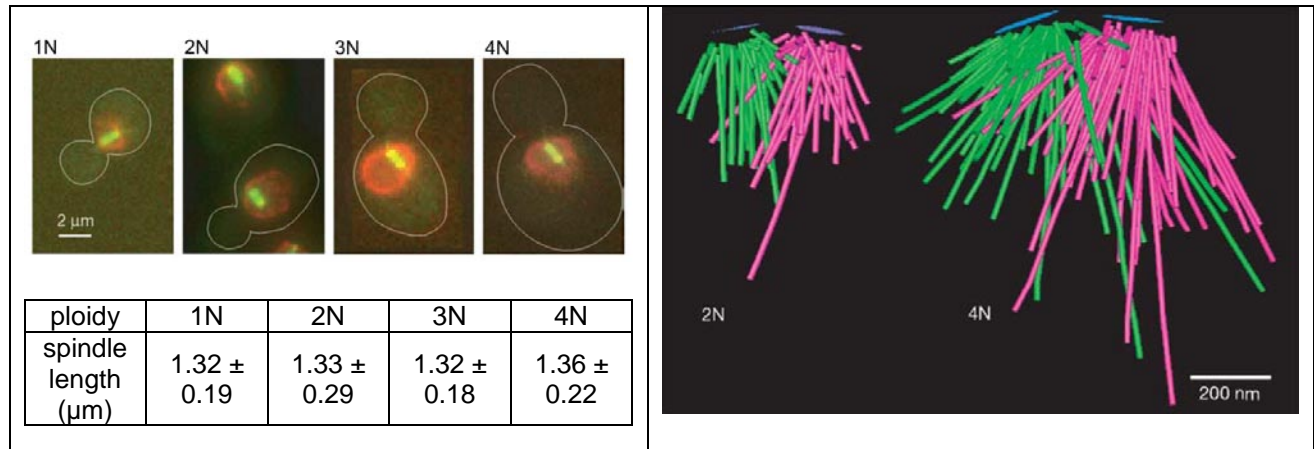


Figure 6. Unequal scaling of pre-anaphase spindle length and spindle pole body surface area (Storchova et al., 2006). **Left:** Fluorescence microscopy images of cells expressing Nup116-YFP (red) to mark the nucleus envelope and Tub1-GFP (green) to label the mitotic spindle. The spindle length is maintained constant, independently of ploidy. **Right:** Models of the mitotic spindle in diploid and tetraploid cells constructed from electron tomography. Central plaques of spindle pole bodies are shown in blue. Green and magenta lines denote microtubules nucleating from different spindle pole bodies. Measured average surface area of spindle pole body is  $0.022 \mu\text{m}^2$  in diploid and  $0.043 \mu\text{m}^2$  in tetraploid.

### Control of cell size in yeast and metazoans

One immediate effect and prominent feature of polyploidy is enlarged cell size (Otto, 2007), the threshold of which is established dynamically as a coordinated outcome of cell growth and cell cycle progression (Cook and Tyers, 2007). How polyploidy raises the cell size threshold is unknown, because the exact mechanism of cell size regulation in haploids or diploids is not yet well understood. Much of the molecular insight into control of cell size comes from elegant studies in budding and fission yeast.

In budding yeast, mutations that alter either cell growth or cell cycle progression change the size threshold. Cell cycle mutants that hasten or delay cell cycle progression lead to reduced or increased cell size, respectively (Cross, 1988; Jorgensen et al., 2002). A systematic screen for mutations altering cell size revealed a role of ribosome biogenesis in cell size control. Mutations

that impair ribosome assembly lower cell size threshold (Jorgensen et al., 2002), reminiscent of the slower ribosome synthesis and reduced cell size during nutrient starvation (Kief and Warner, 1981; Schneider et al., 2004). Details of the functional link between ribosome assembly/activity and cell size regulation await elucidation. Polyploidy may enlarge cell size by increasing the rate of ribosome biogenesis, since the cell division frequency is unchanged by ploidy (Di Talia et al., 2007). A recent discovery, likely a promising lead to a greater understanding of the connection between ribosome activity and size control, is chaperone-dependent release of G1 cyclin Cln3 from the rough ER periphery in late G1 (Verges et al., 2007). Cln3 is the most upstream activator of cell cycle progression (Bloom and Cross, 2007), and its mutant alleles alter the cell size threshold (Cross, 1988). Regulation of Cln3 localization by chaperones at the ribosome-associated ER could represent a simple device for coupling growth and cell cycle progression. The rate of ribosome biogenesis and activity of chaperones likely reflect a cell's growth status and thus the fitness level for mitosis. Only when the capacity for mitosis exceeds a threshold level would the chaperons on the ER release a sufficient amount of Cln3 to initiate cell cycle progression.

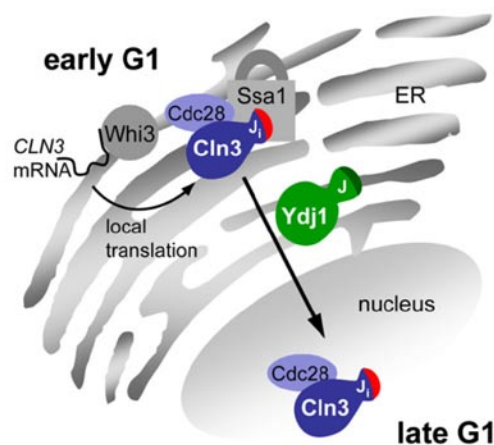


Figure 7: Model for ER-tethering of Cln3 and its release for nuclear accumulation in late G1 (Verges et al., 2007). During most of the cell cycle, Cln3 is associated with the rough ER. Two domains in the Cln3 polypeptide mediate localization to the ER, likely through binding the adaptors Cdc28 and chaperone Ssa1. Ssa1 recognizes the J domain of Cln3 and is thought to maintain a catalytically inactive state when bound to Cln3 *in vivo*. In late

G1, the J domain of another chaperone Ydj1 presumably displaces Cln3 from Ssa1. Localization of the *CLN3* mRNA by Whi3 at the ER is based on findings in a previous study (Gari et al., 2001).

In fission yeast, a recently identified gradient of the kinase Pom1, coupled to a sensor of this gradient, the kinase Cdr2, is involved in the coordinated cell growth and cell cycle progression (Moseley et al., 2009). Activation of Cdr2 is necessary for entry into mitosis, and Pom1 inhibits the activity of Cdr2. Anchoring of Pom1 at the two poles of the cell creates zones of mitotic inhibition. Confined localization of Cdr2 to the middle of the cell ensures mitotic entry does not occur until the cell elongates to a certain dimension so that Cdr2 is sufficiently separated from the inhibition of Pom1.

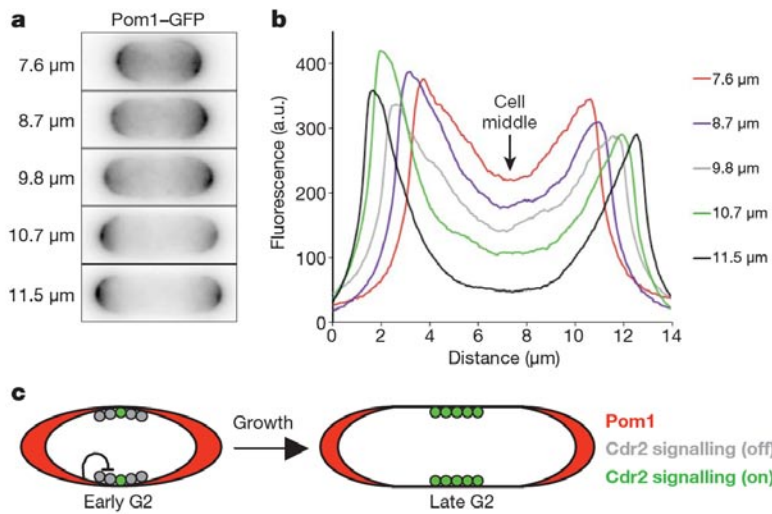


Figure 8: The spatial gradient of Pom1 and the gradual depletion of its abundance in mid-section as the cell elongates (Moseley et al., 2009). (a) Localization of Pom1 in cells of various sizes. (b) Abundance of Pom1 across cells of different sizes, based on quantified GFP fluorescence intensity.

(c) Model for spatial regulations of Pom1 and Cdr2 that enables size-dependent activation of Cdr2 to prevent premature mitotic entry of smaller cells.

Multiple proliferating cell types of vertebrates cultured *in vitro* have demonstrated the existence of a size-sensing mechanism in G1 that regulates timing of S phase onset (Dolznig et al., 2004). This mechanism coordinates cell growth and cell cycle progression, thereby maintaining a size threshold. Human and chicken erythroblasts, as well as mouse fibroblasts, shorten the duration of G1 phase when they have been manipulated to enlarge prior to early G1

in the cell cycle. The result is an efficient reset of cell size in one doubling time. The size threshold is also adjusted accordingly to growth conditions. A faster growth rate promoted by stronger growth signaling raises the size threshold despite more frequent cell division. The cell size threshold, growth rate and doubling time all appear to adapt to changes in growth conditions and reach their defined set points rapidly and reversibly.

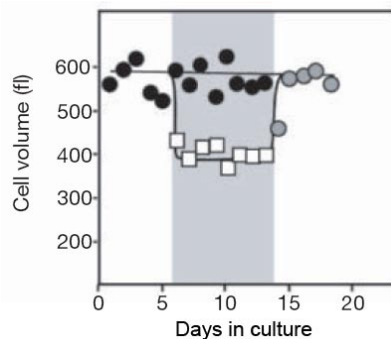


Figure 9: Cultured erythroblasts reversibly alter cell size in response to changing growth conditions (Dolznic et al., 2004). Large cells in a fast growing condition (black filled circles) are either maintained in the same condition or switched to a slower growing condition (open white squares) for 9 days (gray area). The latter population was then switched back to the fast growing condition (gray filled circles).

In cultured mouse lymphoblasts, the cell size appears to be maintained by regulated growth rate and cell division frequency (Tzur et al., 2009). The growth rate positively correlates with cell size until a critical size threshold, beyond which the growth rate declines with increasing cell size. The frequency of cell division also correlates positively with cell size. Both observations reveal how growing cells efficiently reach a desirable size and divide in a regulated fashion. Collectively, the growth and division parameters of multiple cell types support the existence of an exquisite cell autonomous mechanism that maintains size homeostasis in metazoans.

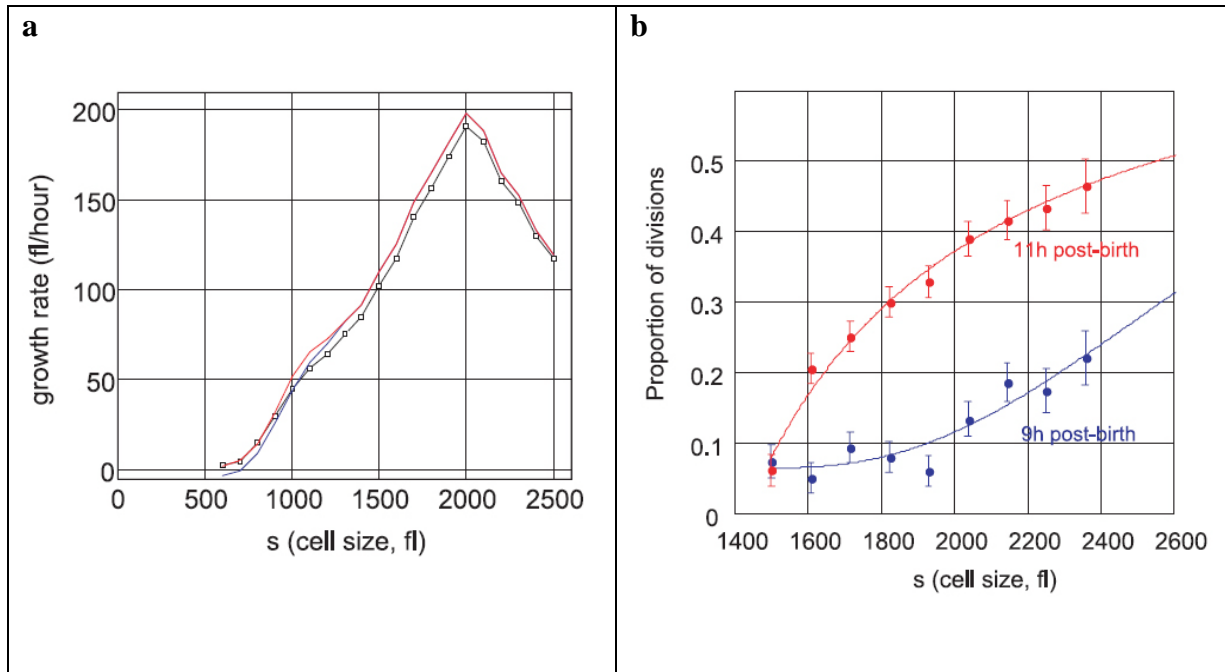


Figure 10: Maintenance of cell size by controlled growth rate and cell division frequency (Tzur et al., 2009). (a)

Growth plot (black line with open squares) of isolated newborn lymphoblasts. Red and blue curves indicate two

different approaches of extrapolating the data. Before reaching the critical cell size 2000 fL, 65% of the population

would have undergone cell division. (b) Populations of cells of the same age at 9 hours and 11 hours after birth were

tracked for the proportion of cells divided at a specified cell size.

## **Summary**

Polyploidy is a prevalent physiological state achieved by multiple mechanisms in evolution, differentiation and disease. In the context of evolution, the duplicated copy of a genome is less functionally constrained and has greater capacity to evolve novel functions in a coordinated fashion on a genome-wide scale. In development, differentiation and stress response, polyploidy is part of an organ's repertoire to rapidly increase biomass and metabolism when proliferation is either undesirable or incapable of achieving the intended physiology. Formation of aneuploid tumors likely requires a polyploid intermediate that is genomically unstable and thus increases the probability of transformation.

Although many polyploid cell types have been discovered, how increasing ploidy enlarges cell size and alters cellular physiology remains enigmatic. Few polyploid cell types have been thoroughly analyzed and compared to their genetically matching haploid or diploid progenitors. Detailed mechanistic investigations on isogenic ploidy series can provide the missing information. In particular, studies directly probing a relationship between cell size and altered physiology in polyploids are lacking. Such a relationship likely exists and plays a fundamental role in cellular biology, since maintenance of cell size homeostasis through sophisticated coordination of cell growth and division is found in a wide range of organisms. The ease of genetic engineering and the extensive information about cell metabolism and growth make yeast an ideal organism for deciphering the intricate relationships among ploidy, size and function.



## **References**

Albertin, W., Balliau, T., Brabant, P., Chevre, A.M., Eber, F., Malosse, C., and Thiellement, H. (2006). Numerous and rapid nonstochastic modifications of gene products in newly synthesized *Brassica napus* allotetraploids. *Genetics* *173*, 1101-1113.

Albertin, W., Brabant, P., Catrice, O., Eber, F., Jenczewski, E., Chevre, A.M., and Thiellement, H. (2005). Autopolyploidy in cabbage (*Brassica oleracea* L.) does not alter significantly the proteomes of green tissues. *Proteomics* *5*, 2131-2139.

Anatskaya, O.V., and Vinogradov, A.E. (2007). Genome multiplication as adaptation to tissue survival: evidence from gene expression in mammalian heart and liver. *Genomics* *89*, 70-80.

Andalis, A.A., Storchova, Z., Styles, C., Galitski, T., Pellman, D., and Fink, G.R. (2004). Defects arising from whole-genome duplications in *Saccharomyces cerevisiae*. *Genetics* *167*, 1109-1121.

Barow, M., and Meister, A. (2003). Endopolyploidy in seed plants is differently correlated to systematics, organ, life strategy and genome size. *Plant, Cell and Environment* *26*, 571-584.

Blanc, G., and Wolfe, K.H. (2004). Widespread paleopolyploidy in model plant species inferred from age distributions of duplicate genes. *Plant Cell* *16*, 1667-1678.

Bloom, J., and Cross, F.R. (2007). Multiple levels of cyclin specificity in cell-cycle control. *Nat Rev Mol Cell Biol* *8*, 149-160.

Cook, M., and Tyers, M. (2007). Size control goes global. *Curr Opin Biotechnol* *18*, 341-350.

Cross, F.R. (1988). DAF1, a mutant gene affecting size control, pheromone arrest, and cell cycle kinetics of *Saccharomyces cerevisiae*. *Mol Cell Biol* *8*, 4675-4684.

Dehal, P., and Boore, J.L. (2005). Two rounds of whole genome duplication in the ancestral vertebrate. *PLoS Biol* *3*, e314.

Di Talia, S., Skotheim, J.M., Bean, J.M., Siggia, E.D., and Cross, F.R. (2007). The effects of molecular noise and size control on variability in the budding yeast cell cycle. *Nature* *448*, 947-951.

Dolznic, H., Grebien, F., Sauer, T., Beug, H., and Mullner, E.W. (2004). Evidence for a size-sensing mechanism in animal cells. *Nat Cell Biol* *6*, 899-905.

Edgar, B.A., and Orr-Weaver, T.L. (2001). Endoreplication cell cycles: more for less. *Cell* *105*, 297-306.

Fujiwara, T., Bandi, M., Nitta, M., Ivanova, E.V., Bronson, R.T., and Pellman, D. (2005). Cytokinesis failure generating tetraploids promotes tumorigenesis in p53-null cells. *Nature* *437*, 1043-1047.

- Galbraith, D.W., Harkins, K.R., and Knapp, S. (1991). Systemic Endopolyploidy in *Arabidopsis thaliana*. *Plant Physiol* 96, 985-989.
- Galitski, T., Saldanha, A.J., Styles, C.A., Lander, E.S., and Fink, G.R. (1999). Ploidy regulation of gene expression. *Science* 285, 251-254.
- Gallego, C., Gari, E., Colomina, N., Herrero, E., and Aldea, M. (1997). The Cln3 cyclin is down-regulated by translational repression and degradation during the G1 arrest caused by nitrogen deprivation in budding yeast. *EMBO J* 16, 7196-7206.
- Ganem, N.J., Storchova, Z., and Pellman, D. (2007). Tetraploidy, aneuploidy and cancer. *Curr Opin Genet Dev* 17, 157-162.
- Gari, E., Volpe, T., Wang, H., Gallego, C., Futcher, B., and Aldea, M. (2001). Whi3 binds the mRNA of the G1 cyclin CLN3 to modulate cell fate in budding yeast. *Genes Dev* 15, 2803-2808.
- Guo, M., Davis, D., and Birchler, J.A. (1996). Dosage effects on gene expression in a maize ploidy series. *Genetics* 142, 1349-1355.
- Hall, D.D., Markwardt, D.D., Parviz, F., and Heideman, W. (1998). Regulation of the Cln3-Cdc28 kinase by cAMP in *Saccharomyces cerevisiae*. *Embo J* 17, 4370-4378.
- Hegarty, M.J., and Hiscock, S.J. (2008). Genomic clues to the evolutionary success of polyploid plants. *Curr Biol* 18, R435-444.
- Herget, G.W., Neuburger, M., Plagwitz, R., and Adler, C.P. (1997). DNA content, ploidy level and number of nuclei in the human heart after myocardial infarction. *Cardiovasc Res* 36, 45-51.
- Hijmans, R.J., Gavrilenko, T., Stephenson, S., Bamberg, J., Salas, A., and Spooner, D.M. (2007). Geographical and environmental range expansion through polyploidy in wild potatoes (*Solanum section Petota*). *Global Ecology and Biogeography* 16, 485-495.
- Ihmels, J., Bergmann, S., Gerami-Nejad, M., Yanai, I., McClellan, M., Berman, J., and Barkai, N. (2005). Rewiring of the yeast transcriptional network through the evolution of motif usage. *Science* 309, 938-940.
- Jorgensen, P., Nishikawa, J.L., Breikreutz, B.J., and Tyers, M. (2002). Systematic identification of pathways that couple cell growth and division in yeast. *Science* 297, 395-400.
- Kasahara, M. (2007). The 2R hypothesis: an update. *Curr Opin Immunol* 19, 547-552.
- Kief, D.R., and Warner, J.R. (1981). Coordinate control of syntheses of ribosomal ribonucleic acid and ribosomal proteins during nutritional shift-up in *Saccharomyces cerevisiae*. *Mol Cell Biol* 1, 1007-1015.

- Lazzerini Denchi, E., Celli, G., and de Lange, T. (2006). Hepatocytes with extensive telomere deprotection and fusion remain viable and regenerate liver mass through endoreduplication. *Genes Dev* 20, 2648-2653.
- Lee, H.O., Davidson, J.M., and Duronio, R.J. (2009). Endoreplication: polyploidy with purpose. *Genes Dev* 23, 2461-2477.
- Lu, P., Prost, S., Caldwell, H., Tugwood, J.D., Betton, G.R., and Harrison, D.J. (2007). Microarray analysis of gene expression of mouse hepatocytes of different ploidy. *Mamm Genome* 18, 617-626.
- Maines, J.Z., Stevens, L.M., Tong, X., and Stein, D. (2004). *Drosophila* dMyc is required for ovary cell growth and endoreplication. *Development* 131, 775-786.
- Mittelsten Scheid, O., Afsar, K., and Paszkowski, J. (2003). Formation of stable epialleles and their paramutation-like interaction in tetraploid *Arabidopsis thaliana*. *Nat Genet* 34, 450-454.
- Moseley, J.B., Mayeux, A., Paoletti, A., and Nurse, P. (2009). A spatial gradient coordinates cell size and mitotic entry in fission yeast. *Nature* 459, 857-860.
- Ohno, S. (1970). *Evolution by Gene Duplication* (New York, Springer-Verlag).
- Olaharski, A.J., Sotelo, R., Solorza-Luna, G., Gonsebatt, M.E., Guzman, P., Mohar, A., and Eastmond, D.A. (2006). Tetraploidy and chromosomal instability are early events during cervical carcinogenesis. *Carcinogenesis* 27, 337-343.
- Osborn, T.C., Pires, J.C., Birchler, J.A., Auger, D.L., Chen, Z.J., Lee, H.S., Comai, L., Madlung, A., Doerge, R.W., Colot, V., *et al.* (2003). Understanding mechanisms of novel gene expression in polyploids. *Trends Genet* 19, 141-147.
- Otto, S.P. (2007). The evolutionary consequences of polyploidy. *Cell* 131, 452-462.
- Raslova, H., Kauffmann, A., Sekkai, D., Ripoché, H., Larbret, F., Robert, T., Le Roux, D.T., Kroemer, G., Debili, N., Dessen, P., *et al.* (2007). Interrelation between polyploidization and megakaryocyte differentiation: a gene profiling approach. *Blood* 109, 3225-3234.
- Ravid, K., Lu, J., Zimmet, J.M., and Jones, M.R. (2002). Roads to polyploidy: the megakaryocyte example. *J Cell Physiol* 190, 7-20.
- Schneider, B.L., Zhang, J., Markwardt, J., Tokiwa, G., Volpe, T., Honey, S., and Futcher, B. (2004). Growth rate and cell size modulate the synthesis of, and requirement for, G1-phase cyclins at start. *Mol Cell Biol* 24, 10802-10813.
- Schughart, K., Kappen, C., and Ruddle, F.H. (1989). Duplication of large genomic regions during the evolution of vertebrate homeobox genes. *Proc Natl Acad Sci U S A* 86, 7067-7071.

Schweizer, L., Yerk-Davis, G.L., Phillips, R.L., Sreenc, F., and Jones, R.J. (1995). Dynamics of maize endosperm development and DNA endoreduplication. *Proc Natl Acad Sci U S A* 92, 7070-7074.

Smith, A.V., and Orr-Weaver, T.L. (1991). The regulation of the cell cycle during *Drosophila* embryogenesis: the transition to polyteny. *Development* 112, 997-1008.

Storchova, Z., Breneman, A., Cande, J., Dunn, J., Burbank, K., O'Toole, E., and Pellman, D. (2006). Genome-wide genetic analysis of polyploidy in yeast. *Nature* 443, 541-547.

Tzur, A., Kafri, R., LeBleu, V.S., Lahav, G., and Kirschner, M.W. (2009). Cell growth and size homeostasis in proliferating animal cells. *Science* 325, 167-171.

Verges, E., Colomina, N., Gari, E., Gallego, C., and Aldea, M. (2007). Cyclin Cln3 is retained at the ER and released by the J chaperone Ydj1 in late G1 to trigger cell cycle entry. *Mol Cell* 26, 649-662.

Wang, J., Tian, L., Madlung, A., Lee, H.S., Chen, M., Lee, J.J., Watson, B., Kagochi, T., Comai, L., and Chen, Z.J. (2004). Stochastic and epigenetic changes of gene expression in *Arabidopsis* polyploids. *Genetics* 167, 1961-1973.

Wolfe, K.H. (2001). Yesterday's polyploids and the mystery of diploidization. *Nat Rev Genet* 2, 333-341.

Wolfe, K.H., and Shields, D.C. (1997). Molecular evidence for an ancient duplication of the entire yeast genome. *Nature* 387, 708-713.

Zybina, T.G., and Zybina, E.V. (2005). Cell reproduction and genome multiplication in the proliferative and invasive trophoblast cell populations of mammalian placenta. *Cell Biol Int* 29, 1071-1083.

## **Chapter 2. Control of gene expression by cell size**

(contents of this chapter have been submitted to the journal PLoS Biology)

### **Summary**

Polyploidy, increased genome content arising from whole genome duplication, plays an important role in evolution, development and tumorigenesis. Polyploids exhibit enlarged cell size and altered gene expression, but the basis for the relationship is not known. My data in this chapter show that ploidy-associated changes in gene expression reflect transcriptional adjustment to a larger cell size, implicating cellular geometry as a key parameter in gene regulation. Using RNA-seq, I identified genes whose regulation was altered in a tetraploid as compared with an isogenic haploid. Regulation of these genes was then examined in haploid genetic mutants that also produce increased cell size. In both contexts, cells with increased cell size share a substantial number of identically differentially regulated genes. Analysis of the size-regulated genes identified a transcription factor that mediates size-dependent regulation. The result suggests a causal relationship between cell size and transcription with a size-sensing mechanism that adjusts gene expression in response to changes in size. Transcriptional responses to enlarged cell size could underlie other cellular changes associated with polyploidy. Furthermore, the causal relationship between cell size and transcription suggests that cell size homeostasis serves a regulatory role in transcriptome maintenance.

### **Introduction**

Mounting genomic evidence suggests that a wide range of diploid eukaryotic species have evolved from polyploid ancestors with duplicated genomes, as hypothesized by Ohno

(Kasahara, 2007; Semon and Wolfe, 2007). Polyploid organisms exist in multiple kingdoms and are especially prevalent among plants. During development, specific cell types in diploid metazoan organisms perform endo-replication and differentiate into polyploid cells that manifest novel functions distinct from their diploid progenitors (Lee et al., 2009). Polyploidy also occurs as an intermediate state in aneuploid tumor formation (Ganem et al., 2007). From yeast to mammals, polyploidy is associated with enlarged cell size and altered cellular physiology (Andalis et al., 2004; Galitski et al., 1999; Lee et al., 2009; Storchova et al., 2006). Despite a plethora of known polyploid cell types, how ploidy changes cellular physiology remains elusive. Moreover, no causal relationship between enlarged cell size and altered physiology has been uncovered. Detailed molecular characterization of polyploid tissues in metazoans and plants has been limited by technical constraints. Methods for precise manipulation of the genome have yet to be fully developed for higher eukaryotes, and therefore it is difficult to access a large quantity of isogenic cells of different ploidies grown in native conditions.

The budding yeast presents an ideal system to decipher the relationship among ploidy, cell size and gene expression. Elegant molecular genetics enables convenient and precise engineering of the yeast genome. Isogenic polyploids can be constructed from haploids and then stably maintained, greatly facilitating ploidy-based experimentation. A small number of ploidy-regulated genes was identified by comparing transcriptomes of isogenic yeast strains in a ploidy series using microarrays (Galitski et al., 1999). Differential regulation of these genes explains some phenotypes displayed by polyploids. However, the small set of ploidy-regulated genes did not reveal any mechanistic relationship between ploidy and gene expression.

This earlier work was technically hampered in two aspects: First, the transcriptomes were isolated from the Sigma 1278b yeast strain, of which the genome sequence was unknown. Hence,

microarrays designed for the S288c strain background was employed. The Sigma 1278b genome has now been sequenced and annotated, and comparative genomics reveals substantial differences in polymorphisms and genomic organizations between the two strain backgrounds (Dowell et al., 2010). The differences in genome sequences limited the power of detection by oligonucleotide hybridization in the earlier study. In addition, transcripts specific to the Sigma 1278b background would elude detection by the S288c-based microarray. Hence, genomic differences between the two strain backgrounds likely resulted in many false negatives. The second technical limitation was inherent to the use of microarrays. Undesirable cross-hybridization is always of concern, and the analog signal output diminishes the quantitation dynamic range. Shotgun transcriptome sequencing (RNA-seq) provides a more powerful profiling platform than the microarray with a greater dynamic range, higher detection sensitivity, and better differentiation between paralogous sequences (Mortazavi et al., 2008; Shendure, 2008). The available Sigma 1278b genome sequence and the advent of RNA-seq now provide the resolution necessary for the genome-wide determination of a functional connection among genes regulated by ploidy.

In this chapter, I present evidence for a size-sensing mechanism in yeast that alters gene expression. Ploidy-associated changes in gene expression thus reflect transcriptional adaptation to a larger cell size. Using RNA-seq, I identified genes differentially regulated in tetraploids when compared to haploids. Gene ontology (GO) analysis shows that ploidy-regulated genes are significantly enriched for those encoding cell surface components. I then found that haploid mutants with enlarged cell size, a prominent physical feature of polyploids, also show altered expression of ploidy regulated genes. These results indicate a causal, regulatory relationship between cell size and gene expression that has not been previously reported.

## **Results**

### **Identification of ploidy regulated genes**

Poly(A) RNA from 2 haploid and 2 tetraploid strains was extracted and processed for RNA-seq as previously described (Mortazavi et al., 2008) (figure 1a). Sequencing reads were mapped to the Sigma 1278b genome by my collaborator P. Alexander Rolfe in the Gifford group of Computer Science and Artificial Intelligence Laboratory. Approximately 9 million reads were reported for each sample, and more than 90% of reads mapped to the ORFs (table 1). A minimal expression threshold for transcripts was determined from read counts of genes known to be silenced under the growth condition, such as hypoxia response and sporulation. Overall, 5613 annotated transcripts were considered expressed in the experiment. The 5613 corresponding ORFs constituted the background gene list for GO term search. The comparison between haploid and tetraploid datasets shows that ploidy only affects the steady-state levels of a small number of transcripts (figure 1b), consistent with previous studies discussed in chapter 1.

Additional steps were taken to identify ploidy-regulated genes: (1) To enrich ploidy-regulated candidates, I eliminated genes whose expression was unaffected by ploidy ( $p > 0.001$ ) in each haploid-tetraploid sample pair. (2) After ranking candidate genes by fold-change in each sample pair, I retained the overlapping, top-ranking candidates from both pairs (figure 1c). Using these criteria, 35 ploidy-repressed genes and 30 ploidy-induced genes were identified (figures 2a-b). Ploidy-associated differential regulation of these genes in this study is largely in agreement with the previous study using the same Sigma 1278b ploidy series (Galitski et al., 1999). Another study comparing the transcriptomes of *MATa/α* and *MATaa/αα* strains in the S288c background found an entirely different and much smaller set of genes that were



differentially expressed in the tetraploid (Storchova et al., 2006). Differences in strain backgrounds and mating types could account for the discrepancy between studies.

### **Ploidy regulated genes show significant bias for encoding cell surface components**

The ploidy regulated genes are significantly enriched for those encoding proteins localized to the cell surface: cell wall, extracellular space and plasma membrane (table 2). Several other ploidy-regulated genes encode regulators of cell surface components (figures 2a-b). Hence, polyploidy preferentially alters expression of cell surface components. Ploidy-repressed genes encode multiple factors important for mating and filamentation/adhesion, while enzymes promoting cytokinesis on the cell surface are predominant among ploidy-induced genes (tables 3-6). The cell cycle does not appear to play a role in ploidy-regulation of these genes (table 7).

### **A hypothesis on cell size and gene expression**

The over-representation of genes encoding cell surface components could result from a geometric limitation: The surface area with respect to volume decreases as cells enlarge with increasing ploidy. For a spherical cell, a 4-fold increase in volume corresponds to only a ~2.5-fold increase in surface area. Reduction in surface area is likely to trigger differential regulation of components associated with the cell surface, where signaling and transport processes take place dynamically. Reduction in surface area could alter interactions between surface and cytoplasmic components in signaling pathways. It could also alter a cell's ability to transport metabolites across the plasma membrane. Both types of alteration could change gene expression in the enlarged cell, and genes could be up- or down-regulated as a result depending on the net effect of cell size on their regulatory pathways.

## Cell size affects expression of *FLO11* independently of ploidy

To test the hypothesis that enlarged cell size alters gene expression, I examined in haploid size mutants the expression level of *FLO11*, a strongly ploidy-repressed gene encoding a cell wall protein (Lambrechts et al., 1996; Lo and Dranginis, 1996). Since cell size expansion and cell cycle progression are intimately linked processes (Cook and Tyers, 2007; Jorgensen et al., 2002), I investigated whether *FLO11* is regulated by cell cycle before devising a method to manipulate cell size. In synchronized haploid cultures, *FLO11* transcript abundance peaks during M-phase (figure 3). I thus focused on expression of *FLO11* during M-phase in cell size mutants identified in a previous genome-wide study (Jorgensen et al., 2002): *bck2Δ*, *eap1Δ* and *cln3Δ*. These mutants were selected because they effectively enlarge cell size without significantly affecting fitness or cell shape (figure 4) and have no reported functional relationship with *FLO11* expression. I also performed experiments using an ATP analog-sensitive allele of *CDC28* (Bishop et al., 2000) that expands cell size upon inhibition by the analog (Goranov et al., 2009). Although this mutant showed an inverse correlation between *FLO11* expression and cell size that was consistent with my hypothesis, concerns about aberrant cell cycle progression and cell shape prompted me to forgo further experiments with this mutant (Materials and Methods).

Expression of *FLO11* is significantly reduced in the two mutants, *bck2Δ* and *eap1Δ*, that exhibit enlarged cell size (figures 5a & 5b), a trend that mimics the down-regulation of *FLO11* in tetraploids (figure 2a). These results suggest a ploidy-independent inverse correlation between *FLO11* expression and cell size. I employed two mutant alleles of the *CLN3* gene to create a size series. The *CLN3-2* haploid arrested as small cells (66% of WT) in nocodazole, whereas the *cln3Δ* haploid mutant arrested as large cells (185% of WT) (figure 5c). In this size series, there is again an inverse correlation between *FLO11* expression and cell size. The *FLO11* transcript

abundance is highest in the small *CLN3-2* haploid and lowest in the large *cln3Δ* haploid, the same relationship observed between *FLO11* expression and cell size in haploid versus tetraploid cells.

### **Reduced activity of *FLO11* promoter in both the *cln3Δ* haploid the WT tetraploid**

To verify further that regulation of *FLO11* is similar in the *cln3Δ* haploid and WT polyploids, I replaced the *FLO11* ORF with a reporter gene to study the effect of cell size on *FLO11* promoter activity. Transcriptional activation at *FLO11* is repressed in the *cln3Δ* mutant as in the WT tetraploid (figure 6). The result further suggests that at least one transcription factor regulating the *FLO11* promoter activity is sensitive to changes in cell size. In addition, the *cln3Δ* haploid could serve as a substitute for polyploids to facilitate the search for regulators sensing cell size and repressing *FLO11*.

### **Multiple ploidy-regulated genes are similarly regulated in the enlarged *cln3Δ* haploid**

To identify the spectrum of genes influenced by cell size, I used quantitative PCR to compare expression of ploidy-regulated genes in WT and the *cln3Δ* mutant haploid. Among the size mutants I examined, the *cln3Δ* haploid displays the most pronounced increase in cell size and arrests in M-phase with efficiency most similar to WT. The set of genes that show differential regulation due to cell size in the *cln3Δ* haploid (table 8) is very similar to those identified in the WT ploidy series (figure 2a-b). Thirty of the ploidy-regulated genes show the same regulatory trend in the *cln3Δ* haploid as was observed in tetraploids. Notably, the top-ranking genes that displayed the strongest ploidy-regulation in tetraploids (figures 2a-b) were significantly affected in the same direction in the *cln3Δ* haploid (table 8). This set of genes likely

represents those that respond most robustly to changes in cell size, since the *cln3Δ* haploid (185% of WT haploid in size) is still much smaller than the tetraploid (400% of WT haploid in size)(Di Talia et al., 2007).

### **Role of pheromone sensing and filamentation MAPK pathways in gene regulation by size**

Differential transcription revealed by RNA-seq gave important clues as to the pathways that could affect size regulation. The genes repressed by large cell size are enriched for those regulated by the pheromone response and filamentation mitogen-activated protein kinase (MAPK) pathways (table 4). Analysis of the promoter regions of size-repressed genes revealed a common binding motif for Dig1, a transcriptional repressor whose activity is repressed by the activated pheromone response or filamentation MAPK pathway (Cook et al., 1996; Tedford et al., 1997). The binding motif of Dig1 was detected ~9 fold more frequently in the promoters of size-regulated genes than the genome-wide average with a corresponding p-value of 4.28 e-9.

The over-representation of Dig1 binding motif suggests that disruption of the pathways that signal to this transcription factor or Dig1 itself should affect size regulation. The effect of such perturbations was examined in enlarged cells. Disruption of signaling in either the pheromone response or the filamentation MAPK pathway reduces the effect of cell size on *FLO11* expression (figure 7a-b). Moreover, loss of Dig1 function renders several size-repressed genes insensitive or much less responsive to the larger size (figure 7c). These results support our observation in WT tetraploid and *cln3Δ* haploid that reduced activities in pheromone response and filamentation pathways contribute to differential gene regulation in large cells.

## **Increasing ploidy raises basal cell wall stress**

The down-regulation of multiple genes involved in mating and filamentation pathways (table 4) prompted me to examine genes regulated by other mitogen-activated protein kinase (MAPK) pathways. In multiple ploidy series, the cell wall integrity (CWI) pathway appears consistently induced in polyploids (figure 8a), indicating a higher basal level of cell wall stress. Polyploidy may also induce the high osmolarity glycerol (HOG) pathway (figure 8b). The RNA-seq data are consistent with the notion that CWI pathway is more active in polyploids. Multiple genes downstream of CWI pathway appear to be similarly regulated in the WT polyploid and a haploid strain over-expressing a gain-of-function allele of *MKK1*, the MAPKK of CWI pathway (Jung and Levin, 1999) (table 9).

## Discussion

In this study, I identified transcripts whose relative level of expression in the transcriptome is altered in the polyploid yeast. Proteins encoded by these transcripts are predominantly cell surface components localized to the cell wall, plasma membrane and extracellular space. This localization bias led me to hypothesize an effect of cell size on expression of these genes. First, increasing ploidy enlarges cell size. Second, the relative surface area of a cell with respect to its volume decreases as the cell enlarges. For a spherical or ellipsoid entity, the volume increases proportionally to the cube of radius but the area only increases proportionally to the square of radius. The significantly larger polyploid therefore is challenged by an intrinsic geometric imbalance: reduced cell surface area per cell volume. This imbalance could alter signaling pathways that involve interactions between cell surface components and their cytoplasmic counterparts. The reduced surface area could also affect transport of molecules across the plasma membrane. Both perturbations could trigger changes in gene expression. To test my hypothesis, I changed cell size in haploids and examined expression of ploidy-regulated genes in them. The strongly ploidy-repressed gene *FLO11* is significantly repressed in enlarged haploids, consistent with the idea that increasing cell size down-regulates *FLO11*. I then found that the change in expression identified in a significant number of ploidy-regulated genes is paralleled in the enlarged *cln3Δ* haploid.

To illustrate further that cell size alters transcription via signaling pathways, I focused on the pheromone response and the filamentation MAPK pathways. Genes regulated by these pathways were preferentially down-regulated in large cells and composed the most significant category in Gene Ontology analysis. Genetic disruption in either one of the MAPKs as well as their common downstream transcriptional repressor Dig1 reduced the effect of cell size on target

gene expression. These results indicate that the pheromone sensing and filamentation MAPK cascades participate in downstream gene repression in the tetraploid and the *cln3Δ* haploid. Both the mating pheromone and the filamentation MAPKs are known to serve dual functions – as inhibitors of transcription in their kinase-inactive state and as activators of downstream transcription in their kinase-active state (Cook et al., 1997; Madhani et al., 1997). Hence, reduced activation of either kinase causes stronger inhibition, rather than a mere lack of activation, of downstream gene expression. In addition, transcriptional activators functioning downstream of both MAPK pathways perform complex positive auto- and cross-regulation (Borneman et al., 2006; Harbison et al., 2004; Kohler et al., 2002; Zeitlinger et al., 2003). The switch-like dual function of MAPKs and the positive feedback loops in these pathways likely exacerbate differences in pathway activity between the active state (in small cells) and the inactive state (in large cells). These attributes of the pathways may account for their pronounced transcriptional response to changes in cell size. Binding motif analysis did not reveal a common transcriptional regulator for genes up-regulated in large cells. Molecular pathways responsible for disproportionately higher expression of these genes will require more detailed computational and genetic examination.

The cause of a higher basal level of cell wall stress in polyploid yeast remains to be elucidated. Polyploids likely have a different cell wall composition because multiple genes encoding cell wall components are strongly differentially regulated (figure 2). Polyploids must also expand the cell wall at a much faster rate in order to reach a larger cell size without increasing the doubling time (Di Talia et al., 2007, figures 2 & 3 in Appendix). The combination of an altered cell wall composition and a faster cell wall expansion rate could generate a higher basal level of stress.

I examined the activity of CWI pathway in *cln3Δ* haploid and did not observe a difference when compared with WT haploid (data not shown). Two factors might explain why the CWI pathway is not more active in the *cln3Δ* haploid. First, the *cln3Δ* haploid mutant is similar to the WT diploid in size, about 2-fold larger than WT haploid. As seen in figure 6a, reporter genes of the CWI pathway are significantly induced in tetraploids but not in diploids. It is possible that a 2-fold increase in cell size is not sufficient to elevate cell wall stress. Second, the WT and *cln3Δ* haploids were treated with nocodazole for cell cycle arrest, whereas cells of the WT ploidy series were cultured without cell cycle inhibitors. The difference in growth conditions could influence the response of CWI pathway to cell size. Regardless of the underlying reason, results in the *cln3Δ* mutant indicate that induction of CWI pathway is not necessary for differential expression of the size-regulated genes in enlarged cells. Hence, elevated cell wall stress in polyploids likely occurs independently of, or as a result of, differential regulation of the set of genes identified in this study.

Collectively my data show a causal relationship between cell size and gene regulation, suggesting the existence of a size-sensing mechanism that can alter transcription. Also considered was an alternative model, in which polyploidy and the aforementioned mutations change transcription of size-regulated genes, whose altered expression then enlarges cell size. I found this model to be improbable on two bases. First, a previous genome-wide screen for size mutants in yeast identified a large set of genes distinct from the set of size-regulated genes in this study (Jorgensen et al., 2002). Second, the WT polyploid and the haploid size mutants are physiologically discrete in growth, and they likely achieve the enlarged size via different modes (Cook and Tyers, 2007; Di Talia et al., 2007). Polyploids seem to achieve a larger size by



increasing growth rate. Mutants of cell cycle regulation such as *cln3Δ* and *bck2Δ* are thought to enlarge size by delaying the onset of START.

Control of gene expression by cell size may occur in a wide range of organisms and could partake in higher level physiological consequences of polyploidy such as differentiation and tumorigenesis. In fungi and mammals, cell size thresholds are actively maintained by regulated growth rates and cell division frequencies (Cook and Tyers, 2007; Tzur et al., 2009). The regulatory relationship between cell size and gene expression uncovered here suggests that the uniformity of cell size in unicellular organisms and within a tissue in multi-cellular organisms could be necessary to maintain the homeostasis of transcription.

## **Materials and Methods**

### **Yeast strains and growth conditions**

Strains are listed at the end of this section. Prior to analysis, cultures were inoculated from diluted overnight pre-cultures and grown until mid-log phase in the SC medium supplemented with 2% glucose on a rotary shaker at 30°C. Synchronization of the mitotic cell cycle with  $\alpha$ -factor was performed as described in (Amon, 2002).

### **Technical observations and concerns about the *cdc28-as1* allele:**

I treated a mid-log culture of asynchronously grown *cdc28-as1* mutant with 50 $\mu$ M of the 1-NM-PP1(**9**) inhibitor (Bishop et al., 2000) and split the culture four ways: (1) no additional drug treatment (2) 0.1% azide (3) 10 $\mu$ M rapamycin (4) 100 $\mu$ g/mL cycloheximide. The PP1 treatment was intended to inhibit cell cycle progression while permitting cell growth, thereby enabling cells to enlarge. Azide, rapamycin and cycloheximide were used to inhibit cell growth in addition to PP1 treatment. Samples were taken hourly in a 4-hour time course to track *FLO11* expression and cell size. Over time, cells treated with PP1 alone had significantly enlarged cell size and reduced *FLO11* expression compared to cells treated with additional growth inhibitors. However, I also found increasing expression of *CLN1* concurrent with the decreasing *FLO11* expression in the PP1 treated cells. Since expression of *FLO11* is repressed in the G1-stage of the cell cycle, I reasoned that the G1-like state in PP1 treated cells might repress *FLO11* independently of cell size.

I considered using PP1 at a lower concentration (500nM) to arrest cells in G2/M in the aforementioned experiment to avoid complications associated with G1. However, cells became

hyperpolarized and thus had a fundamentally different morphology, as shown in the original article (Bishop et al., 2000). Since the effect of cell shape on *FLO11* expression is also unclear, I would not be able to draw informative conclusions from this experiment.

I also considered releasing  $\alpha$ -factor (G1) synchronized cells into PP1 to enlarge cell size, followed by washing away PP1 after different amounts of incubation time to obtain cells of varying sizes in M-phase. However, I was not able to wash off PP1 efficiently (on a filter disk with 25x volumes of medium), presumably due to the extraordinarily high affinity of PP1 for the Cdc28-as1 enzyme (Bishop et al., 2000). As a result, the washed cells became hyperpolarized as described above.

The intrinsic temperature sensitivity of the Sigma 1278b strain background was also of technical concern. For this reason, I did not use temperature sensitive mutant alleles of cell cycle regulators to enlarge cell size as described (Goranov et al., 2009).

### **Construction of cDNA libraries and deep sequencing**

Total RNA was extracted from yeast cultures in mid-log phase with acid phenol. Enriched poly(A) RNA (Qiagen Oligotex mRNA kit) was processed for cDNA library construction and sequencing as described in (Mortazavi et al., 2008). The libraries were sequenced for 36 cycles on Illumina Genome Analyzer 2 using the standard protocol.

The RNA-seq data have been deposited in NCBI's Gene Expression Omnibus and are accessible through GEO Series accession number GSE19685.

## **Mapping algorithm for RNA-seq reads**

Reads were mapped to the Sigma1278b genome using the Bowtie alignment software (version 0.10.0; <http://bowtie-bio.sourceforge.net/index.shtml>). Reads were mapped multiply (bowtie --solexa-quals -k 100 -m 100 --best --strata -p 2 --strandfix). A read that mapped to  $n$  genomic locations was assigned a weight of  $1/n$  and the "number of reads" mapping to a repetitive element was the sum of the weights of the hits in that element.

## **Calling differentially expressed genes in the RNA-seq data**

Reads were stored in David K. Gifford group's in-house ChIP/RNA-seq database and analyzed with the code in DifferentialExpression.java. To find differentially expressed genes, the following procedure was performed on each annotated ORF in the Sigma 1278b genome:

- Determine the total number of uniquely mapped reads in the haploid and tetraploid experiments.
- Count, for the haploid and tetraploid experiments, the number of uniquely mapped reads on both strands in the ORF.
- Compute  $\text{frequency\_haploid} = (\text{haploid count for gene}) / (\text{total haploid count})$  and similarly for the tetraploid.
- Compute  $1 - \text{CDF}$  of observing the number of reads in the haploid sample using a binomial distribution given the frequency in the tetraploid sample and the total number of haploid reads. This is the p-value for the haploid observation given the tetraploid observation.
- Compute the p-value for the tetraploid observation given the haploid observation.
- Retain genes with a p-value less than some threshold (eg  $p < 0.001$ ) and to which at least 15 reads mapped. These genes are considered differentially expressed.

## **Identification of ploidy-regulated genes from the RNA-seq data**

Based on read counts of known silenced genes (hypoxia response and sporulation specific), a threshold of 15 was set as the minimal expressed level. In total, 5613 genes were considered expressed and constituted the “background gene list” for subsequent Gene Ontology analysis. The list of differentially expressed genes with read counts > 15 provided the set of ploidy-regulated candidates.

The ploidy-regulated candidates were sorted by fold change (normalized by total number of reads in each experiment). The top-ranking genes in common between the two replicates were identified as ploidy-regulated. The number of top-ranking candidates from each replicate was selected to obtain a sufficient number of genes for GO analysis while ensuring the overlap between replicates was highly statistically significant ( $p < e-10$ ) by hypergeometric test in MatLab.

## **Binding motif analysis for ploidy-regulated genes**

Using the Sigma1278b ORF annotations, we determined an upstream intergenic region for each ORF. We limited each region to at most 5kb and limited each region such that it did not overlap any other ORF (thus producing empty promoter regions in the case of some overlapping ORF annotations). Using our in-house database of DNA sequence motifs (taken from Transfac, MacIsaac06, JASPAR, and several other sources), we searched for each motif in the promoters of ploidy-induced genes, the promoters of ploidy-repressed genes, and the promoters of all genes. We counted a motif as present in a promoter region if the occurrence of the match was at least 70% of the maximum possible score. We retained motifs that were enriched in the ploidy-induced or -repressed set compared to all genes according to a binomial test with a p-value less

than .001. We expected .882 false positives at this p-value given the 882 motifs in our database.

### **Growth condition for haploid size variants**

Cultures in YPD + 1% DMSO were inoculated at low density from over-night pre-cultures and incubated at 30 degrees on a shaker for aeration. Cultures in exponential phase were diluted to ~0.15 O.D.<sub>600</sub> in pre-warmed fresh medium and incubated for another 30 min. Nocodazole was then added to a final concentration of 15 µg/mL (Day et al., 2004) to arrest cell cycle for 3 hours. Cells were collected by centrifugation for RNA extraction and microscopy.

### **Gene-specific quantification of expression levels**

Total RNA extracted from yeast was processed for cDNA synthesis using QuantiTect Reverse Transcription Kit (Qiagen). Expression levels were measured on Applied Biosystems 7500 Real-Time PCR System with SYBR Green in Absolute Quantification mode following manufacture's procedure. Unless specified, I used the abundance of *ACT1* transcript to normalize the expression levels of other genes. The representation of *ACT1* transcript in the transcriptome is found to be consistent in all strains used in this study (data not shown and Galitski et al., 1999).

### **Measurement of cell size**

Cells were fixed in 3.7% formaldehyde at 4°C overnight and digested with a mixture of zymolyase and glucanase at 30°C in the presence of 1.2M sorbitol citrate to relieve aggregation. Microscopy images of more than 50 large-budded cells per strain were analyzed using ImageJ.

Cell size was calculated from measured width and length of both mother and bud, assuming rotational symmetry about the long axis.

## Yeast strains used in this study

All strains are in the Sigma 1278b background with the genotype *ura3-52, leu2::hisG his3::hisG* unless noted otherwise.

<u>Strain ID</u>	<u>Genotype or Description</u>	<u>Reference/Source</u>
Haploid and tetraploid used for RNA-seq:		
L6437	<i>MATa</i>	Galitski et al. Science, 1999
L6440	4n, isogenic to L6437	"
Haploid size variants:		
L7613	<i>MATa, CLN3, leu2::hisG::LEU2</i>	Andalis et al. Genetics, 2004
L7641	<i>MATa, cln3Δ::LEU2</i>	"
L7646	<i>MATa, CLN3-2</i>	Gerald Fink lab
L7609	<i>MATa, cln3Δ::LEU2</i>	"
L7618	<i>MATa, CLN3, leu2::hisG::LEU2</i>	"
	<i>MATa, bck2::kanMX</i>	Charles Boone lab
	<i>MATa, eap1::kanMX</i>	"
	<i>MATa</i> , isogenic WT strain	"
yCW151	<i>MATa, flo11Δ::yEGFP-URA3</i>	Gerald Fink lab
yCW175	isogenic <i>MATaaaa</i>	
yCW755	<i>MATa, flo11Δ::yEGFP-URA3, cln3Δ::LEU2, trp1::hisG</i>	this study
yCW754	isogenic to yCW755 but <i>CLN3</i>	this study
yCW763	<i>MATa dig1Δ::kanMX</i>	this study
yCW764	<i>MATa dig1Δ::kanMX, cln3Δ::LEU2</i>	this study
L7320	<i>MATa fus3Δ::LEU2, HIS3</i> , cured of <i>URA3</i> plasmid	Gerald Fink lab
yCW318	<i>MATaa</i> isogenic to L7320	this study
L6237	<i>MATa kss1Δ::ura3::LEU2, ste7Δ::HIS3, trp1::hisG</i> , cured of plasmid	Gerald Fink lab
yCW582	<i>MATaa</i> isogenic to L6237	this study



## **References**

- Amon, A. (2002). Synchronization procedures. *Methods Enzymol* 351, 457-467.
- Andalis, A.A., Storchova, Z., Styles, C., Galitski, T., Pellman, D., and Fink, G.R. (2004). Defects arising from whole-genome duplications in *Saccharomyces cerevisiae*. *Genetics* 167, 1109-1121.
- Bishop, A.C., Ubersax, J.A., Petsch, D.T., Matheos, D.P., Gray, N.S., Blethrow, J., Shimizu, E., Tsien, J.Z., Schultz, P.G., Rose, M.D., *et al.* (2000). A chemical switch for inhibitor-sensitive alleles of any protein kinase. *Nature* 407, 395-401.
- Borneman, A.R., Leigh-Bell, J.A., Yu, H., Bertone, P., Gerstein, M., and Snyder, M. (2006). Target hub proteins serve as master regulators of development in yeast. *Genes Dev* 20, 435-448.
- Chial, H.J., Stemm-Wolf, A.J., McBratney, S., and Winey, M. (2000). Yeast Eap1p, an eIF4E-associated protein, has a separate function involving genetic stability. *Curr Biol* 10, 1519-1522.
- Cook, J.G., Bardwell, L., Kron, S.J., and Thorner, J. (1996). Two novel targets of the MAP kinase Kss1 are negative regulators of invasive growth in the yeast *Saccharomyces cerevisiae*. *Genes Dev* 10, 2831-2848.
- Cook, J.G., Bardwell, L., and Thorner, J. (1997). Inhibitory and activating functions for MAPK Kss1 in the *S. cerevisiae* filamentous-growth signalling pathway. *Nature* 390, 85-88.
- Cook, M., and Tyers, M. (2007). Size control goes global. *Curr Opin Biotechnol* 18, 341-350.
- Cosentino, G.P., Schmelzle, T., Haghighat, A., Helliwell, S.B., Hall, M.N., and Sonenberg, N. (2000). Eap1p, a novel eukaryotic translation initiation factor 4E-associated protein in *Saccharomyces cerevisiae*. *Mol Cell Biol* 20, 4604-4613.
- Day, A., Schneider, C., and Schneider, B.L. (2004). Yeast cell synchronization. *Methods Mol Biol* 241, 55-76.
- Di Talia, S., Skotheim, J.M., Bean, J.M., Siggia, E.D., and Cross, F.R. (2007). The effects of molecular noise and size control on variability in the budding yeast cell cycle. *Nature* 448, 947-951.
- Dowell, R.D., Ryan, O., Jansen, A., Cheung, D., Agarwala, S., Danford, T., Bernstein, D.A., Rolfe, A., Chin, B., Fink, G.R., *et al.* (2010). Genotype to Phenotype: Comparison of Two Interbreeding Yeast Strains Reveals Complex Genetics of Conditional Essential Genes. *Science*, In press.
- Epstein, C.B., and Cross, F.R. (1994). Genes that can bypass the CLN requirement for *Saccharomyces cerevisiae* cell cycle START. *Mol Cell Biol* 14, 2041-2047.

Galitski, T., Saldanha, A.J., Styles, C.A., Lander, E.S., and Fink, G.R. (1999). Ploidy regulation of gene expression. *Science* 285, 251-254.

Ganem, N.J., Storchova, Z., and Pellman, D. (2007). Tetraploidy, aneuploidy and cancer. *Curr Opin Genet Dev* 17, 157-162.

Goranov, A.I., Cook, M., Ricicova, M., Ben-Ari, G., Gonzalez, C., Hansen, C., Tyers, M., and Amon, A. (2009). The rate of cell growth is governed by cell cycle stage. *Genes Dev* 23, 1408-1422.

Harbison, C.T., Gordon, D.B., Lee, T.I., Rinaldi, N.J., Macisaac, K.D., Danford, T.W., Hannett, N.M., Tagne, J.B., Reynolds, D.B., Yoo, J., *et al.* (2004). Transcriptional regulatory code of a eukaryotic genome. *Nature* 431, 99-104.

Jorgensen, P., Nishikawa, J.L., Breikretz, B.J., and Tyers, M. (2002). Systematic identification of pathways that couple cell growth and division in yeast. *Science* 297, 395-400.

Jung, U.S., and Levin, D.E. (1999). Genome-wide analysis of gene expression regulated by the yeast cell wall integrity signalling pathway. *Mol Microbiol* 34, 1049-1057.

Kasahara, M. (2007). The 2R hypothesis: an update. *Curr Opin Immunol* 19, 547-552.

Kohler, T., Wesche, S., Taheri, N., Braus, G.H., and Mosch, H.U. (2002). Dual role of the *Saccharomyces cerevisiae* TEA/ATTS family transcription factor Tec1p in regulation of gene expression and cellular development. *Eukaryot Cell* 1, 673-686.

Lambrechts, M.G., Bauer, F.F., Marmur, J., and Pretorius, I.S. (1996). Muc1, a mucin-like protein that is regulated by Mss10, is critical for pseudohyphal differentiation in yeast. *Proc Natl Acad Sci U S A* 93, 8419-8424.

Lee, H.O., Davidson, J.M., and Duronio, R.J. (2009). Endoreplication: polyploidy with purpose. *Genes Dev* 23, 2461-2477.

Lo, W.S., and Dranginis, A.M. (1996). FLO11, a yeast gene related to the STA genes, encodes a novel cell surface flocculin. *J Bacteriol* 178, 7144-7151.

Madhani, H.D., Styles, C.A., and Fink, G.R. (1997). MAP kinases with distinct inhibitory functions impart signaling specificity during yeast differentiation. *Cell* 91, 673-684.

Mortazavi, A., Williams, B.A., McCue, K., Schaeffer, L., and Wold, B. (2008). Mapping and quantifying mammalian transcriptomes by RNA-Seq. *Nat Methods* 5, 621-628.

Roberts, C.J., Nelson, B., Marton, M.J., Stoughton, R., Meyer, M.R., Bennett, H.A., He, Y.D., Dai, H., Walker, W.L., Hughes, T.R., *et al.* (2000). Signaling and circuitry of multiple MAPK pathways revealed by a matrix of global gene expression profiles. *Science* 287, 873-880.

Semon, M., and Wolfe, K.H. (2007). Consequences of genome duplication. *Curr Opin Genet Dev* 17, 505-512.

Shendure, J. (2008). The beginning of the end for microarrays? *Nat Methods* 5, 585-587.

Spellman, P.T., Sherlock, G., Zhang, M.Q., Iyer, V.R., Anders, K., Eisen, M.B., Brown, P.O., Botstein, D., and Futcher, B. (1998). Comprehensive identification of cell cycle-regulated genes of the yeast *Saccharomyces cerevisiae* by microarray hybridization. *Mol Biol Cell* 9, 3273-3297.

Storchova, Z., Breneman, A., Cande, J., Dunn, J., Burbank, K., O'Toole, E., and Pellman, D. (2006). Genome-wide genetic analysis of polyploidy in yeast. *Nature* 443, 541-547.

Tedford, K., Kim, S., Sa, D., Stevens, K., and Tyers, M. (1997). Regulation of the mating pheromone and invasive growth responses in yeast by two MAP kinase substrates. *Curr Biol* 7, 228-238.

Tzur, A., Kafri, R., LeBleu, V.S., Lahav, G., and Kirschner, M.W. (2009). Cell growth and size homeostasis in proliferating animal cells. *Science* 325, 167-171.

Zeitlinger, J., Simon, I., Harbison, C.T., Hannett, N.M., Volkert, T.L., Fink, G.R., and Young, R.A. (2003). Program-specific distribution of a transcription factor dependent on partner transcription factor and MAPK signaling. *Cell* 113, 395-404.

**Figures**

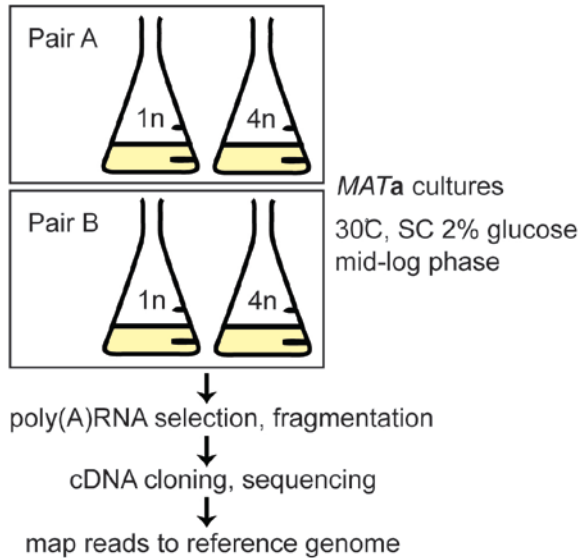


**Figure 1a.** Analysis of the haploid and tetraploid transcriptomes by RNA-seq. Two pairs of haploid and tetraploid cultures, A and B, were harvested for poly(A) RNA isolation. cDNA libraries were constructed and sequenced on the Illumina platform. Reads were mapped to the annotated Sigma 1278b genome. Expression of an ORF was calculated from the number of reads mapping inside the ORF.

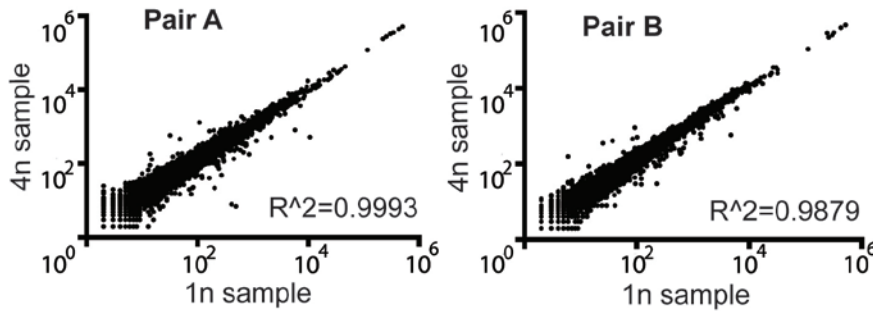
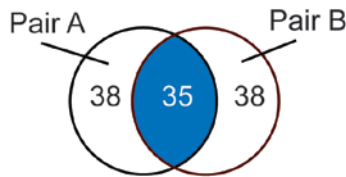


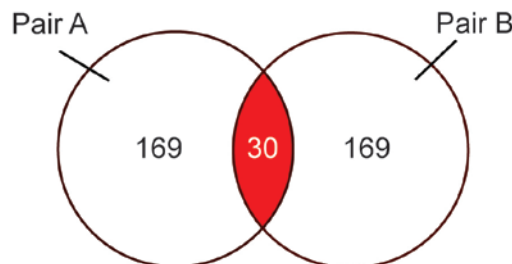
**Figure 1b.** Ploidy alters expression of only a small number of genes. Read counts for each expressed transcript at the two ploidy states are plotted. Statistical treatment with linear regression was performed using all data points.

Ploidy-repressed genes:



significance of overlap:  $p \ll e-10$

Ploidy-induced genes:



significance of overlap:  $p < e-10$

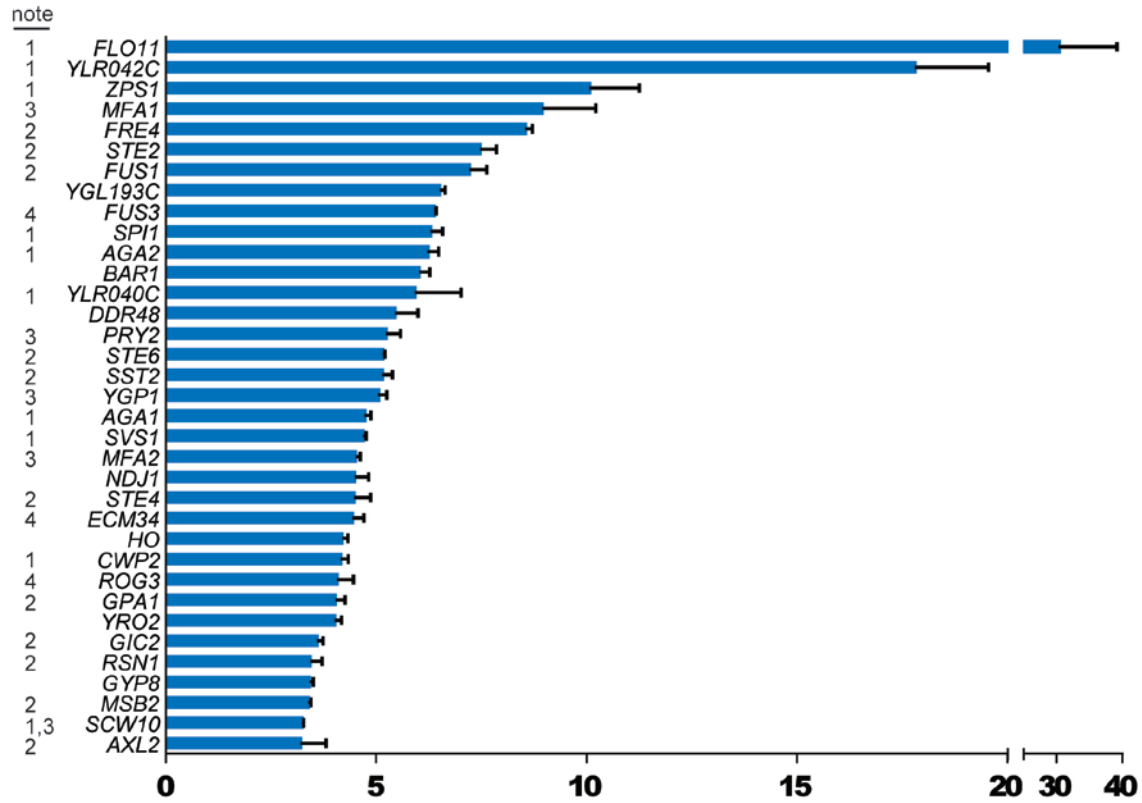
**Figure 1c.** Strategy to identify ploidy-regulated genes. Within each pair of 1n-4n RNA-seq datasets, ploidy-regulated candidate genes

were enriched and ranked by fold-change in expression. As shown in the Venn diagrams, top-ranking candidates from both pairs of datasets were compared, and the overlapping candidates

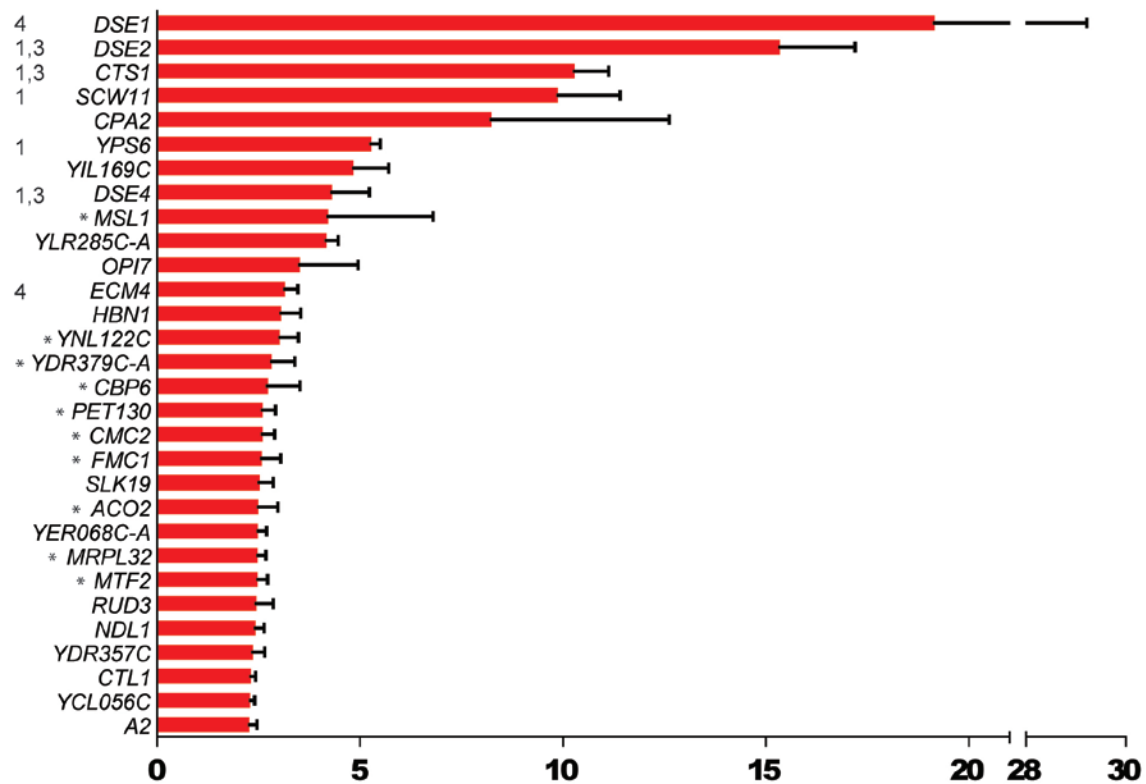
were identified as ploidy-regulated. Cut-offs for top-ranking candidates were selected to obtain a sufficient set of overlapping genes for GO analysis while ensuring that the overlap remained highly statistically significant ( $p < e^{-10}$ ) by hypergeometric test.

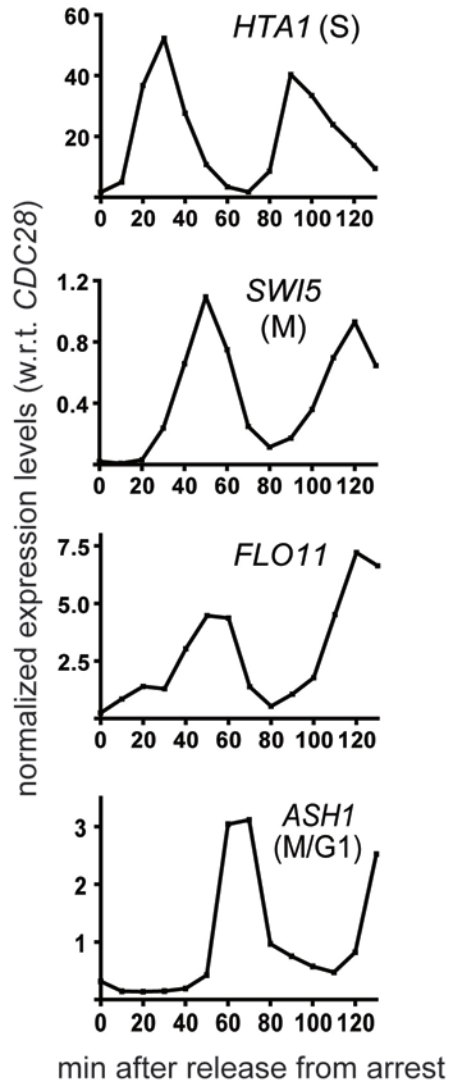
**Figures 2a & 2b (next page).** Ploidy-regulated genes ranked by the average fold-change in expression from both pairs of RNA-seq datasets. (a) Ploidy-repressed genes. (b) Ploidy-induced genes. Error bar represents standard deviation. Characterized genes are shown with their standard names in the *Saccharomyces* Genome Database (SGD). These results are largely in agreement with data from the previous study (Galitski et al., 1999). Notes on localization of encoded protein based on SGD: **1**: cell wall. **2**. plasma membrane. **3**. extra-cellular space. **4**. regulator of cell surface components with intracellular or unknown localization. Asterisk: mitochondrial localization. This category is not statistically significant in our GO analysis but nevertheless represents a third of ploidy-induced genes.

**Figure 2a:** Ploidy-repressed genes.



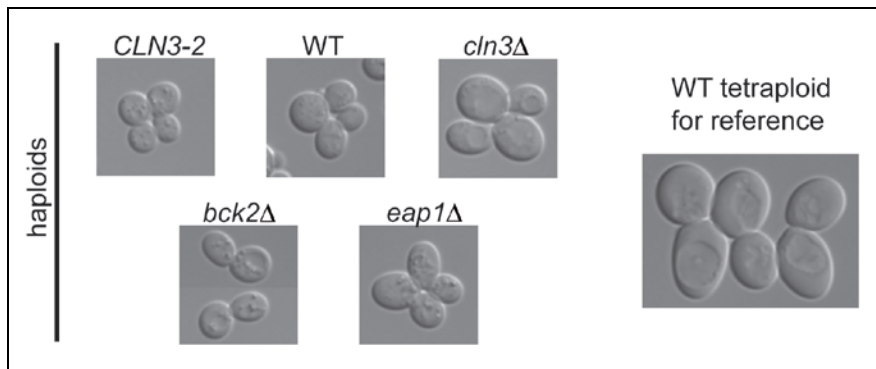
**Figure 2b:** Ploidy-induced genes.





**Figure 3.** *FLO11* transcript abundance peaks in M-phase during the mitotic cell cycle. Upon release from alpha-factor arrest in G1, WT haploid cells were harvested at 10-min intervals. Cell cycle stages were assessed using expression profiles of known standard transcripts: *SWI5*(M-phase), *ASH1*(M/G1 transition) and *HTA1*(S-phase) (Spellman et al., 1998). The expression pattern of *FLO11* resembles that of *SWI5*.

**Figure 4.** Live cell images of WT and size mutant haploids.



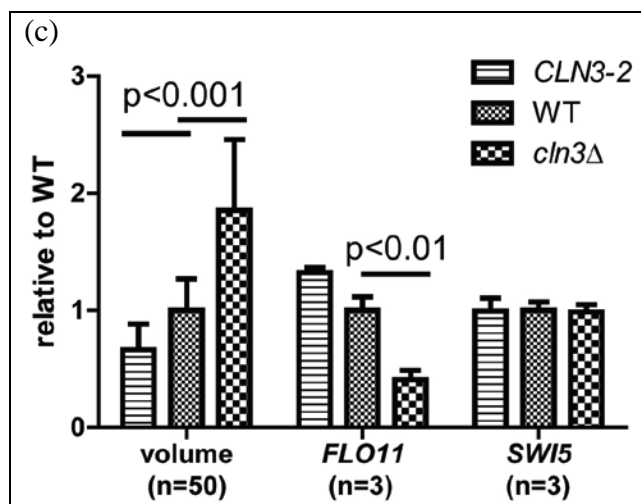
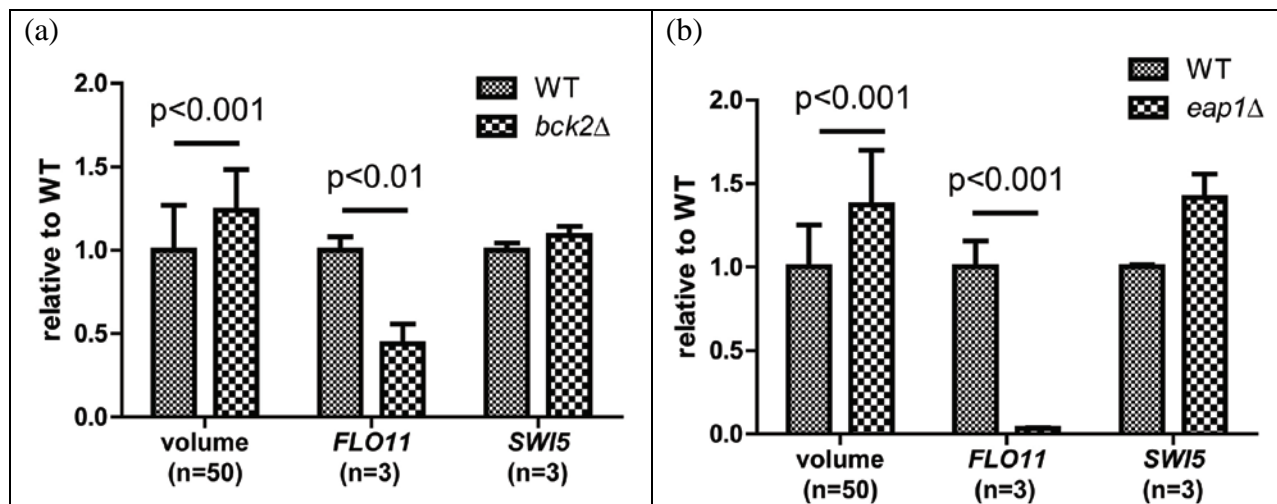


**Figure 5.** Abundance of the *FLO11* transcript inversely correlates with cell size in haploids. (a) WT and *bck2Δ*. (b) WT and *eap1Δ*. (c) *CLN3*-based size series. Bck2 promotes the G1-S transition independently of Cln3 (Epstein and Cross, 1994). Eap1 regulates translation by binding the eukaryotic translation initiation factor 4E (Cosentino et al., 2000) and has a separate role in chromosome segregation (Chial et al., 2000). Cln3 is the most upstream activator of G1-S transition and maintains the size threshold of mitotic START (Cook and Tyers, 2007). Cell volume was measured from microscopy

images. Gene expression was measured by quantitative PCR. Expression of *SWI5* was monitored to rule out the effect of cell cycle in data interpretation. Enrichment of M-phase cells was also monitored by percentage of large budded cells with DAPI-stained nuclei at the mother-bud junction. Error bar = standard deviation. Statistical significance was calculated using Student's t-test (unpaired, for two-tail p value).

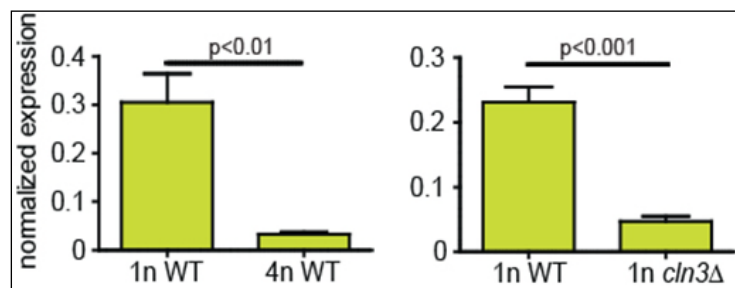
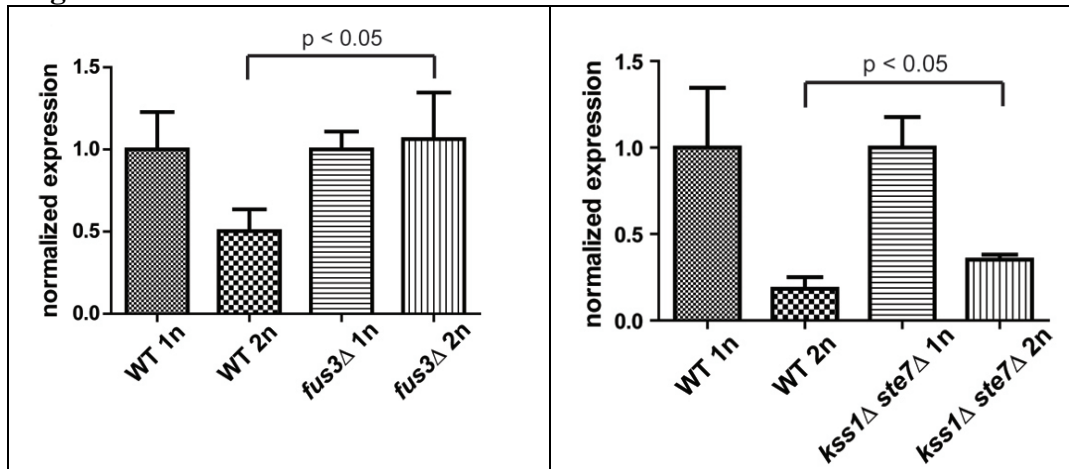


**Figure 6.** Promoter activity of *FLO11* is reduced in WT tetraploid and *cln3Δ* haploid. Reporter gene = GFP. Haploid and tetraploid WT strains were grown in SC with 2% glucose. WT and *cln3Δ* haploids were grown in YPD + nocodazole as described in methods section. Comparable *SWI5*

expression levels in WT and *cln3Δ* haploids were verified to ensure equal enrichment of cells in M-phase (data not shown).

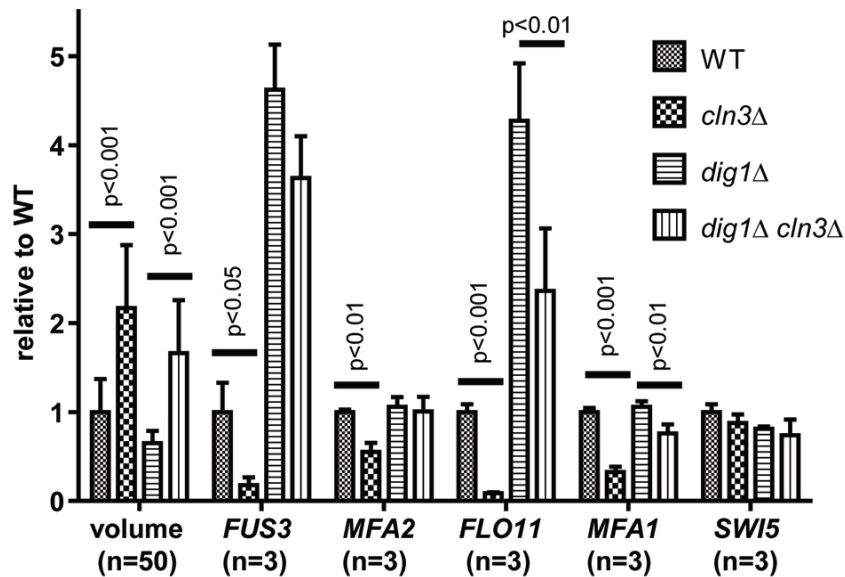


**Figure 7a-b.**



(a) Repression of *FLO11* in large cells involves the pheromone response MAPK Fus3. Expression levels of *FLO11* in *MAT $\alpha$*  diploids, which are twice larger in size than haploids, are normalized to the expression levels in corresponding isogenic *MAT $\alpha$*  haploids.  $n=3$ , error bar=standard deviation. (b) The filamentation MAPK cascade contributes to differential regulation of *FLO11* in large cells. Instead of the *kss1* $\Delta$  single mutant, the *kss1* $\Delta$  *ste7* $\Delta$  double mutant was employed since it is capable of agar adhesion as a haploid and pseudohyphal growth as a *MAT $\alpha$* /alpha diploid (Cook et al., 1997), suggesting that this mutant expresses a moderate level of *FLO11* transcript.

**Figure 7c.**



(c) The transcription factor Dig1 is involved in size-dependent gene regulation. Several size-repressed genes are significantly de-repressed in the *dig1* $\Delta$  *cln3* $\Delta$  haploid mutant as compared with the *dig1* $\Delta$  mutant.

**Figure 8a.**

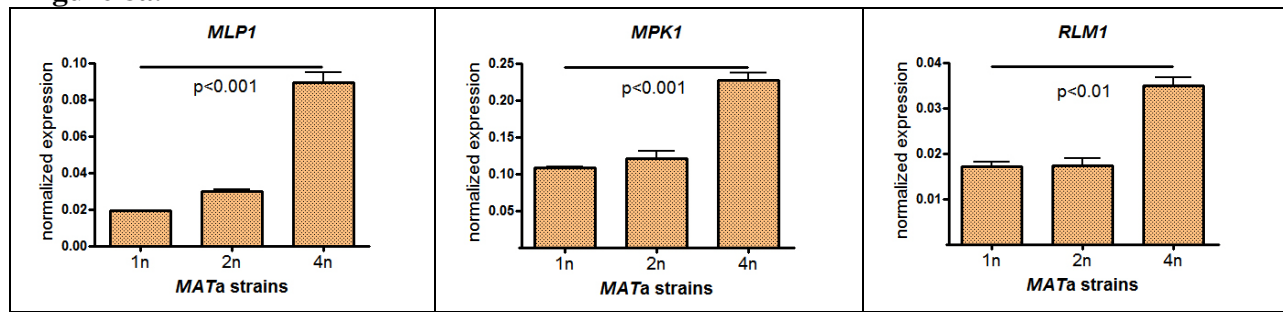
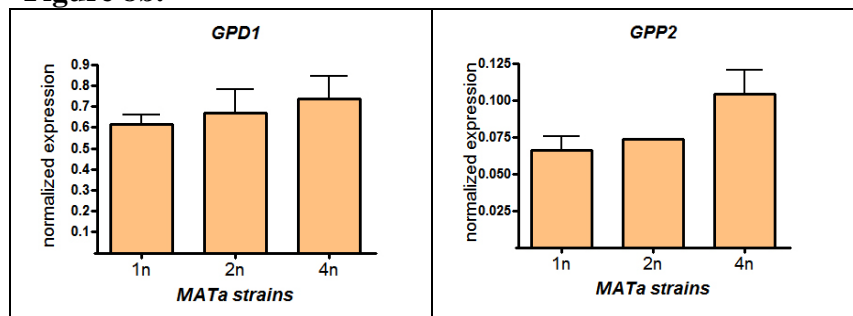


**Figure 8b.**



**Figures 8a & 8b.** Activities of the CWI and HOG MAPK pathways in WT *MATa* ploidy series. (a) Reporters of CWI pathway. (b) Reporters of HOG pathway. Expression of reporter genes of each pathway (Roberts et al., 2000) was measured by quantitative PCR.  $n=3$ . Error bar = standard deviation. p-values were calculated with Student's t-test by comparing the expression levels in haploids and the isogenic tetraploids.

## Tables

Sample		Read counts in millions		
		Total	ORF	Other
Pair A	1n	8.70	6.26	1.92
	4n	9.60	6.81	2.22
Pair B	1n	9.02	5.88	2.62
	4n	9.10	6.40	2.15

**Table 1.** RNA-seq read counts. More than 90% of the ~9 million reads in each sample were mapped to the genome. More than 60% of the mapped reads fell within annotated ORFs. The majority of remaining reads mapped to rDNA locus and Ty elements.

GO term	Cluster freq.	Background freq.	p-value
Cell wall	15/65, 23.1%	85/5613, 1.5%	1.5 e-14
Extracellular	8/65, 12.3%	22/5613, 3.9%	5.8 e-11
Plasma membrane	11/65, 16.9%	254/5613, 4.5%	1.1 e-4

**Table 2.** Cellular compartmental GO terms for ploidy-regulated genes.

GO term	Cluster frequency	Background frequency	P-value	Genes
Cell wall	10/35, 28.6%	80/5613, 1.4%	2.7 e-11	<i>AGA1, AGA2, ZPS1, SPI1, SVS1, YGP1, CWP2, SCW10, YLR040C, FLO11</i>
Plasma membrane	11/35, 31.4%	251/5613, 4.5%	1.9 e-7	<i>FRE4, STE2, FUS1, STE6, SST2, STE4, GPA1, GIC2, MSB2, AXL2, RSN1</i>

**Table 3.** Cellular compartmental GO terms for ploidy-repressed genes.

GO term	Cluster frequency	Background frequency	P-value	Genes
Mating & adhesion	13/35, 37.1%	123/5613, 2.2%	1.4 e-13	<i>FLO11, MFA1, MFA2, STE2, STE4, FUS1, FUS3, AGA1, AGA2, BAR1, SST2, GPA1, SCW10</i>
Cell surface receptor linked signal transduction	7/35, 20%	50/5613, 0.9%	1.6 e-8	<i>MFA1, MFA2, STE2, STE4, FUS3, GPA1, MSB2</i>

**Table 4.** Biological process GO terms for ploidy-repressed genes. A significant number of ploidy-repressed genes participate in the processes of mating, filamentation/adhesion and cell surface related signaling.

GO term	Cluster frequency	Background frequency	P-value	Genes
Receptor binding	2/35, 5.7%	2/5613, 0.03%	3.8 e-5	<i>MFA1, MFA2</i>
Cell adhesion molecule binding	2/35, 5.7%	3/5613, 0.1%	1.1 e-4	<i>AGA1, AGA2</i>
Signal transducer	4/35, 11.4%	42/5613, 0.7%	1.2 e-4	<i>FUS3, MSB2, STE2, STE4</i>

**Table 5.** GO terms of molecular functions for ploidy-repressed genes.

GO term	Cluster frequency	Background frequency	P-value	Genes
Cytokinesis (process)	5/30, 16.7%	11/5613, 0.2%	1.4 e-9	<i>DSE1, DSE2, DSE4, CTS1, SCW11</i>
Hydrolase (function)	4/30, 13.3%	30/5613, 0.5%	1.7 e-5	<i>DSE2, DSE4, CTS1, SCW11</i>
Cell wall (compartment)	5/30, 16.7%	80/5613, 1.4%	5.6 e-5	<i>DSE2, DSE4, CTS1, SCW11, YPS6</i>

**Table 6.** GO terms for ploidy-induced genes.

Ploidy-repressed genes			Ploidy-induced genes		
ORF	Symbol	Peak expression	ORF	Symbol	Peak expression
YIR019C	FLO11	M	YER124C	DSE1	G1
YLR042C		(no effect)	YHR143W	DSE2	G1
YOL154W	ZPS1	*	YLR286C	CTS1	G1
YDR461W	MFA1	G1	YGL028C	SCW11	G1
YNR060W	FRE4	*	YJR109C	CPA2	*
YFL026W	STE2	M	YIR039C	YPS6	*
YCL027W	FUS1	M/G1	YIL169C	YIL169C	*
YGL193C		*	YNR067C	DSE4	M/G1
YBL016W	FUS3	*	YIR009W	MSL1	*
YER150W	SPI1	M/G1	YLR285C-A		no data
YGL032C	AGA2	M/G1	YDR360W	OPI7	(no effect)
YIL015W	BAR1	*	YKR076W	ECM4	*
YLR040C		M/G1	YCL026C-B	HBN1	no data
YMR173W	DDR48	*	YNL122C		*
YKR013W	PRY2	G1	YDR379C-A		no data
YKL209C	STE6	M	YBR120C	CBP6	*
YLR452C	SST2	M/G1	YJL023C	PET130	*
YNL160W	YGP1	M/G1	YBL059C-A	CMC2	no data
YNR044W	AGA1	M/G1	YIL098C	FMC1	*
YPL163C	SVS1	G1	YOR195W	SLK19	G1
YNL145W	MFA2	M	YJL200C	ACO2	*
YOL104C	NDJ1	*	YER068C-A		no data
YOR212W	STE4	*	YCR003W	MRPL32	*
YHL043W	ECM34	*	YDL044C	MTF2	*
YDL227C	HO	G1	YOR216C	RUD3	*
YKL096W-A	CWP2	G2	YLR254C	NDL1	G2/M
YFR022W	ROG3	*	YDR357C		*
YHR005C	GPA1	M/G1	YMR180C	CTL1	*
YBR054W	YRO2	M	YCL056C	YCL056C	*
YDR309C	GIC2	G1	YCR096C	A2	*
YMR266W	RSN1	*			
YFL027C	GYP8	*			
YKR012C		G1			
YGR014W	MSB2	G1			
YMR305C	SWC10	G1			
YIL140W	AXL2	G1			

Distribution:	Distribution:
G1: 9	G1: 5
G2: 1	G2/M: 2
M: 5	M/G1: 1
M/G1: 8	





\*: magnitude of change in expression throughout the cell cycle did not exceed a defined threshold to be considered cell-cycle regulated

**Table 7.** Ploidy-regulation of the identified genes is not correlated with stages in the mitotic cell cycle. Except for *FLO11*, cell cycle regulation information is obtained from the systematic study by (Spellman et al., 1998).

Ploidy-repressed genes	Ploidy-induced genes
<i>FLO11</i>	<i>DSE1</i>
<i>YLR042C</i>	<i>DSE2</i>
<i>MFA1</i>	<i>CTS1</i>
<i>FRE4</i>	<i>SCW11</i>
<i>STE2</i>	<i>CPA2</i>
<i>FUS1</i>	<i>YPS6</i>
<i>FUS3</i>	<i>YIL169C</i>
<i>AGA2</i>	<i>DSE4</i>
<i>BAR1</i>	<i>MSL1</i>
<i>YLR040C</i>	<i>OPI7</i>
<i>DDR48</i>	<i>ECM4</i>
<i>PRY2</i>	<i>HBN1</i>
<i>STE6</i>	<i>YNL122C</i>
<i>SST2</i>	<i>YDR379C-A</i>
<i>AGA1</i>	<i>CBP6</i>
<i>SVS1</i>	<i>CMC2</i>
<i>MFA2</i>	<i>FMC1</i>
<i>NDJ1</i>	<i>SLK19</i>
<i>STE4</i>	<i>ACO2</i>
<i>HO</i>	<i>MRPL32</i>
<i>CWP2</i>	<i>MTF2</i>
<i>GPA1</i>	<i>RUD3</i>
<i>GIC2</i>	<i>NDL1</i>
<i>RSN1</i>	<i>YDR357C</i>
<i>GYP8</i>	<i>CTL1</i>
<i>MSB2</i>	
<i>SCW10</i>	

**Table 8.** The *cln3Δ* haploid resembles WT tetraploid. Among the ploidy-regulated genes listed in figure 2, fifty-two remain expressed and ploidy-regulated when cells are grown in the YPD medium. These genes are sorted here in the same order (by fold-change) as in figures 2a & 2b. Expression levels in WT and *cln3Δ* haploids in YPD + nocodazole was measured by quantitative PCR (n=3) and analyzed with Student's t-test (unpaired, for two-tail p-value). Genes expressed at significantly different levels (p<0.05) are highlighted. Blue and red shades indicate significant repression and induction in the *cln3Δ* mutant, respectively.

Regulation of Mkk1-targets in polyploids:

<i>PST1</i>	<i>PIR1</i>	<i>PGK1</i>	<i>SEC28</i>	 Identical trend  Ploidy independent  Opposite trend  No expression
<i>SED1</i>	<i>PIR2</i>	<i>MPK1</i>	<i>DFG5</i>	
<i>CRH1</i>	<i>PIR3</i>	<i>MLP1</i>	<i>PRM5</i>	
<i>CWP1</i>	<i>CIS3</i>	<i>FKS1</i>	<i>YNL058C</i>	
<i>YLR194C</i>	<i>BGL2</i>	<i>FKS2</i>	<i>YMR295C</i>	
<i>CCW14</i>	<i>SPS100</i>	<i>CHS3</i>		
<i>FIT2</i>	<i>YGP1</i>	<i>CTT1</i>		

**Table 9.** Multiple targets of Mkk1 are regulated in the same direction in WT polyploids. Listed here are genes whose expression was significantly altered by over-expression of a gain-of-function allele of *MKK1* (Jung and Levin, 1999). Expression levels of these genes were examined in the RNA-seq datasets using  $p < 0.001$  as the cut-off probability for differential expression between haploid and tetraploid.



### **Chapter 3: Reduced binding of transcriptional activators of *FLO11* in polyploids**

#### **Summary**

The reduction in *FLO11* expression in polyploids as a consequence of increased cell size indicates some communication between the cell surface and the transcriptional apparatus. The reduction requires the *FLO11* promoter, suggesting that at least one of the *FLO11* transcriptional regulators is affected. To test this possibility, the activity or binding of transcription factors to the *FLO11* promoter was examined in isogenic strains of different ploidies. Chromatin immunoprecipitation results show that in tetraploids, there is a reduction in binding of Ste12, Tec1, and Flo8, the key transcription factors that activate *FLO11* expression. The steady-state levels of these transcription factors appear to be unaffected by ploidy. None of the known pathways (including multiple MAP kinase pathways) that regulate these transcription factors is necessary for the down-regulation of *FLO11* in polyploids. Therefore, the circuitry connecting increased cell size to repression of *FLO11* is still not understood. It is possible that multiple pathways function redundantly to repress *FLO11* in polyploids, so disruption of a single pathway is not sufficient to restore expression of *FLO11* in polyploids.

Several considerations should be taken into account in evaluating these data. First, the finding that haploid cell size mutants recapitulate the polyploidy effect was made only recently, after data presented in this chapter had been obtained from various isogenic ploidy series. Second, the construction of tetraploids with desirable genotypes was laborious and time-consuming (see Materials and Methods). Third, tetraploids are genomically unstable as they lose chromosomes at a higher rate and undergo homologous recombination to repair DNA damage much more frequently. Therefore, many of the observations on the circuitry were made in

tetraploids, with the constraints noted. For simplicity, “ploidy-regulation” will be used below to refer to the repression of *FLO11* in polyploids, although the down-regulation is caused by enlarged cell size.

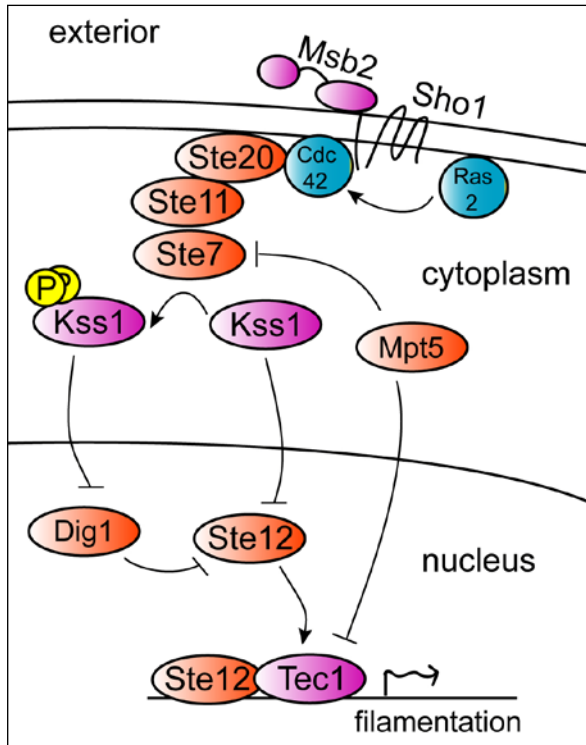
## **Introduction**

The gene encoding a cell surface glycoprotein, *FLO11*, is of great interest in gene regulation studies since multiple pathways control *FLO11* expression. The promoter of *FLO11* is greater than 3Kb in length, contains recognition motifs of many transcriptional regulators, and therefore integrates the inputs of many more pathways than the average promoter in the genome of *S. cerevisiae* (Bumgarner et al., 2009; Harbison et al., 2004; Rupp et al., 1999). The Flo11 protein promotes adhesion among yeast cells and to substratum (Guo et al., 2000; Lo and Dranginis, 1996). Flo11 plays a critical role in agar invasion of haploids and in pseudohyphal growth of diploids during starvation (Lambrechts et al., 1996; Lo and Dranginis, 1998). As summarized below, multiple signaling pathways combinatorially modify the ensemble of transcription factors at the *FLO11* promoter to regulate complex physiological processes in response to changes in environmental conditions.

### **The filamentous growth pathway controls *FLO11* expression by regulating the activity of transcription factors Ste12 and Tec1**

For simplicity, the mitogen-activated protein kinase (MAPK) pathway regulating invasive and pseudohyphal growth is termed the filamentous growth (FG) pathway. In haploids,

glucose deprivation induces invasive growth (Cullen and Sprague, 2000). In diploids, nitrogen starvation in the presence of high glucose concentration induces pseudohyphal growth (Gimeno et al., 1992).



Shown on the left is a diagram of the MAPK pathway. Upstream of the FG MAPK cascade is the G-protein Ras2 signaling via the Rho family protein Cdc42 upon nutrient starvation (Mosch et al., 1996). An independent study shows that surface proteins Msb2 and Sho1 interact physically and are both required for filamentous growth (Cullen et al., 2004). Msb2 also negatively regulates FG. Deletion of the mucin tandem repeats in Msb2 causes hyperactivity of FG pathway. Mutants with

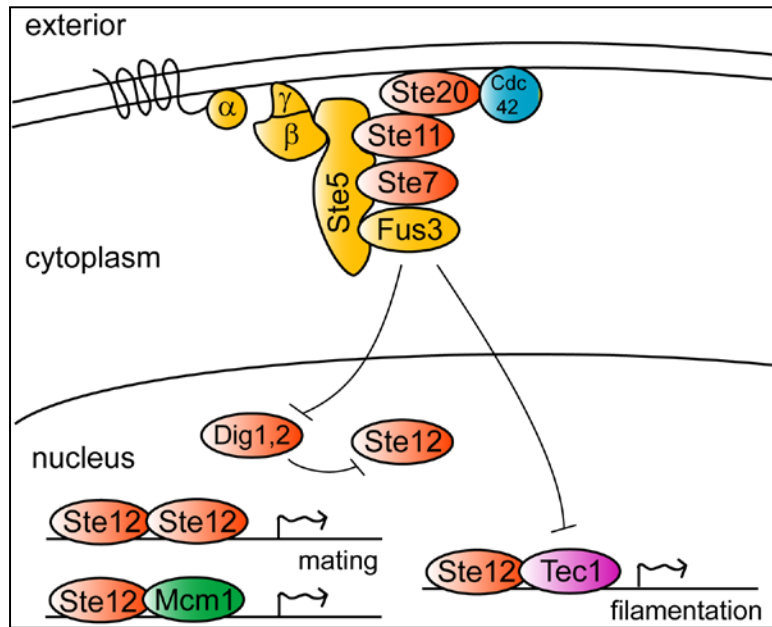
decreasing numbers of mucin repeats showed increasingly stronger signaling in the FG pathway (Cullen et al., 2004). The relationship between Ras2 and Msb2/Sho1 remains to be established. In the GTP-bound form, Cdc42 activates Ste20 at the tip of small budded cells (Peter et al., 1996). This sub-cellular localization pattern is essential for filamentous growth. Localization of Ste20 to the emerging bud tip is facilitated by the adaptor protein Bem1 (Winters and Pryciak, 2005). Similarly, interaction of the MAPKKK Ste11 with Cdc42 and Ste20 is promoted by the adaptor protein Ste50 (Ramezani-Rad, 2003). Activated Ste11 (MAPKKK) then initiates activation of downstream kinases Ste7 (MAPKK) and Kss1 (MAPK).

The inactive form of Kss1 and a regulatory protein Dig1 both bind to the transcription factor Ste12 to inhibit its function (Chou et al., 2006; Cook et al., 1996; Cook et al., 1997; Madhani et al., 1997). Upon activation by the kinase Ste7, Kss1 dissociates from Ste12 (Cook et al., 1997; Madhani et al., 1997) and phosphorylates both Ste12 and Dig1, releasing Ste12 from Dig1's repression (Cook et al., 1996; Tedford et al., 1997). Relieved of inhibition, Ste12 and a FG-specific transcription factor Tec1 activate expression of FG-specific genes including *FLO11* (Kohler et al., 2002; Zeitlinger et al., 2003). Ste12 is also crucial for expression of *TEC1* (Kohler et al., 2002). Ste12 and Tec1 cooperatively bind to a composite motif element termed filamentation response element (FRE) *in vitro* (Madhani and Fink, 1997), and Tec1 is required for localization of Ste12 to FG-specific genes *in vivo* (Zeitlinger et al., 2003). It is worth emphasizing that Kss1 acts either as a potent repressor or a crucial activator of Ste12 activity, depending on the phosphorylation state. The *kss1Δ ste7Δ* double mutant is capable of invasive growth (Cook et al., 1997). Hence, the FG MAPK pathway implements a switch-like control on its target genes and is not necessary for their expression per se.

The activity of FG pathway is also controlled at the level of translation by the RNA-binding protein Mpt5. Deletion of *MPT5* increases protein levels of Ste7 and Tec1 without affecting their transcript levels, and diploids homozygous for *mpt5Δ* shows enhanced pseudohyphal growth (Prinz et al., 2007). It is unclear how Mpt5 is regulated to mediate translational control on its target transcripts.

**The pheromone response pathway inhibits *FLO11* expression by triggering degradation of Tec1**

Numerous elegant studies have contributed to an extensive understanding of the pheromone response pathway (Dohlman and Slessareva, 2006). Diagrammed to the right are the major components of the pheromone response MAPK pathway.



Binding of mating pheromone to the 7-pass transmembrane G-protein coupled receptor (Ste2 and Ste3 in *MATa* and  $\alpha$  cells, respectively) results in dissociation of a trimeric G-protein complex. Dissociated from the  $G\alpha$  subunit (Gpa1), the  $G\beta\gamma$  complex (Ste4/Ste18) triggers activation of Cdc42, which recruits and activates Ste20. The  $G\beta$  subunit also interacts with the scaffold Ste5, which brings the remaining kinases in the cascade to the vicinity of activated Ste20.

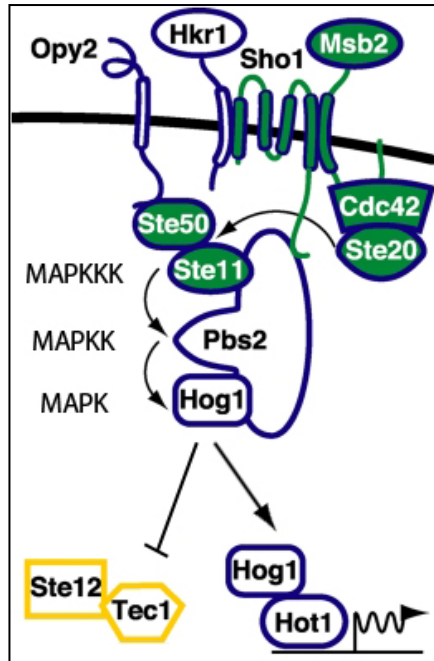
Although the pheromone response pathway shares multiple components with the FG pathway (Cdc42, Ste20, Bem1, Ste11, Ste50 and Ste7) (Roberts and Fink, 1994), pheromone signal transduction specificity is ensured by the scaffold protein Ste5 (Choi et al., 1994; Good et al., 2009; Whiteway et al., 1995) and by the mating-specific MAPK Fus3 mediated destruction of Tec1 (Bao et al., 2004; Bruckner et al., 2004; Chou et al., 2004). Absence of Tec1 prevents induction of FG-specific genes, as Ste12 alone does not localize to promoters of those genes

(Zeitlinger et al., 2003). On the other hand, genes required for mating are successfully induced by Ste12 without Tec1. Similar to Kss1, activated Fus3 phosphorylates Dig1 and Dig2 to relieve Ste12 from inhibition (Cook et al., 1996). Fus3 therefore promotes the mating response while repressing the filamentation pathway upon activation by Ste7. In its uninhibited form, Ste12 induces pheromone response genes as homo-dimers or hetero-dimers with a number of other transcription factors (Bruhn and Sprague, 1994).

Recent biochemical and genetic studies reveal the mechanistic details of destruction of Tec1. In the presence of mating pheromone, activated Fus3 phosphorylates Tec1 at threonines 273 and 276, triggering ubiquitylation of Tec1 by SCF(Cdc4) followed by proteolytic degradation in the proteasome (Bao et al., 2009; Chou et al., 2004). Amino acid substitutions at residue 273 or 276 prevent phosphorylation by Fus3 and block the pheromone-dependent degradation of Tec1. These Tec1 mutants cause erroneous induction of filamentation genes in the presence of mating pheromone (Bao et al., 2004; Bao et al., 2009; Bruckner et al., 2004; Chou et al., 2004).

### **The high osmolarity glycerol pathway represses *FLO11* transcription by inhibiting the activity of Tec1**

The high osmolarity glycerol (HOG) pathway is critical for adaptation to external hypertonic stress as it increases glycerol production to counteract the osmotic differential between the internal and external osmolarity of the cell. The molecular mechanism for signal transduction is well-summarized by Hohmann (Hohmann et al., 2007). Shown below are components of the Sho1 branch of the HOG pathway (modified from (Shock et al., 2009). Two



sensors on the cell surface, Hkr1 and Msb2, are structurally similar and functionally redundant in initiating HOG signaling (Tatebayashi et al., 2007). Another cell surface protein, Opy2, promotes activation of Ste11 by interacting with Ste50 and is required for signaling in the Sho1 branch (Wu et al., 2006). For simplicity, I omitted the Sln1 branch of the HOG pathway involving a histidine kinase on the plasma membrane (Sln1), a phospho-transferase (Ypd1), a cytoplasmic response regulator Ssk1, and two redundant MAPKKK Ssk2 and Ssk22.

The fact that multiple components are shared among the pheromone response, FG and HOG pathways (Cdc42, Ste20, Ste50 and Ste11 in all three; Sho1 and Msb2 in both FG and HOG) raises the question of how these signaling pathways are insulated from one another. Specifically, the mechanism that prevents the activation of the HOG pathway upon activation of either pheromone response or the FG pathway is not known. Both Pbs2 and Hog1 are required to prevent erroneous activation of pheromone response and FG genes from the Sho1 branch of the HOG pathway (Davenport et al., 1999; O'Rourke and Herskowitz, 1998). Recently, it has been discovered that Hog1 inhibits the DNA binding activity of Tec1 to prevent cross-talk from HOG to FG pathway (Shock et al., 2009). Inhibition of Tec1 largely depends on the kinase activity of Hog1. The mechanism of inhibition by Hog1 is unclear. It does not affect the abundance or nuclear localization of Tec1. Nor does it appear to involve any of the known regulators of Tec1.

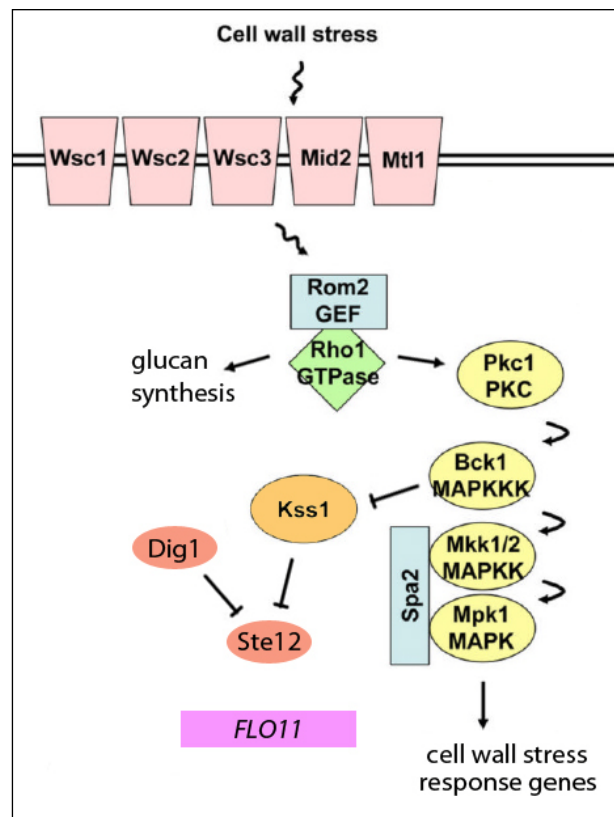
## The cell wall integrity pathway represses *FLO11* through crosstalk to the FG MAPK

The cell wall integrity (CWI) MAPK pathway regulates the dynamic expansion and remodeling of the cell wall during normal vegetative proliferation, exposure to cell wall damaging agents, hypo-osmotic shock, oxidative stress, depolarization of actin cytoskeleton, mating response (Levin, 2005) and likely filamentous growth. Shown in the figure below are major components of the CWI pathway (modified from (Chen and Thorner, 2007)). Briefly, cell wall stress is sensed by the Wsc1-3/Mid2/Mtl1 glycoproteins on the cell surface, which trigger the activation of the G protein Rho1 through Rom2. Pkc1, one of the downstream effectors of Rho1, activates the CWI MAPK cascade.

Activated MAPK Mpk1 regulates gene expression largely through the induction of transcription factor *RLM1*. A comprehensive description of CWI signaling and function is detailed in a recent review (Levin, 2005).

While characterizing *FLO11* regulation, I discovered that deletion of *BCK1* increases *FLO11* expression, and this increase depends on Kss1. Deletion of the CWI MAPK *MPK1*, on the other hand, does not increase *FLO11* expression (see results

section below). These results suggest inhibitory crosstalk from CWI to FG pathway. The crosstalk would occur upstream of the CWI MAPK Mpk1, likely initiated by Bck1, and would involve the MAPK Kss1 as shown in the figure above.

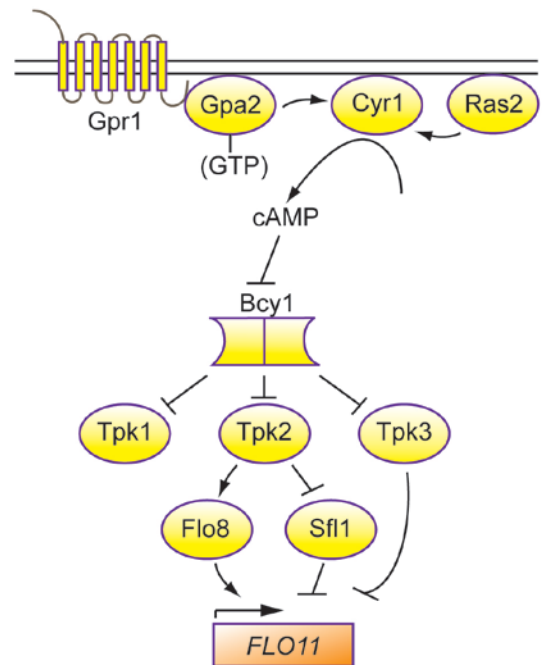




## The cAMP/PKA pathway modulates *FLO11* expression by regulating transcription factors Sfl1 and Flo8

The cAMP/protein kinase A (PKA) pathway functions in parallel to the FG MAPK pathway to induce *FLO11* expression (Mosch et al., 1999). The G-protein coupled receptor Gpr1 senses nutrient levels and is required for FG (Lorenz et al., 2000). Gpr1 activates Gpa2 (G $\alpha$ ), which then stimulates the adenylate cyclase Cyr1 to produce cAMP (Xue et al., 1998). Elevated cellular concentration of cAMP relieves the catalytic subunits of PKA (Tpk1-3) from inhibitory binding of the regulatory subunit, Bcy1.

Tpk2 is required for *FLO11* induction and pseudohyphal growth, because non-functional alleles show a dramatic reduction in both phenotypes. Deletion of *TPK3* increases *FLO11* expression and promotes pseudohyphal growth. Deletion of *TPK1* did not affect *FLO11* expression or pseudohyphal growth (Robertson and Fink, 1998). Tpk2 binds and exerts opposite effects on two targets: the transcriptional activator Flo8 and



the transcriptional repressor Sfl1 (Pan and Heitman, 2002). Tpk2 stimulates the DNA binding capability of Flo8. Although phosphorylation of Flo8 by Tpk2 was not detected *in vivo*, binding of Flo8 to DNA required both Tpk2 and ATP *in vitro*. Tpk2 phosphorylates Sfl1 *in vivo* and inhibits its DNA binding function in the presence of ATP *in vitro*. Tpk2 thus operates a switch to induce *FLO11* expression. It removes the repression mediated by Sfl1 and enables induction by activating Flo8. Notably, Flo8 and Sfl1 bind to the same region (between -1400 and -1150nt) of

the *FLO11* promoter. Hence, the two transcription factors function in an antagonistic, mutually exclusive fashion, further ensuring a switch-like mechanism of *FLO11* regulation.

### **The cAMP/PKA and FG MAPK pathways function in concert to induce *FLO11***

The cAMP/PKA and FG MAPK pathways have a common upstream regulator, Ras2, that activates Cyr1 in the cAMP/PKA pathway and Cdc42/Ste20 in the FG MAPK pathway (Mosch et al., 1999). Transcription factors downstream of the two pathways, Flo8, Ste12 and Tec1, are all required to induce *FLO11* and FG (Gavrias et al., 1996; Liu et al., 1996; Lo and Dranginis, 1998; Pan and Heitman, 2002; Roberts and Fink, 1994). Hence, both pathways are important for FG, and each of these transcription factors plays a distinct and critical role.

In the yeast *Saccharomyces diastaticus*, regulation of *STAI* whose promoter is nearly identical to that of *FLO11* (Gagiano et al., 1999) provides detailed molecular insight on the functional relationship among Flo8, Ste12 and Tec1 (Kim et al., 2004). Under inducing conditions, Ste12 and Tec1 bind to the *STAI* promoter cooperatively first to recruit the chromatin remodeling complex Swi/Snf. Remodeling of the chromatin allows Flo8 and another transcription factor, Mss11 (van Dyk et al., 2005), to associate cooperatively with the promoter. Flo8/Mss11 then recruit RNA polymerase II to induce expression of *STAI*. These data led to the model in the figure below. The details of intermolecular interactions and DNA looping have not been verified experimentally at the *FLO11* promoter in *S. cerevisiae*.

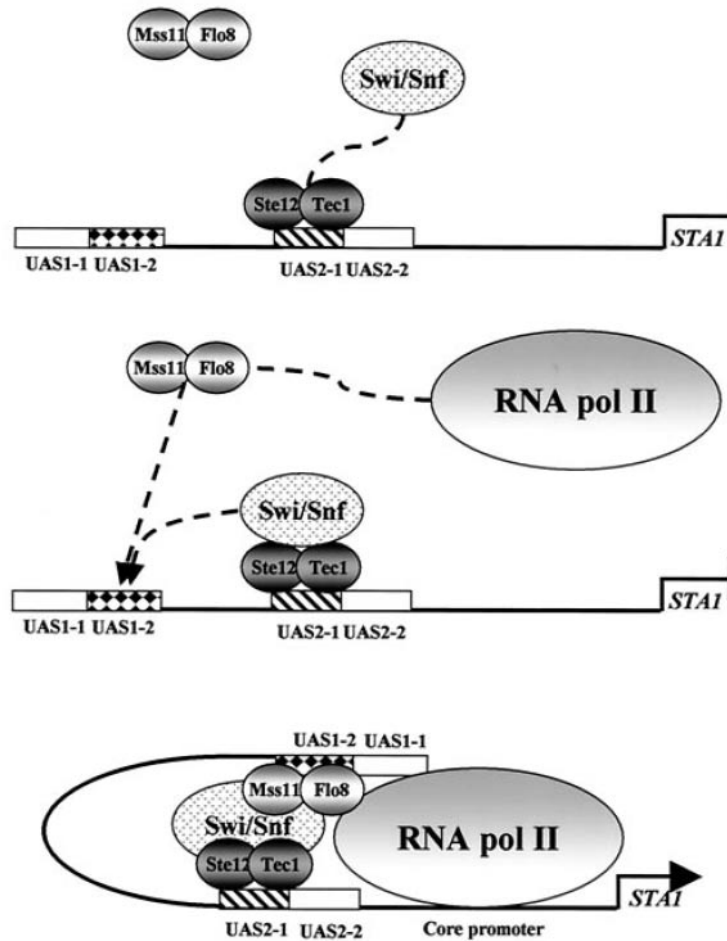


Figure: Model for *STAI* induction by sequential actions of Ste12/Tec1, Swi/Snf and Flo8/Mss11 (Kim et al., 2004).

UAS: upstream activating sequence.

### **Nrg1 and Nrg2 repress *FLO11* when glucose is abundant**

The zinc finger transcription repressors Nrg1 and Nrg2 function downstream of the glucose sensing Snf1 kinase to repress *FLO11* transcription when glucose is limiting (Kuchin et al., 2002). Deletion of both *nrg1* and *nrg2* significantly promotes pseudohyphal formation, suggesting that nitrogen abundance also regulates the activities of these transcription repressors in diploids.

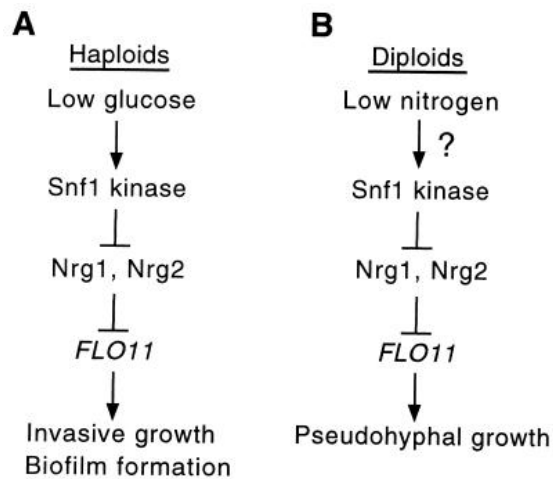


Figure: Models for regulation of *FLO11* expression by Nrg1 and Nrg2 in haploids (A) and diploids (B) (Kuchin et al., 2002).

### The histone deacetylase Hda1 is required for variegated repression of *FLO11*

*FLO11* expression is controlled not only by many transcription factors that modulate its response to environmental conditions, but also by chromatin alterations that lead to epigenetic variegation. Halme *et al.* showed that the WT Sigma 1278b grows as a mixture of cells with Flo11 present and absent on the cell surface (Halme et al., 2004). Cells within a diploid colony undergoing filamentous growth show a strong correlation between Flo11 surface expression and morphology: The elongated, filament-forming cells express Flo11 whereas the oval, vegetatively growing cells do not. The variegation phenomenon requires expression of *FLO11* at its native genomic location and is independent of the telomere position effect. The authors then demonstrated that both the “on” and “off” expression phenotypes can be stable for multiple generations and are fully reversible.

This non-genetic, reversible switch between Flo11-expressed and -silenced states requires the histone deacetylase Hda1, which is recruited to the *FLO11* promoter by the aforementioned transcription repressor Sfl1. Halme *et al.* found that null deletion mutants of either *HDA1* or

*SFLI* display Flo11 on the cell surface uniformly. This implies that in a WT population, Hda1 mediates *FLO11* silencing in only a fraction of cells.

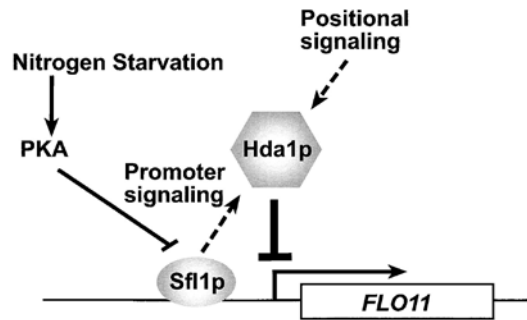


Figure: Model for the mechanism of variegated *FLO11* expression. Sfl1 confers the specificity of silencing by binding to the *FLO11* promoter. Hda1, recruited by Sfl1, likely integrates the promoter-specific and location-specific silencing. (modified from (Halme et al., 2004)

### ***cis*-acting non-coding RNAs mediate a toggle switch of *FLO11* expression**

Bumgarner *et al.* identified a pair of long non-coding RNAs transcribed within the upstream intergenic region of *FLO11* (Bumgarner et al., 2009). Transcription of *ICRI* (interfering Crick RNA 1) starts at 3.1 to 3.4 Kb upstream of *FLO11* ORF, proceeds through most of the promoter region, and ends at about ~200nt upstream of or further towards the ORF. The second non-coding RNA, *PWRI* (promoting Watson RNA 1), initiates at ~2.3 Kb upstream of *FLO11* ORF and ends near the initiation site of *ICRI* (see diagram below). Transcription of *ICRI* occludes binding of transcription factors, thereby silences *FLO11*. Under *FLO11*-expressing conditions, transcription of *PWRI* interferes with that of *ICRI*. Absence of *ICRI* transcription allows transcriptional activators (Ste12, Tec1, Flo8 etc.) to associate with the *FLO11* promoter, especially within 2Kb upstream of *FLO11* ORF. Binding sites of multiple key transcriptional activators have been predicted and confirmed in this region (Bumgarner et al., 2009; Harbison et al., 2004; Rupp et al., 1999)(also see results section below).

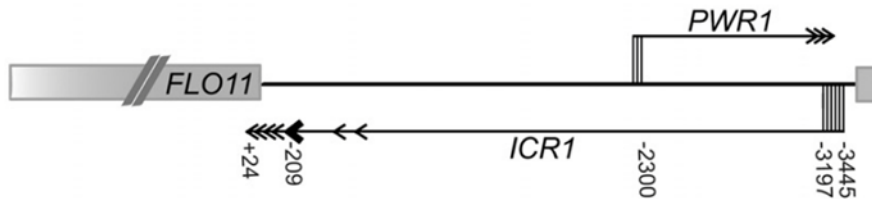


Figure: Regulation of *FLO11* expression by the non-coding RNAs *ICR1* and *PWR1*. The transcription initiation and termination sites of both transcripts are shown with respect to the chromosomal location of *FLO11* ORF. (modified from (Bumgarner et al., 2009))

### **Induction of *FLO11* by aromatic alcohols at high cell density**

The expression of *FLO11* is induced at high cell density through a quorum sensing mechanism. As cell density increases, nitrogen source depletes, causing increased production of alcohol derivatives of the amino acids Tyr, Phe and Trp, abbreviated as TyrOH, PheOH and TrpOH, respectively (Chen and Fink, 2006). Both PheOH and TrpOH but not TyrOH induce expression of *FLO11* in a Tpk2 and Flo8 dependent fashion. When supplemented with TrpOH but not PheOH or TyrOH, cells at low density behave as if they were at high density in nitrogen poor conditions: they up-regulate expression of enzymes necessary for production of the alcohol derivatives. These results illustrate a positive feedback loop for *FLO11* expression as cell density increases.

## **Results**

A series of quantitative PCR results from mutant ploidy series will be presented in this section. Unless otherwise specified, these are the default conditions of experiments and data analysis: Cells were grown to mid-log phase in SC medium + 2% glucose at 30°C prior to harvest. All data were statistically analyzed with Student's t-test (unpaired & two-tailed) or one-way ANOVA with n=3 and error bar = standard deviation. Notation for significance: \* = p-value less than 0.05, \*\* = p-value less than 0.01, \*\*\* = p-value less than 0.001.

### **The *FLO11* promoter is required for ploidy-regulation**

To determine whether the reduction in *FLO11* expression in tetraploids required specific regulatory elements in the *FLO11* gene, I replaced the endogenous *FLO11* ORF and 3'UTR with exogenous sequences without affecting the 5' promoter region (figure 1a). Expression of the reporter gene is still ploidy-repressed in tetraploids even when the 3' UTR and coding region is different. When this construct is transferred to the genomic location of *URA3*, the construct is still ploidy-repressed (figure 1a), showing that the *FLO11* promoter is sufficient for conferring ploidy-regulation and does not require the native genomic location of *FLO11* to cause the down-regulation observed in polyploids.

I also attempted to measure the half-life of *FLO11* transcript in haploids and tetraploids. My preliminary result suggests that increasing ploidy does not destabilize the *FLO11* transcript. In this experiment, the *FLO11* ORF and 3'UTR were inserted downstream of the *GALI* promoter on a centromere-based plasmid carried by *flo11Δ* haploid and tetraploid strains. After 3 hour induction in galactose, expression of *FLO11* was turned off by the presence of glucose. Cells

were collected at regular intervals to quantify abundance of *FLO11* RNA. Based on the preliminary data shown in figure 1b, the degradation rate of the *FLO11* transcript is not faster in the tetraploid. Therefore, ploidy does not appear to affect the stability of *FLO11* RNA, a result consistent with the conclusion that the reduced *FLO11* promoter activity is likely responsible for the lower steady-state level of *FLO11* RNA in polyploids.

A technical note on the experiment: This experiment was performed only once as an exploratory attempt. The data are not conclusive and raise some interesting questions. Between the two ploidy states, why was there such a large difference in the initial abundance of *FLO11* transcript after galactose induction? Was the plasmid retained poorly in the tetraploid? Such instability would not be surprising because polyploids have defects in chromosome segregation. Does ploidy affect galactose sensing or the promoter activity of *GALI*? In addition, the 5'UTR of *FLO11* transcript is likely different when expressed from the *GALI* promoter. Differences in nucleotide sequences could affect the degradation rate of *FLO11* transcript. Last, a briefer induction period in galactose would create a more physiological relevant context in the experiment. More frequent sampling right after addition of glucose would also be needed to extrapolate the kinetic details of transcript degradation. In summary, technical improvements would be required to fully investigate the effect of ploidy on *FLO11* transcript stability.

### **Association of RNA polymerase II with the *FLO11* promoter is reduced in polyploids**

To further understand the mechanism underlying the regulation of *FLO11* in polyploids, I examined binding of RNA pol II to the *FLO11* promoter in haploids and tetraploids. I had previously mapped the transcription start site of *FLO11* by 5' RACE and located it at 29nt



upstream of the start codon (data not shown). I also identified a putative TATA box 100nt upstream of the ORF. I thus decided to examine binding of RNA pol II to the predicted TATA box by ChIP. As shown in figure 2a, association of RNA pol II is significantly reduced in tetraploids, suggesting that polyploidy represses recruitment of RNA pol II to the *FLO11* promoter. This observation is consistent with the aforementioned reduction in transcript abundance of *FLO11* in polyploids (figure 1a).

### **Reduced binding of transcriptional activators to the *FLO11* promoter in polyploids**

Consistent with the model for *STA1* induction in *S. diastolicus*, binding of Flo8, Ste12 and Tec1 to the *FLO11* promoter is reduced in *S. cerevisiae* polyploids (figure 2b), a result that likely accounts for the reduced recruitment of RNA pol II. Association of RNA pol II with the *FLO11* promoter in WT tetraploid is similar to that in the haploid *tec1Δ* mutant (figure 2a), consistent with a lack of transcriptional activation at *FLO11* in WT tetraploids. A control experiment with a transcription factor, Gcn4, that does not bind to *FLO11* shows that this reduction in tetraploids is specific for the *FLO11* promoter (figure 2c). The abundance of Flo8, Ste12 and Tec1 proteins relative to total protein does not appear to change in tetraploids based on western blot (data not shown). Their RNA expression levels also appear to be unaffected by ploidy (data not shown). Polyploidy likely regulates the activity of these transcription factors post-translationally.

Since multiple signaling pathways regulate the activities of Flo8, Ste12 and Tec1, the remaining experimental results will focus on these pathways. In particular, the roles of negative

regulators of *FLO11* in these pathways are of primary interest since they are known to repress the activity of these transcription activators.

### **Kss1, Dig1, Mpt5 and Msb2 in the FG pathway**

In its inactive state, the FG MAPK Kss1 represses *FLO11* expression by inhibiting the activity of Ste12. The lack of transcriptional activation of *FLO11* in polyploids could be caused by a lack of activation of Kss1. To test this possibility, expression of *FLO11* was quantified in the *kss1Δ ste7Δ* double mutant. The double mutant is useful in this experiment since it is capable of invasive growth. By contrast, the single *kss1Δ* mutant expresses *FLO11* poorly and is strongly defective in FG (Cook et al., 1997). Deletion of *KSS1* and *STE7* did not affect ploidy-regulation of *FLO11* (figure 3a). I also examined expression of *FLO11* in the *dig1Δ* ploidy series. Acting downstream of Kss1, Dig1 is another negative regulator of Ste12 and Tec1 in the FG pathway. Similarly, deletion of *DIG1* did not abolish the ploidy-regulation of *FLO11* in tetraploids (figure 3b). These results indicate that inactivity of the FG pathway alone cannot explain repression of *FLO11* in polyploids. Translational repression of *STE7* and *TEC1* by Mpt5 cannot explain ploidy-regulation of *FLO11*, as evidenced by the significantly reduced expression of *FLO11* in *mpt5Δ* diploid compared to haploid (figure 3c). The mucin domain of Msb2 does not appear to cause repression of *FLO11* in polyploids, either (figure 3d). In summary, the currently known negative regulators of *FLO11* in the FG pathway are not required for repression of *FLO11* in polyploids.

### **The Fus3 kinase of the pheromone response pathway and the Tec1 T273M mutant**

The pheromone response pathway MAPK Fus3 is known to inhibit transcriptional activation of *FLO11* by triggering degradation of the transcription factor Tec1 (Bao et al., 2009). Multiple lines of evidence suggest that Fus3 is not necessary for silencing of *FLO11* in polyploids. First, *FUS3* is not expressed in the *MATa/a* cell type, but ploidy-regulation occurs in all three *MAT* cell types (Galitski et al., 1999). Second, RNA-seq data suggest that Fus3 is less active in tetraploids, since a number of genes in the pheromone response pathway, including *FUS3* itself, are ploidy-repressed (table 4 in chapter 2). Third, the T273M mutant of Tec1 protein is resistant to phosphorylation by activated Fus3 and not degraded during pheromone response (Bao et al., 2004; Bruckner et al., 2004; Chou et al., 2004). In the *TEC1* T273M mutant background, *FLO11* is still repressed by increasing ploidy (figure 4).

### **The high osmolarity glycerol pathway MAPK Hog1**

The fact that Hog1 inhibits the DNA binding function of Tec1 makes Hog1 an attractive candidate for an agent of gene regulation by ploidy. However, deletion of *HOG1* also did not restore the promoter activity of *FLO11* in polyploids (figure 5).

### **Bck1, the MAPKKK of the cell wall integrity (CWI) pathway**

I had found that deletion of the CWI MAPKKK *BCK1* causes de-repression of *FLO11* in haploids, whereas deletion of the CWI MAPK *MPK1* has little or a negative effect on *FLO11* expression (figure 6a). Probing the mechanism further, I found that the double mutant *kss1Δ*

*ste7Δ* is epistatic to *bck1Δ* (figure 6b). One interpretation of these results is inhibitory crosstalk from Bck1 to the FG MAPK cascade. Higher activity of CWI pathway observed in tetraploids (figure 6a in chapter 2) could cause of *FLO11* repression. To test this hypothesis, I constructed the *bck1Δ* ploidy series and compared expression of *FLO11* within the series. In the *bck1Δ* tetraploid, expression of *FLO11* is significantly lower than in the isogenic haploid (figure 6c). Hence, the repressive effect of ploidy on *FLO11* persists in the *bck1Δ* background.

### **Sfl1 and Tpk3 in the cAMP/PKA pathway**

Sfl1 is a key transcriptional repressor of *FLO11*. By precluding Flo8 from binding to the *FLO11* promoter, Sfl1 prevents recruitment of general transcription factors and RNA pol II. Sfl1 also promotes transcriptional silencing by recruiting the general repressor Ssn6-Tup1 (Conlan and Tzamarias, 2001). Having these functions, Sfl1 could be regulated by ploidy and confer the down-regulation of *FLO11* in polyploids. I constructed a ploidy series of the *sfl1Δ* mutant to study its effect and found that repression of *FLO11* by polyploidy persists in this mutant background (figure 7a). Hence, Sfl1 is not required for ploidy-regulation. While investigating roles of the protein A kinases in FG, Robertson *et al.* discovered that Tpk3 might function upstream of Tpk2 to inhibit FG (Robertson and Fink, 1998). As shown in figure 7b, it is unlikely that Tpk3 mediates ploidy-based silencing of *FLO11*, because the repression on *FLO11* remains in *tpk3Δ* polyploids.

## **Nrg1 in the glucose repression pathway**

Kuchin *et al.* reported that the zinc finger transcriptional repressors Nrg1 and Nrg2 function downstream of the Snf1 kinase to repress *FLO11* when nutrients are abundant (Kuchin *et al.*, 2002). Nrg1 is of particular interest as its activity is regulated by glucose content (Berkey *et al.*, 2004). It is possible that polyploids respond to nutrient depletion poorly due to signaling defects, as shown in a previous study (Andalis *et al.*, 2004). Polyploids may be defective in sensing glucose depletion in the medium and maintains *FLO11* repression in a growing culture. I investigated this possibility by ChIP to quantify association of Nrg1 with the *FLO11* promoter. As shown in figure 8, binding of Nrg1 to the *FLO11* promoter is diminished in polyploids. Binding of Nrg1 to the *GAT4* promoter, on the other hand, is not affected by ploidy. These results suggest that Nrg1 does not contribute to repression of *FLO11* in polyploids. The results again show that in polyploids, the *FLO11* promoter is somehow less accessible to transcription factors.

## **Variation factor histone deacetylase Hda1**

In haploids and diploids, Hda1 is required for variegated silencing of *FLO11* (Halme *et al.*, 2004). One possibility is that polyploidy increases the fraction of silenced cells in the population through Hda1. Consequently, the average level of *FLO11* expression would decrease when assayed on the population level. To probe this possibility, I constructed the *hda1* $\Delta$  ploidy series. The repressive effect of ploidy remains in this mutant background (figure 9). Results from the *hda1* $\Delta$  and *sf11* $\Delta$  ploidy series are in agreement and consistent with a role of Sfl1 in recruiting Hda1 to the *FLO11* promoter.

### **Upstream intergenic transcription of *ICRI***

Bumgarner *et al.* show that transcription of *ICRI* initiates far upstream of the *FLO11* ORF and progresses through most of the *FLO11* promoter (in some cases even further into the *FLO11* ORF), preventing transcription activators from binding to the promoter (Bumgarner *et al.*, 2009). To investigate whether *ICRI* is involved in ploidy-regulation, I quantified the abundance of *ICRI* and *FLO11* transcripts in multiple isogenic haploid, diploid and tetraploid strains. Although in one ploidy series the expression of *ICRI* appears to increase with increasing ploidy, the other ploidy series did not show such a trend (figure 10). Regardless of the levels of *ICRI* expression, expression of *FLO11* consistently decreases with increasing ploidy in all series. The inverse relationship between *ICRI* and *FLO11* expression observed in haploids by Bumgarner *et al.* is not established in polyploids. It is unlikely that *ICRI* mediates repression of *FLO11* in polyploids.

### **Cell density**

The expression of *FLO11* is induced at high cell density through a quorum sensing mechanism involving alcohol derivatives of phenylalanine and tryptophan. A comparison between optical density and cell density shows that the same optical density corresponds to ~3 fold lower cell density for the tetraploid when compared to haploid (table 1 in Appendix). Because comparisons of *FLO11* expression had only been performed in cultures controlled for optical density, effects caused by a difference cell density in ploidy series were unknown albeit systematic. Hence, it was important to compare *FLO11* expression in cultures at the same cell density. As shown in table 1, expression of *FLO11* in tetraploids remains significantly lower than

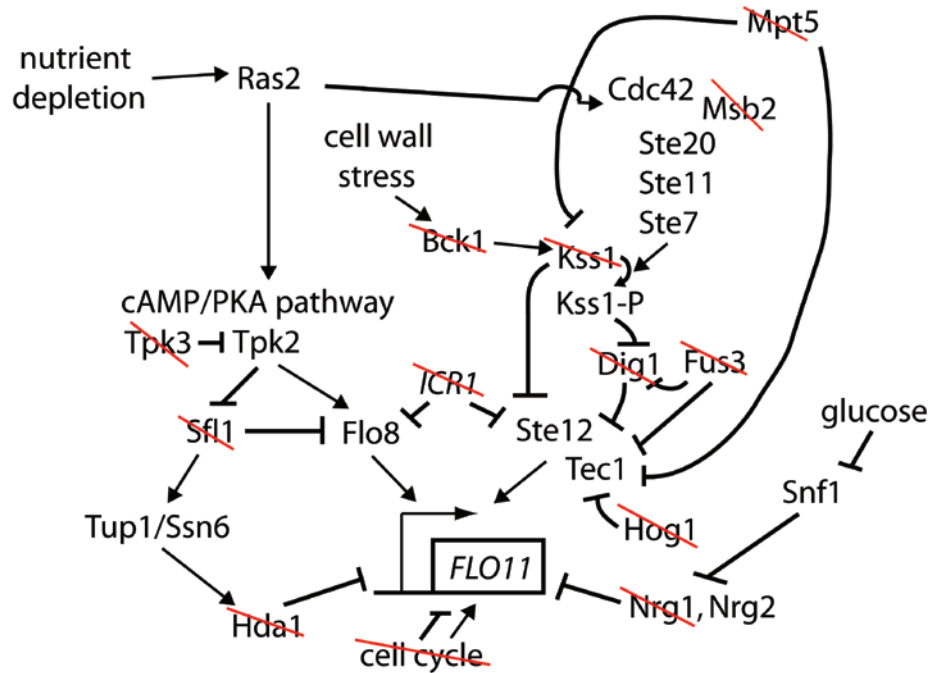
in haploids at similar cell densities. The result rules out differences in cell density as a determinant of repression of *FLO11* in polyploids.

### **Cell cycle**

As discussed earlier (figure 3 in chapter 2), expression of *FLO11* is regulated by the mitotic cell cycle. It peaks during M-phase and drops at the onset of G1, a pattern identical to that of *SWI5*. One explanation for the ploidy-regulation of *FLO11* would be an alteration in the polyploid mitotic cell cycle – such as a much longer G1-phase – causing under-representation of cells in M-phase in polyploid cultures. Consequently, the average expression level of *FLO11* would be lower. Data from the cell size haploid mutants (figures 5 in chapter 2) argue against this explanation. Another line of evidence is shown in figure 11: expression of *SWI5* appears to increase with increasing ploidy. If changes in the cell cycle were to account for differential expression of *FLO11*, then expression of *FLO11* would have been higher in polyploids. The fact that *FLO11* is strongly repressed in polyploids means that a cell cycle independent process causes ploidy-repression.

## Discussion

Results presented in this chapter are summarized in the diagram below. I selectively looked at a number of repressors of *FLO11* that function upstream of Flo8, Ste12 and Tec1. When individually examined, none of the repressors was necessary for down-regulation of *FLO11*. Hence, these repressors are individually dispensable for the regulation and are thus crossed out in the diagram. Implications of these results, combined with findings in chapter 2, will be discussed in the next chapter along with future directions to identify potential pathways mediating repression of *FLO11* in polyploids.



The candidate-based genetic survey of the regulators employed in this chapter is certainly far from complete. A small number of mutants are worth consideration but have not been explored: *bcy1Δ*, *msb2* without its N-terminal domain, and *nrg2Δ* (Cullen et al., 2004; Kuchin et al., 2002; Prinz et al., 2007; Robertson and Fink, 1998). In these mutants, it was observed that



*FLO11* expression levels were increased as compared with WT, suggesting that these proteins of interest act as repressors of *FLO11*. I also did not explore combinations of mutations in different pathways. Due to the complex regulation of *FLO11*, it is formally possible that two or more regulators function redundantly and that individually each of the regulators is sufficient for strong repression of *FLO11* in polyploids.

A few improvements in experimental design would have led to more informative results in this chapter. First, the growth condition of yeast cultures could have been better standardized to minimize variations among experiments. For example, the WT haploid strain L6437 and tetraploid strain L6440 in figures 9, 10 (1<sup>st</sup> panel) and 11 showed 2.8, 7, and 15 fold reduction in *FLO11* transcript levels in the tetraploid, respectively. Although it is clear that *FLO11* is consistently down-regulated in the tetraploid, such large variations in fold changes compromise the quantitative quality of the data. Gene expression analysis was performed using cultures grown on shakers in a 30C warm room, a condition that could have been optimized to improve experimental reproducibility. Since the facility is shared by multiple investigators who need to frequently access the room and turn on/off the shakers, changes in growth conditions caused by fluctuations in temperature and aeration can be common. These changes could influence expression of *FLO11*, whose regulation is controlled by multiple signaling pathways responsive to changes in the environment. Growing cultures in a water bath with finer control over temperature and rotary speed could have helped to minimize variations among different experiments.

Second, a significant portion of the data was obtained from mutants without their WT counterparts that would have generated more useful data. Without proper WT controls, it is difficult to quantitatively assess the contribution of each regulator to the down-regulation of

*FLO11*. In other words, the fold changes in *FLO11* expression levels between mutant haploids and polyploids could have been more meaningful if fold changes in isogenic WT controls had been available in the same experiments. If several mutations were found to individually restore *FLO11* expression in polyploids by a small degree, these mutations would be suitable to combine to further examine functional redundancy among their associated signaling pathways.

Another technical improvement would be to verify euploidy in each tetraploid strain prior to gene expression analysis. Genome instability occurs more often in polyploids due to more frequent chromosomal loss (Andalis et al., 2004; Ganem et al., 2007; Storchova et al., 2006). Aneuploidy in polyploids can lead to false interpretations of gene expression data, especially when chromosomes carrying genes of interest are lost. A comprehensive way to confirm euploidy is to perform comparative genomic hybridization using microarrays to examine the genome content of a polyploid against a reference haploid genome. Transcriptomic profiling can also reveal aneuploidy of a chromosome, based on the large-scale indicative perturbation in transcriptome observed in aneuploid haploids (Torres et al., 2007). Alternatively, genome integrity can be assessed by using chromosome specific probes in quantitative PCR to make sure equal representation of all chromosomes in a polyploid as compared with a haploid control.

## **Materials and Methods**

### **Yeast strains, genetic engineering and growth conditions**

Strains used in this study are listed at the end of this section. Standard molecular techniques were employed to engineer mutant and epitope-tagged strains. All engineered strains were verified by polymerase chain reaction and/or western blotting. Functions of epitope-tagged alleles were assessed by their ability to complement expression or phenotypic defects of null mutants. Prior to analysis, all cultures were grown from diluted overnight pre-cultures until mid-log phase in the SC medium supplemented with 2% glucose at 30°C on a shaker.

### **Construction of isogenic ploidy series**

Repeated rounds of mating-type switching and zygote selection were performed to obtain isogenic ploidy series. Typically the process of generating a *MAT $\alpha\alpha\alpha\alpha$*  or *MAT $aaaa$*  tetraploid from an isogenic haploid takes 4 to 6 weeks. Briefly, haploid strains with suitable genotypes were transformed with a plasmid encoding the HO endonuclease inducible by galactose to enable mating-type switching. Transformed strains were pre-grown overnight in SC drop-out medium supplemented with 0.1% glucose. After sufficient washing with water, cells were resuspended in SC drop-out medium + 2% galactose and grown for 3 hours to enable mating type switching before plating on YPD. Mating-type switched candidates were passaged multiple times on YPD to ensure loss of the HO-encoding plasmid prior to mating-type assessment by auxotrophic marker complementation or a pheromone-dependent growth inhibition assay.

## **Chromatin Immunoprecipitation**

Chromatin Immunoprecipitation was performed as described (Zeitlinger et al., 2003). Monoclonal antibody against the 9E11 epitope (Covance) was used to precipitate myc-tagged proteins. Anti-Rpb3 antibody (NeoClone) was used to precipitate RNA polymerase II complex. Enrichment of chromatin of interest was measured by quantitative PCR. Primer specificity was evaluated by the dissociation melting temperature of amplicon. Specificity was also confirmed by the absence of amplicons when the target sequence had been deleted in the genome used as qPCR template, when applicable. Quantitative ChIP results were analyzed as previously described (Keogh and Buratowski, 2004).

## **Measurement of gene expression by quantitative PCR**

See methods section in chapter 2.

## Yeast strains

All strains are in the Sigma 1278b background with the genotype *ura3-52, leu2::hisG*

*his3::hisG* and were created in this study unless noted otherwise.

<u>Strain ID</u>	<u>Genotype or Description</u>	<u>Reference/Source</u>
(figure 1)		
yCW93	<i>MATa, flo11Δ::lacZ-LEU2, NUP49-GFP-HIS3</i>	
yCW157	<i>MATaaaa</i> isogenic strain to yCW93	
yCW111	<i>MATa, FLO11</i> promoter and ORF replaced with kanMX, p <i>FLO11-lacZ-LEU2</i> at <i>URA3</i> locus, <i>NUP49-GFP-HIS3</i>	
yCW173	<i>MATaaaa</i> isogenic strain to yCW111	
yCW497	yCW93 transformed with bCW78 (see below)	
yCW499	yCW157 transformed with bCW78	
(figure2)		
L6437	<i>MATa</i> WT	Galitski <i>et al.</i> , Science 1999
L6440	<i>MATaaaa</i> isogenic strain to L6437	"
L7003	<i>MATa, tec1Δ::HIS3</i>	Gerald Fink lab stock
yCW180	<i>MATa, FLO8-9myc-TRP1</i>	
yCW207	<i>MATαααα</i> isogenic strain to yCW180	
yCW10	<i>MATa, 3myc-TEC1</i>	
yCW28	<i>MATaaaa</i> isogenic strain to yCW10	
yCW1	<i>MATa, STE12-9myc-TRP1, trp1::hisG</i>	
yCW41	<i>MATaaaa</i> isogenic strain to yCW1	
yCW43	<i>MATa, GCN4-9myc-TRP1, trp1::hisG</i>	
yCW76	<i>MATaaaa</i> isogenic strain to yCW43	
(figure 3)		
yCW552	<i>MATa, kss1Δ::ura3::LEU2, ste7Δ::HIS3, trp1::hisG</i>	Fink strain L6237
yCW582	<i>MATaa</i> , isogenic strain to yCW552	
yCW686	<i>MATa, dig1Δ::kanMX</i>	Charles Boone
yCW758	<i>MATaaaa</i> , isogenic strain to yCW686	
yCW493	<i>MATa, mpt5Δ::kanMX</i>	Charles Boone
yCW490	isogenic <i>MATaa</i>	

yCW372	<i>MATa</i> , <i>msb2</i> without mucin repeats	
yCW441	<i>MATaaaa</i> , isogenic strain to yCW372	
(figure 4)		
yCW350	<i>MATa</i> , <i>leu2::3myc-TEC1 T273M</i>	Hans-Ulrich Mosch
yCW423	<i>MATaaaa</i> , isogenic to yCW350	
(figure 5)		
yCW745	<i>MATa</i> , <i>hog1Δ::TRP1, flo11Δ::yEGFP-URA3</i>	
yCW796	<i>MATaaaa</i> isogenic to yCW745	
(figure 6)		
yCW478	<i>MATa</i> , WT	Charles Boone
yCW514	<i>MATa</i> , isogenic to yCW478 except <i>bck1Δ::kanMX</i>	"
yCW492	<i>MATa</i> , isogenic to yCW478 except <i>mpk1Δ::kanMX</i>	"
yCW610	<i>MATa</i> , <i>flo11Δ::yEGFP-URA3</i>	
yCW612	<i>MATa</i> , isogenic to yCW610 except <i>bck1Δ::kanMX</i>	
yCW479	<i>MATa</i> , WT	Charles Boone
yCW625	<i>MATaaaa</i> , isogenic to yCW479	
yCW560	<i>MATa</i> , <i>bck1Δ::kanMX</i>	
yCW555	<i>MATaaaa</i> , isogenic to yCW560	
(figure 7)		
yCW506	<i>MATa</i> , <i>sfl1Δ::HIS3, flo11Δ::yEGFP-URA3</i>	
yCW530	<i>MATaa</i> , isogenic to yCW506	
yCW511	<i>MATa/α</i> , isogenic to yCW506	
yCW675	<i>MATaa/aa</i> , isogenic to yCW506	
yCW749	<i>MATa</i> , <i>tpk3Δ::HIS3, flo11Δ::yEGFP-URA3, trp1</i>	
yCW794	<i>MATaaaa</i> isogenic to yCW749	
(figure 8)		
yCW4	<i>MATa</i> , <i>NRG1-9myc-TRP1</i>	
yCW57	<i>MATaaaa</i> isogenic to yCW4	
(figure 9)		
L6437	<i>MATa</i> , WT	Galitski <i>et al.</i> , Science 1999
L6440	<i>MATaaaa</i> isogenic to L6440	"
yCW98	<i>MATa</i> , <i>hda1Δ::kanMX, FLO11-HA</i>	S. Bumgarner/Fink lab
yCW153	<i>MATaaaa</i> isogenic to yCW153	
(figure 10)		
L6437	<i>MATa</i> , WT	Galitski <i>et al.</i> , Science 1999
L6438	isogenic <i>MATaa</i>	"

L6439	isogenic <i>MATaaa</i>	"
L6440	isogenic <i>MATaaaa</i>	"
L6441	<i>MATα</i> , WT	"
L6442	isogenic <i>MATaa</i>	"
L6443	isogenic <i>MATaaa</i>	"
L6444	isogenic <i>MATaaaa</i>	"
yCW43	<i>MATa</i> , <i>GCN4-9myc-TRP1</i> , <i>trp1::hisG</i>	
yCW60	isogenic <i>MATaa</i>	
yCW76	isogenic <i>MATaaaa</i>	
yCW48	isogenic <i>MATα</i>	
yCW54	isogenic <i>MATaa</i>	
yCW77	isogenic <i>MATaaaa</i>	
yCW151	<i>MATa</i> , <i>flo11Δ::yEGFP-URA3</i>	S. Chen/Fink lab
yCW163	isogenic <i>MATaa</i>	
yCW175	isogenic <i>MATaaaa</i>	
yCW92	isogenic <i>MATα</i>	
yCW164	isogenic <i>MATaa</i>	

(figure 11)  
WT *MATa* ploidy series, as in figure 10

### Plasmids

<u>Plasmid ID</u>	<u>Description</u>	<u>Reference/Source</u>
bCW78	<i>GALIS</i> promoter driving <i>FLO11</i> ORF and 3'UTR cloned from an S288c genomic DNA library, <i>URA3</i> as selectable marker, CEN.	
B4099	<i>FLO11</i> promoter upstream of <i>lacZ</i> ORF, for integrative transformation to use <i>lacZ</i> as a reporter for <i>FLO11</i> promoter activity. <i>LEU2</i> as selectable marker.	Gerald Fink lab stock

## **References**

- Andalis, A.A., Storchova, Z., Styles, C., Galitski, T., Pellman, D., and Fink, G.R. (2004). Defects arising from whole-genome duplications in *Saccharomyces cerevisiae*. *Genetics* 167, 1109-1121.
- Bao, M.Z., Schwartz, M.A., Cantin, G.T., Yates, J.R., and Madhani, H. (2004). Pheromone-dependent destruction of the Tec1 transcription factor is required for MAP kinase signaling specificity in yeast. *Cell* 119, 991-1000.
- Bao, M.Z., Shock, T.R., and Madhani, H.D. (2009). Multisite phosphorylation of the *S. cerevisiae* filamentous growth regulator Tec1 is required for its recognition by the E3 ubiquitin ligase adaptor Cdc4 and its subsequent destruction in vivo. *Eukaryot Cell*.
- Berkey, C.D., Vyas, V.K., and Carlson, M. (2004). *Nrg1* and *nrg2* transcriptional repressors are differently regulated in response to carbon source. *Eukaryot Cell* 3, 311-317.
- Bruckner, S., Kohler, T., Braus, G.H., Heise, B., Bolte, M., and Mosch, H.U. (2004). Differential regulation of Tec1 by Fus3 and Kss1 confers signaling specificity in yeast development. *Curr Genet* 46, 331-342.
- Bruhn, L., and Sprague, G.F., Jr. (1994). MCM1 point mutants deficient in expression of alpha-specific genes: residues important for interaction with alpha 1. *Mol Cell Biol* 14, 2534-2544.
- Bumgarner, S.L., Dowell, R.D., Grisafi, P., Gifford, D.K., and Fink, G.R. (2009). Toggle involving cis-interfering noncoding RNAs controls variegated gene expression in yeast. *Proc Natl Acad Sci U S A* 106, 18321-18326.
- Chen, H., and Fink, G.R. (2006). Feedback control of morphogenesis in fungi by aromatic alcohols. *Genes Dev* 20, 1150-1161.
- Chen, R.E., and Thorner, J. (2007). Function and regulation in MAPK signaling pathways: lessons learned from the yeast *Saccharomyces cerevisiae*. *Biochim Biophys Acta* 1773, 1311-1340.
- Choi, K.Y., Satterberg, B., Lyons, D.M., and Elion, E.A. (1994). Ste5 tethers multiple protein kinases in the MAP kinase cascade required for mating in *S. cerevisiae*. *Cell* 78, 499-512.
- Chou, S., Huang, L., and Liu, H. (2004). Fus3-Regulated Tec1 Degradation through SCF(Cdc4) Determines MAPK Signaling Specificity during Mating in Yeast. *Cell* 119, 981-990.
- Chou, S., Lane, S., and Liu, H. (2006). Regulation of mating and filamentation genes by two distinct Ste12 complexes in *Saccharomyces cerevisiae*. *Mol Cell Biol* 26, 4794-4805.
- Conlan, R.S., and Tzamarias, D. (2001). Sfl1 functions via the co-repressor Ssn6-Tup1 and the cAMP-dependent protein kinase Tpk2. *J Mol Biol* 309, 1007-1015.



- Cook, J.G., Bardwell, L., Kron, S.J., and Thorner, J. (1996). Two novel targets of the MAP kinase Kss1 are negative regulators of invasive growth in the yeast *Saccharomyces cerevisiae*. *Genes Dev* 10, 2831-2848.
- Cook, J.G., Bardwell, L., and Thorner, J. (1997). Inhibitory and activating functions for MAPK Kss1 in the *S. cerevisiae* filamentous-growth signalling pathway. *Nature* 390, 85-88.
- Cullen, P.J., Sabbagh, W., Jr., Graham, E., Irick, M.M., van Olden, E.K., Neal, C., Delrow, J., Bardwell, L., and Sprague, G.F., Jr. (2004). A signaling mucin at the head of the Cdc42- and MAPK-dependent filamentous growth pathway in yeast. *Genes Dev* 18, 1695-1708.
- Cullen, P.J., and Sprague, G.F., Jr. (2000). Glucose depletion causes haploid invasive growth in yeast. *Proc Natl Acad Sci U S A* 97, 13619-13624.
- Davenport, K.D., Williams, K.E., Ullmann, B.D., and Gustin, M.C. (1999). Activation of the *Saccharomyces cerevisiae* filamentation/invasion pathway by osmotic stress in high-osmolarity glycogen pathway mutants. *Genetics* 153, 1091-1103.
- Dohlman, H.G., and Slessareva, J.E. (2006). Pheromone signaling pathways in yeast. *Sci STKE* 2006, cm6.
- Gagiano, M., Van Dyk, D., Bauer, F.F., Lambrechts, M.G., and Pretorius, I.S. (1999). Divergent regulation of the evolutionarily closely related promoters of the *Saccharomyces cerevisiae* STA2 and MUC1 genes. *J Bacteriol* 181, 6497-6508.
- Galitski, T., Saldanha, A.J., Styles, C.A., Lander, E.S., and Fink, G.R. (1999). Ploidy regulation of gene expression. *Science* 285, 251-254.
- Ganem, N.J., Storchova, Z., and Pellman, D. (2007). Tetraploidy, aneuploidy and cancer. *Curr Opin Genet Dev* 17, 157-162.
- Gavrias, V., Andrianopoulos, A., Gimeno, C.J., and Timberlake, W.E. (1996). *Saccharomyces cerevisiae* TEC1 is required for pseudohyphal growth. *Mol Microbiol* 19, 1255-1263.
- Gimeno, C.J., Ljungdahl, P.O., Styles, C.A., and Fink, G.R. (1992). Unipolar cell divisions in the yeast *S. cerevisiae* lead to filamentous growth: regulation by starvation and RAS. *Cell* 68, 1077-1090.
- Good, M., Tang, G., Singleton, J., Remenyi, A., and Lim, W.A. (2009). The Ste5 scaffold directs mating signaling by catalytically unlocking the Fus3 MAP kinase for activation. *Cell* 136, 1085-1097.
- Guo, B., Styles, C.A., Feng, Q., and Fink, G.R. (2000). A *Saccharomyces* gene family involved in invasive growth, cell-cell adhesion, and mating. *Proc Natl Acad Sci U S A* 97, 12158-12163.

- Halme, A., Bumgarner, S., Styles, C., and Fink, G.R. (2004). Genetic and epigenetic regulation of the FLO gene family generates cell-surface variation in yeast. *Cell* 116, 405-415.
- Harbison, C.T., Gordon, D.B., Lee, T.I., Rinaldi, N.J., Macisaac, K.D., Danford, T.W., Hannett, N.M., Tagne, J.B., Reynolds, D.B., Yoo, J., *et al.* (2004). Transcriptional regulatory code of a eukaryotic genome. *Nature* 431, 99-104.
- Hohmann, S., Krantz, M., and Nordlander, B. (2007). Yeast osmoregulation. *Methods Enzymol* 428, 29-45.
- Keogh, M.C., and Buratowski, S. (2004). Using chromatin immunoprecipitation to map cotranscriptional mRNA processing in *Saccharomyces cerevisiae*. *Methods Mol Biol* 257, 1-16.
- Kim, T.S., Kim, H.Y., Yoon, J.H., and Kang, H.S. (2004). Recruitment of the Swi/Snf complex by Ste12-Tec1 promotes Flo8-Mss11-mediated activation of STA1 expression. *Mol Cell Biol* 24, 9542-9556.
- Kohler, T., Wesche, S., Taheri, N., Braus, G.H., and Mosch, H.U. (2002). Dual role of the *Saccharomyces cerevisiae* TEA/ATTS family transcription factor Tec1p in regulation of gene expression and cellular development. *Eukaryot Cell* 1, 673-686.
- Kuchin, S., Vyas, V.K., and Carlson, M. (2002). Snf1 protein kinase and the repressors Nrg1 and Nrg2 regulate FLO11, haploid invasive growth, and diploid pseudohyphal differentiation. *Mol Cell Biol* 22, 3994-4000.
- Lambrechts, M.G., Bauer, F.F., Marmur, J., and Pretorius, I.S. (1996). Muc1, a mucin-like protein that is regulated by Mss10, is critical for pseudohyphal differentiation in yeast. *Proc Natl Acad Sci U S A* 93, 8419-8424.
- Levin, D.E. (2005). Cell wall integrity signaling in *Saccharomyces cerevisiae*. *Microbiol Mol Biol Rev* 69, 262-291.
- Liu, H., Styles, C.A., and Fink, G.R. (1996). *Saccharomyces cerevisiae* S288C has a mutation in FLO8, a gene required for filamentous growth. *Genetics* 144, 967-978.
- Lo, W.S., and Dranginis, A.M. (1996). FLO11, a yeast gene related to the STA genes, encodes a novel cell surface flocculin. *J Bacteriol* 178, 7144-7151.
- Lo, W.S., and Dranginis, A.M. (1998). The cell surface flocculin Flo11 is required for pseudohyphae formation and invasion by *Saccharomyces cerevisiae*. *Mol Biol Cell* 9, 161-171.
- Lorenz, M.C., Pan, X., Harashima, T., Cardenas, M.E., Xue, Y., Hirsch, J.P., and Heitman, J. (2000). The G protein-coupled receptor *gpr1* is a nutrient sensor that regulates pseudohyphal differentiation in *Saccharomyces cerevisiae*. *Genetics* 154, 609-622.

Madhani, H.D., and Fink, G.R. (1997). Combinatorial control required for the specificity of yeast MAPK signaling. *Science* 275, 1314-1317.

Madhani, H.D., Styles, C.A., and Fink, G.R. (1997). MAP kinases with distinct inhibitory functions impart signaling specificity during yeast differentiation. *Cell* 91, 673-684.

Mosch, H.U., Kubler, E., Krappmann, S., Fink, G.R., and Braus, G.H. (1999). Crosstalk between the Ras2p-controlled mitogen-activated protein kinase and cAMP pathways during invasive growth of *Saccharomyces cerevisiae*. *Mol Biol Cell* 10, 1325-1335.

Mosch, H.U., Roberts, R.L., and Fink, G.R. (1996). Ras2 signals via the Cdc42/Ste20/mitogen-activated protein kinase module to induce filamentous growth in *Saccharomyces cerevisiae*. *Proc Natl Acad Sci U S A* 93, 5352-5356.

O'Rourke, S.M., and Herskowitz, I. (1998). The Hog1 MAPK prevents cross talk between the HOG and pheromone response MAPK pathways in *Saccharomyces cerevisiae*. *Genes Dev* 12, 2874-2886.

Pan, X., and Heitman, J. (2002). Protein kinase A operates a molecular switch that governs yeast pseudohyphal differentiation. *Mol Cell Biol* 22, 3981-3993.

Peter, M., Neiman, A.M., Park, H.O., van Lohuizen, M., and Herskowitz, I. (1996). Functional analysis of the interaction between the small GTP binding protein Cdc42 and the Ste20 protein kinase in yeast. *Embo J* 15, 7046-7059.

Prinz, S., Aldridge, C., Ramsey, S.A., Taylor, R.J., and Galitski, T. (2007). Control of signaling in a MAP-kinase pathway by an RNA-binding protein. *PLoS One* 2, e249.

Ramezani-Rad, M. (2003). The role of adaptor protein Ste50-dependent regulation of the MAPKKK Ste11 in multiple signalling pathways of yeast. *Curr Genet* 43, 161-170.

Roberts, R.L., and Fink, G.R. (1994). Elements of a single MAP kinase cascade in *Saccharomyces cerevisiae* mediate two developmental programs in the same cell type: mating and invasive growth. *Genes Dev* 8, 2974-2985.

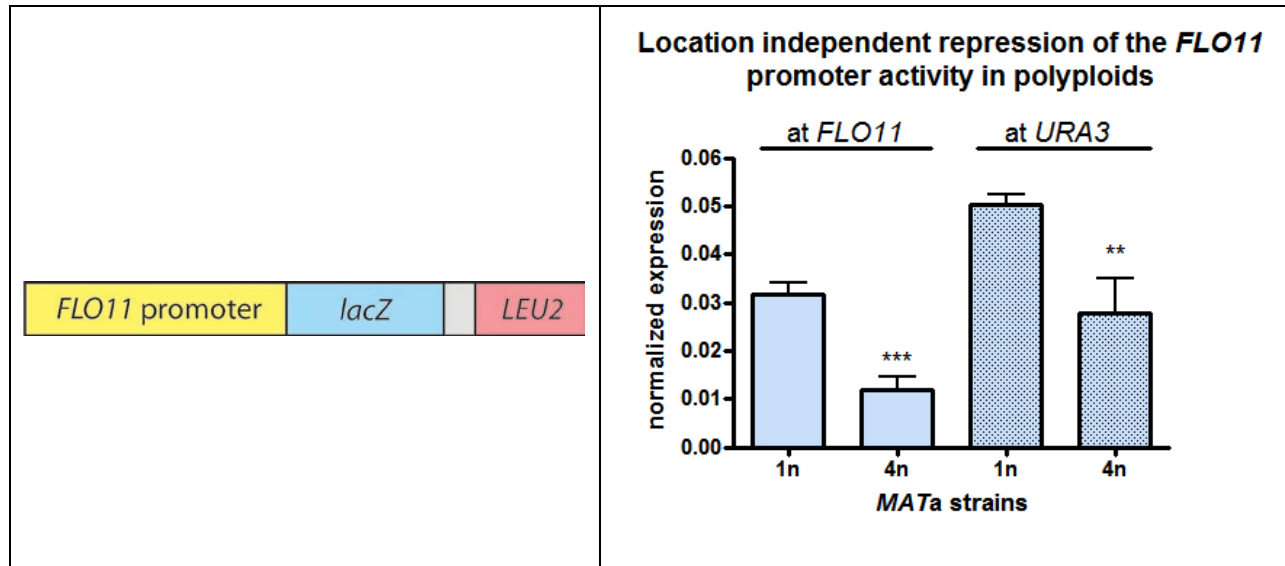
Robertson, L.S., and Fink, G.R. (1998). The three yeast A kinases have specific signaling functions in pseudohyphal growth. *Proc Natl Acad Sci U S A* 95, 13783-13787.

Rupp, S., Summers, E., Lo, H.J., Madhani, H., and Fink, G. (1999). MAP kinase and cAMP filamentation signaling pathways converge on the unusually large promoter of the yeast FLO11 gene. *Embo J* 18, 1257-1269.

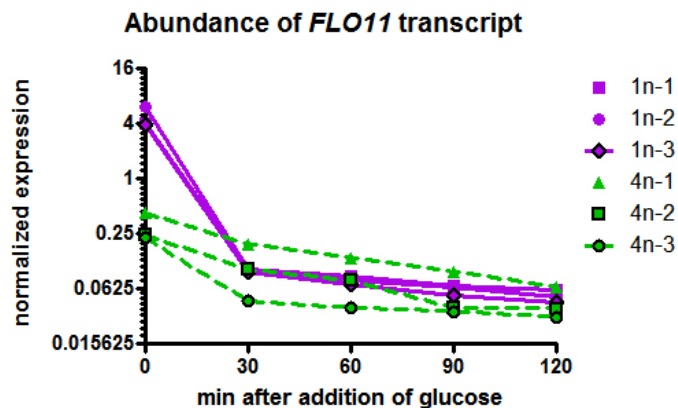
Shock, T.R., Thompson, J., Yates, J.R., 3rd, and Madhani, H.D. (2009). Hog1 mitogen-activated protein kinase (MAPK) interrupts signal transduction between the Kss1 MAPK and the Tec1 transcription factor to maintain pathway specificity. *Eukaryot Cell* 8, 606-616.

- Storchova, Z., Breneman, A., Cande, J., Dunn, J., Burbank, K., O'Toole, E., and Pellman, D. (2006). Genome-wide genetic analysis of polyploidy in yeast. *Nature* 443, 541-547.
- Tatebayashi, K., Tanaka, K., Yang, H.Y., Yamamoto, K., Matsushita, Y., Tomida, T., Imai, M., and Saito, H. (2007). Transmembrane mucins Hkr1 and Msb2 are putative osmosensors in the SHO1 branch of yeast HOG pathway. *Embo J* 26, 3521-3533.
- Tedford, K., Kim, S., Sa, D., Stevens, K., and Tyers, M. (1997). Regulation of the mating pheromone and invasive growth responses in yeast by two MAP kinase substrates. *Curr Biol* 7, 228-238.
- Torres, E.M., Sokolsky, T., Tucker, C.M., Chan, L.Y., Boselli, M., Dunham, M.J., and Amon, A. (2007). Effects of aneuploidy on cellular physiology and cell division in haploid yeast. *Science* 317, 916-924.
- van Dyk, D., Pretorius, I.S., and Bauer, F.F. (2005). Mss11p is a central element of the regulatory network that controls FLO11 expression and invasive growth in *Saccharomyces cerevisiae*. *Genetics* 169, 91-106.
- Whiteway, M.S., Wu, C., Leeuw, T., Clark, K., Fourest-Lieuvin, A., Thomas, D.Y., and Leberer, E. (1995). Association of the yeast pheromone response G protein beta gamma subunits with the MAP kinase scaffold Ste5p. *Science* 269, 1572-1575.
- Winters, M.J., and Pryciak, P.M. (2005). Interaction with the SH3 domain protein Bem1 regulates signaling by the *Saccharomyces cerevisiae* p21-activated kinase Ste20. *Mol Cell Biol* 25, 2177-2190.
- Wu, C., Jansen, G., Zhang, J., Thomas, D.Y., and Whiteway, M. (2006). Adaptor protein Ste50p links the Ste11p MEKK to the HOG pathway through plasma membrane association. *Genes Dev* 20, 734-746.
- Xue, Y., Batlle, M., and Hirsch, J.P. (1998). GPR1 encodes a putative G protein-coupled receptor that associates with the Gpa2p Galpha subunit and functions in a Ras-independent pathway. *Embo J* 17, 1996-2007.
- Zeitlinger, J., Simon, I., Harbison, C.T., Hannett, N.M., Volkert, T.L., Fink, G.R., and Young, R.A. (2003). Program-specific distribution of a transcription factor dependent on partner transcription factor and MAPK signaling. *Cell* 113, 395-404.

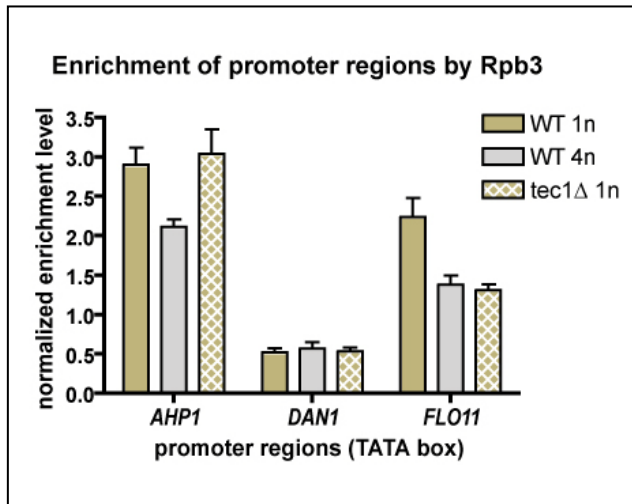
## Figures and Table



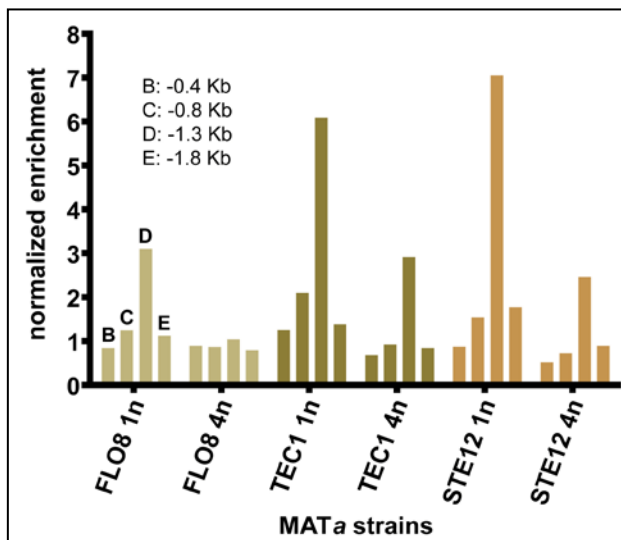
**Figure 1a.** The *FLO11* promoter is sufficient for conferring ploidy-regulation. **Left:** By integrative transformation, the *FLO11* ORF and 3'UTR was replaced with the *lacZ* reporter gene followed by the *LEU2* selection marker. The *LacZ* and *LEU2* sequence came from vector YEp365 and was used to construct the Fink lab plasmid B4099 for integration at the *FLO11* locus. In a separate strain, the entire region shown in the diagram was inserted at the *URA3* locus by integrative transformation. **Right:** Like the *FLO11* ORF, *lacZ* reporter expression levels are significantly reduced in the isogenic tetraploids. The down-regulation of *FLO11* promoter activity occurs at both genomic locations.



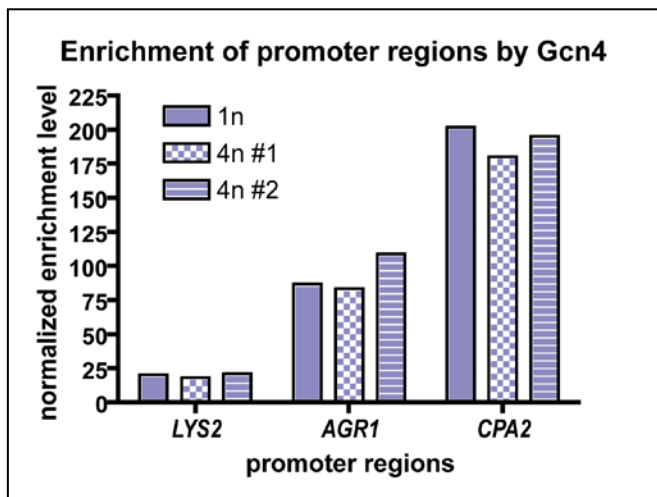
**Figure 1b.** Degradation of *FLO11* RNA in haploids (solid purple lines) and tetraploids (dotted green lines) after addition of glucose to turn off *FLO11* expression from the *GALI* promoter.



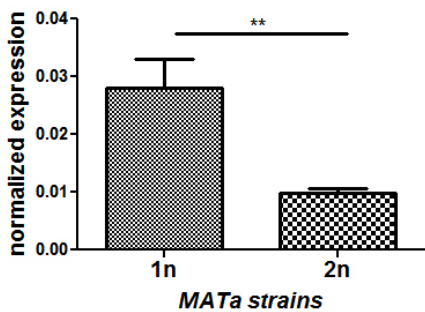
**Figure 2a.** Reduced association of RNA pol II with the *FLO11* promoter in polyploids. Chromatin was co-immunoprecipiated with Rpb3, a component of RNA pol II. *AHP1* (a well expressed gene) and *DAN1* (a silenced gene) are reference chromatin regions with strong and little binding of RNA pol II, respectively. In all strains, expression levels of *FLO11* are between those of *AHP1* and *DAN1* (data not shown). The intermediate enrichment levels of *FLO11* promoter by ChIP correlate well with its relative transcript abundance, validating reduced association of RNA pol II in tetraploids.



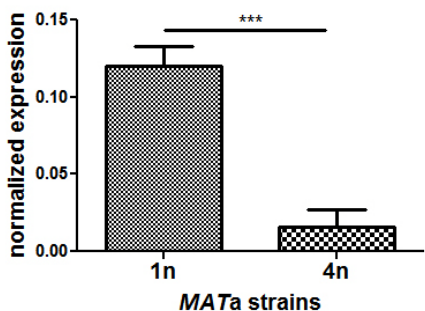
**Figure 2b.** Reduced binding of key transcription activators to the *FLO11* promoter in polyploids. Epitope-tagged transcription factors had been confirmed to be functional by invasive growth in haploids, and isogenic tetraploids were then constructed. Different primer sets (B-E) were used to detect enrichment of various regions of the promoter. Region D, about 1.3Kb upstream of the ORF, was most enriched by all three transcription factors in haploids. Enrichment of *FLO11* promoter in tetraploids displays the same pattern but a smaller magnitude for region D.



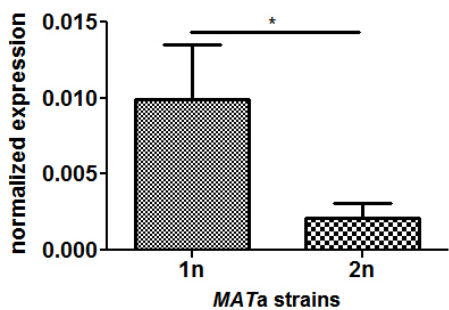
**Figure 2c.** Binding of Gcn4 to chromatin is not reduced in polyploids.



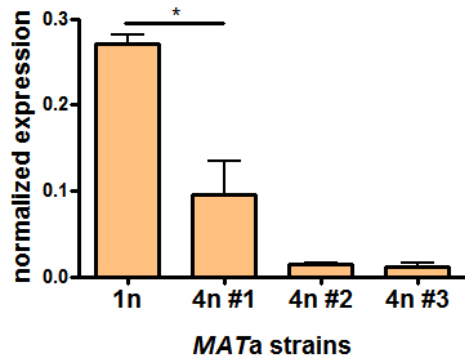
**Figure 3a.** Ploidy-associated reduction in *FLO11* expression in the *kss1Δ ste7Δ* double mutant background.



**Figure 3b.** Repression of *FLO11* in polyploids in the *digΔ* mutant background.

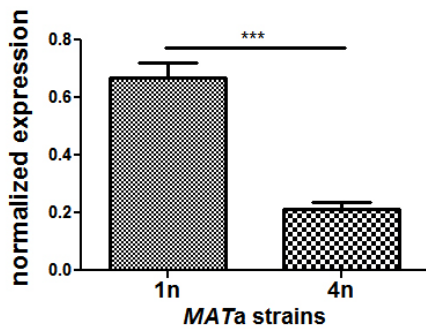
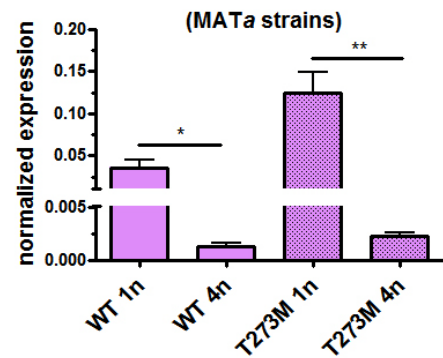


**Figure 3c.** Ploidy-dependent repression of *FLO11* in *mpt5Δ* mutants.



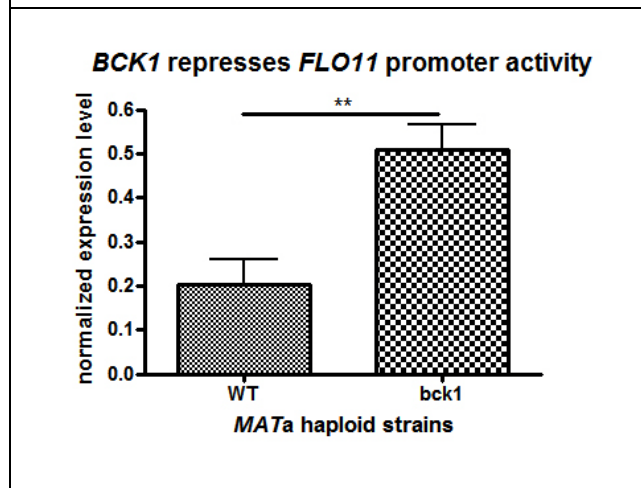
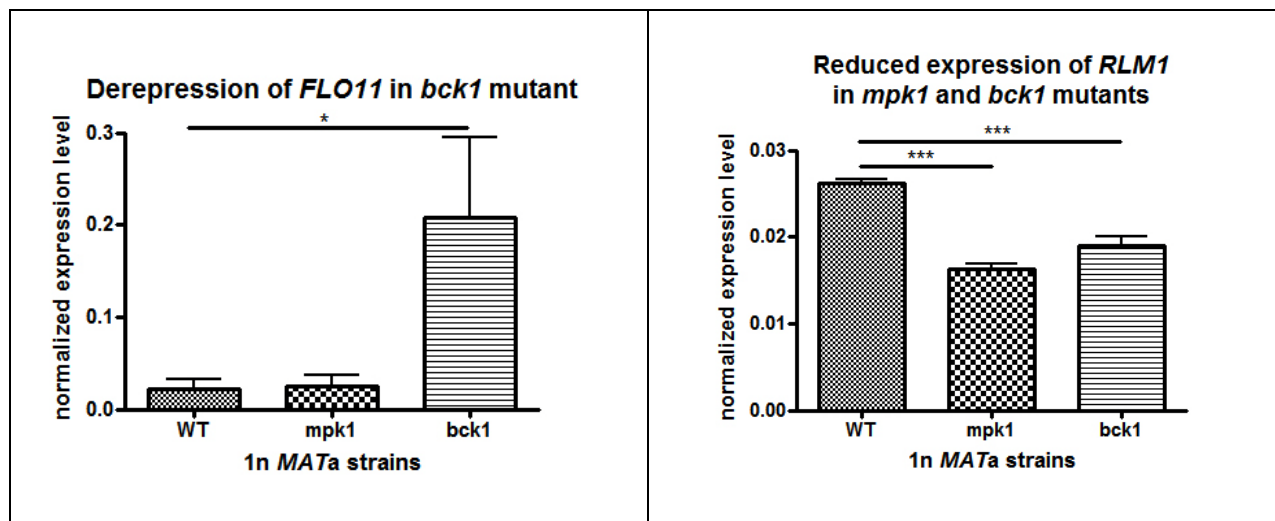
**Figure 3d.** The mucin repeats in *Msb2* are not required for ploidy-regulation of *FLO11*.

**Figure 4.** Ploidy regulation of *FLO11* in the *TEC1* T273M mutant background. T273M amino acid substitution stabilizes Tec1 protein. However, repression of *FLO11* still occurs in the polyploid.

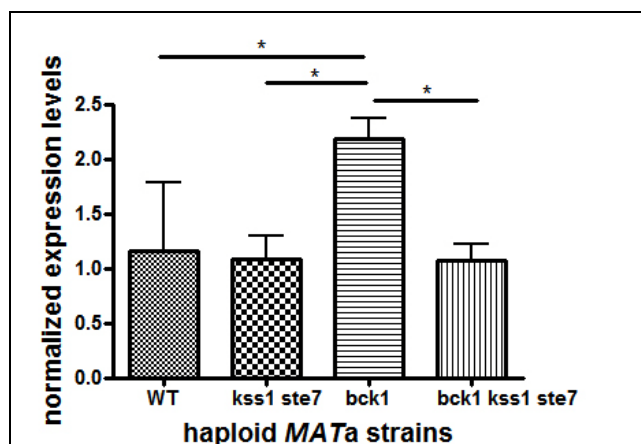


**Figure 5.** Promoter activity of *FLO11* in the *hog1Δ* haploid and tetraploid mutants. The *FLO11* ORF was replaced with GFP as a reporter of promoter strength.

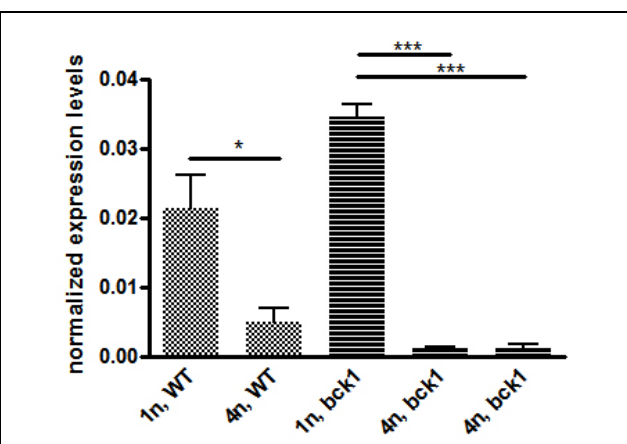




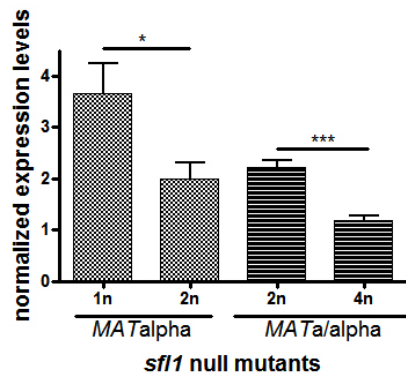
**Figure 6a.** *Bck1* represses *FLO11* expression. Diagonal: Expression of *FLO11* is de-repressed in *bck1* $\Delta$  but not *mpk1* $\Delta$  mutant. Above: On the contrary, *RLM1*, a target gene of the CWI pathway, is similarly repressed in both mutants, suggesting similar degrees of defect in CWI signaling in both mutants. Left: *Bck1* inhibits transcription at *FLO11* promoter. The GFP ORF is used as a reporter of *FLO11* promoter activity.



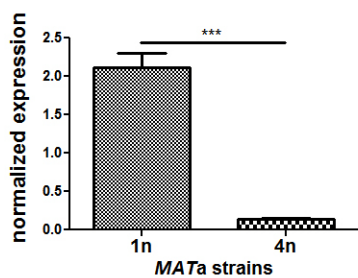
**Figure 6b.** The double mutant *kss1* $\Delta$  *ste7* $\Delta$  is epistatic to *bck1* $\Delta$ . Expression of *FLO11* was quantified in haploids with the designated genotypes.



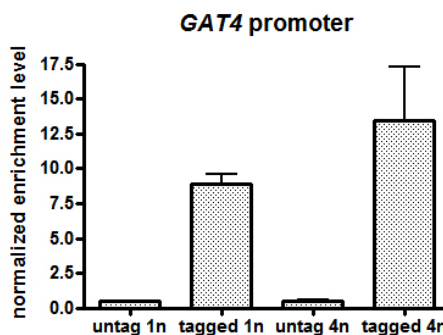
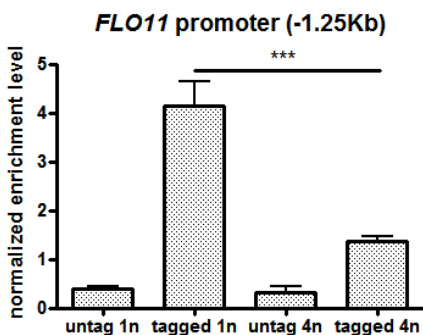
**Figure 6c.** Expression of *FLO11* in *bck1* $\Delta$  haploid and tetraploid mutants.



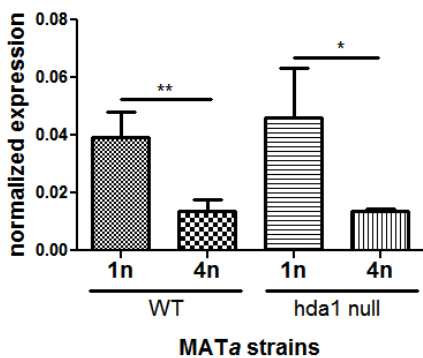
**Figure 7a.** Ploidy-mediated repression of *FLO11* expression (reporter = GFP) does not require Sfl1.



**Figure 7b.** The promoter activity of *FLO11* remains repressed by polyploidy in the *tpk3Δ* mutant background. The GFP ORF is used as a reporter for expression from the *FLO11* promoter.

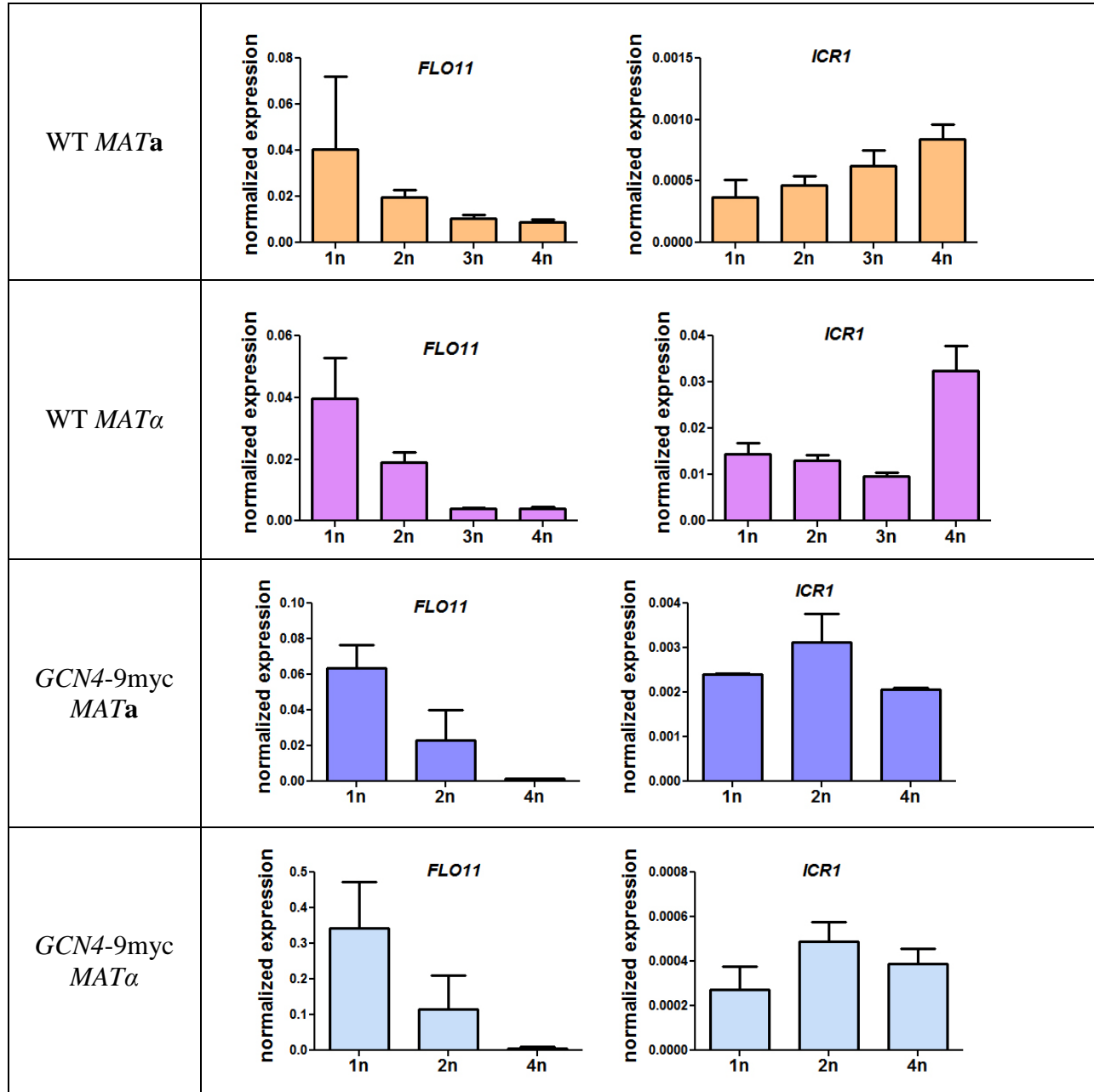


**Figure 8.** Enrichment of promoter chromatin by Nrg1 in isogenic haploid and tetraploid. (untagged = WT *NRG1*. tagged = *NRG1* C-terminally tagged with 9myc at endogenous locus.)



**Figure 9.** Ploidy-mediated repression of *FLO11* does not require Hda1.

**Figure 10.** Expression of *FLO11* (or *FLO11* promoter activity) and *ICR1* in multiple ploidy series. Genotypes of the isogenic ploidy series are noted above. Expression of *ICR1* was measured using qPCR primers amplifying ~1.3Kb upstream of the *FLO11* start codon, a region where transcription of *ICR1* would interfere with binding of Flo8, Ste12 and Tec1.



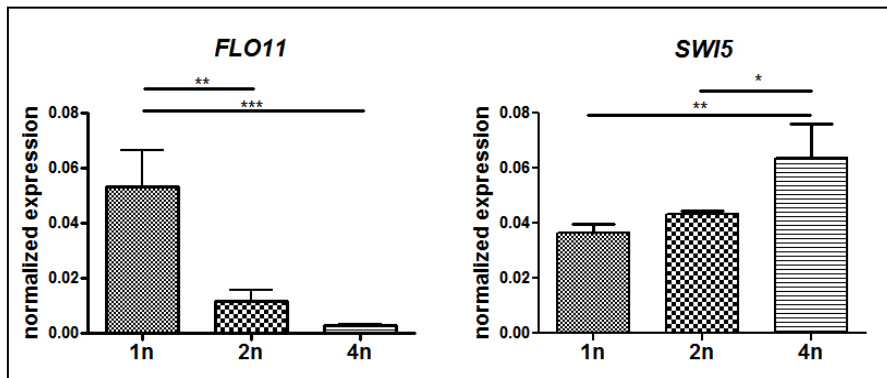
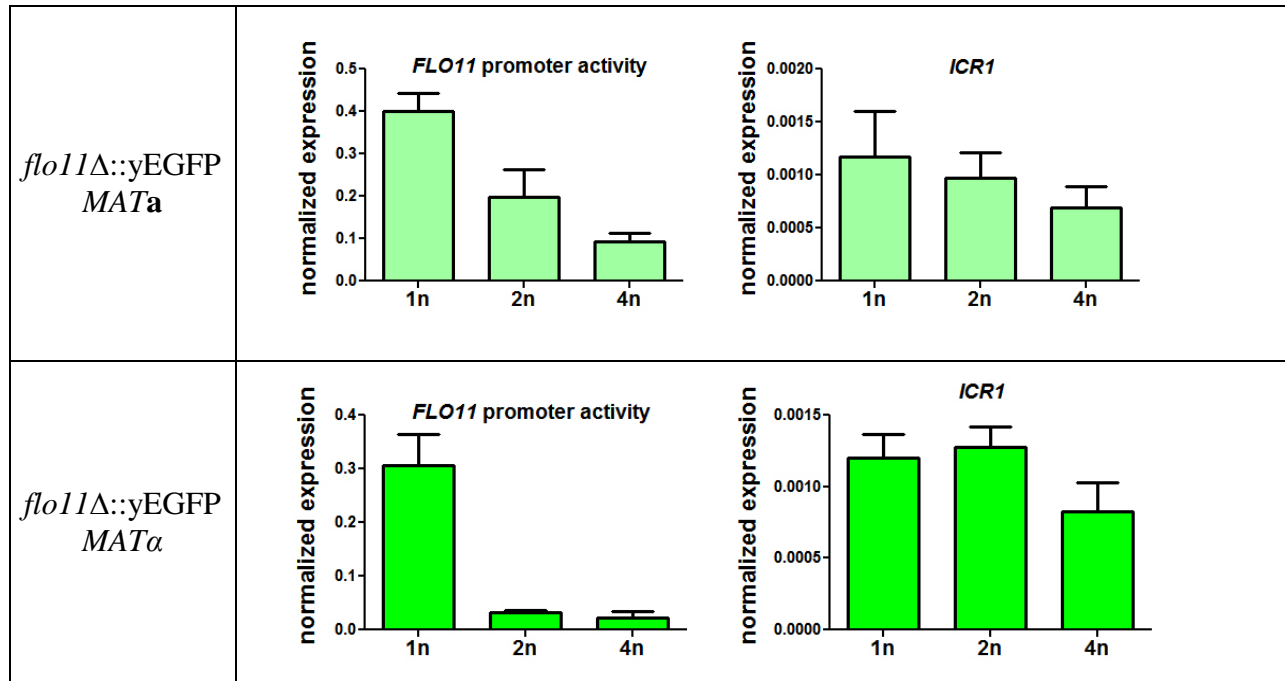


**Figure 11.** Expression of *FLO11* and *SWI5* in the WT *MATa* ploidy series.

**Table 1.** Normalized expression levels of *FLO11* (relative to *ACT1*) in *MATa* and *MATaaaa* WT strains at  $\sim 3 \times 10^7$  cells/mL.

strain	1n #1	1n #2	4n #1	4n #2
<i>FLO11</i>	0.19	0.19	0.025	0.011

## Chapter 4. Discussion and future directions

### Cell size and ploidy

Although the exact mechanism by which polyploidy enlarges cell size is unclear, recent studies on polyploid *S. cerevisiae* have provided considerable insight to aid further investigation. While cell volume increases proportionally with increasing ploidy, the doubling time remains unchanged in a ploidy series (Di Talia et al., 2007 and Appendix I). Earlier work suggests that the cell size threshold is established by the balance between rate of cell growth and frequency of mitotic division (Cook and Tyers, 2007; Jorgensen et al., 2002). Hence, an increase in cell size without a reduction in cell division frequency in polyploids must result from a faster rate of biomass accumulation. Since the cell volume scales linearly with ploidy in yeast, the rate of biomass accumulation is likely proportional to ploidy. The unchanged doubling time also raises interesting questions concerning cell cycle regulation. The fact that polyploidy does not significantly alter cell cycle progression (Storchova et al., 2006) suggests that the relative but not absolute abundance of cell cycle regulators with respect to the genome determines timely progression of mitotic cell cycle.

An *in vitro* study using synthetic macromolecules illustrates how a greater cellular biomass could increase cell size by simple physical principles. The study showed that RNA polymers encapsulated in fatty acid vesicles can generate sufficient osmotic pressure to expand the vesicles, provided that additional fatty acid molecules are available in the system to enable vesicle growth (Chen et al., 2004). In light of this physical observation, the concentration of macromolecules in a cell could dictate cell size. High concentrations of macromolecules inside a cell increase the internal osmotic pressure, which in turn triggers water inflow and thus provides

the turgor pressure to expand the cellular boundary. The physical principles provide an intuitively simple explanation for the positive correlation between cell size and ploidy: In tetraploids the quadrupled genome encodes a four-fold larger capacity for production of macromolecules, whose four-fold greater abundance then enlarges the cell size by four fold.

### **Stress and compositional changes in the cell wall in response to enlarged cell size**

The budding yeast cell wall comprises at least 20% of the cellular dry weight (Smits et al., 1999). As an organelle, the cell wall performs dynamic and controlled re-structuring in order to maintain cellular morphology while enabling growth. The enlarged cell size appears to have a unique impact on the cell wall, as my RNA-seq data show that genes encoding cell wall components and their regulators are preferentially regulated both in the enlarged *cln3Δ* haploid and the naturally large tetraploid. The cell wall composition is thus likely altered in large cells, although the molecular content and organization of cell wall remain to be compared in strains of different cell sizes.

Despite the higher basal cell wall stress, polyploids do not appear to suffer gross defects in the cell wall. Using fluorescence microscopy, I detected no difference in the exposure levels of glucan and chitin on the cell surface between haploids and tetraploids grown to mid-log phase in YPD (data not shown). However, the basal level of cell wall stress appears significantly higher in polyploids, as evidenced by the elevated activity of cell wall integrity (CWI) pathway (see chapter 2). The increased pathway activity could result from a number of changes in the polyploids. First, polyploids must expand their cell wall at a faster rate than haploids to enable faster growth with an unchanged doubling time but a much larger cell size. Expansion of cell

wall requires rigorous and highly controlled wall remodeling – loosening the cell wall in targeted regions for addition of new wall components yet maintaining a sufficient force to counter the turgor pressure at the same time - to prevent bursting at structurally loosened sites. Since the remodeling process is coordinated by the CWI pathway (Levin, 2005), a faster cell wall expansion rate in polyploids likely demands a higher activity of the CWI pathway.

A second factor contributing to the elevated CWI pathway activity could be the increased turgor pressure and therefore the greater physical stress on the cell wall. The faster accumulation of cellular content in polyploids likely generates greater turgor pressure, while the relative cell wall surface area with respect to cell volume decreases due to geometric limitations. Consequently, in polyploids, each unit of the cell wall would endure a higher amount of turgor pressure and would require more rigorous CWI pathway activity to stabilize the cell wall.

Third, the likely altered cell wall composition in polyploids could induce the CWI pathway, which monitors and copes with structural changes in the cell wall (Levin, 2005). An altered composition of cell wall could weaken its structural integrity, which would exacerbate the stress endured by the wall and demand a stronger response from the CWI pathway. Whether the physical strength and structural integrity of cell wall are affected by the enlarged size of polyploids could be assessed by biochemical means. For example, resistance to digestion by glucanases and chitinases could be quantified by the degree of permeability of reporter molecules normally excluded by the intact cell wall. If larger cells have structurally compromised cell wall, they may display greater cell wall permeability given a constant amount of enzymatic treatment.

The nuclear envelope, like the cell surface, also experiences a reduction in area with respect to their enclosed volume as the cell enlarges. It has been observed that the nuclear volume in yeast is proportional to cell volume (Jorgensen et al., 2007; Neumann and Nurse, 2007). Using fluorescence microscopy to measure the diameter of nuclear envelope labeled with GFP (as a fusion protein to the nucleoporin Nup49), I also found that the nucleus in a tetraploid is indeed about four times larger than its haploid counterpart in budding yeast. Although the nuclear size enlarges with increasing cell size and is thus also under sophisticated size control (Huber and Gerace, 2007), transcriptional data from this work and previous studies (Galitski et al., 1999; Storchova et al., 2006) did not suggest a perturbation in the nuclear envelope in polyploids. Hence, the effect of polyploidy and cell size on nuclear function and structure remain unclear. Certainly, the absence of transcriptional effects does not eliminate other types of physiological perturbations that could be caused by changes in nuclear size.

### **Pathway specific responses to enlarged cell size**

The enlarged cell size does not equally affect all molecular pathways concerning the cell surface. My transcriptome data show that among the four MAPK pathways active during vegetative growth, the pheromone response and filamentation pathways are down-regulated in large cells. In tetraploids, the cell wall integrity MAPK pathway is significantly induced. As discussed earlier, data from the high osmolarity glycerol (HOG) MAPK pathway are inconclusive. These MAPK pathways may be affected differently by cell size and manifest varying degrees of differential regulation. Alternatively, they could experience a similar degree of perturbation in large cells but adapt differently. For example, the HOG pathway shows a robust response to osmotic perturbation (Hohmann, 2009). Upon hyper-osmotic shocks, the



active, dually phosphorylated MAPK Hog1 promptly translocates from cytoplasm to nucleus and induces transcription of a broad range of genes. The duration of nuclear retention of Hog1 is correlated with the osmotic differential across the plasma membrane rather than the absolute intra-cellular osmolarity. After restoration of turgor pressure by increasing intra-cellular glycerol content, the nuclear enrichment level of Hog1 returns to the baseline level observed prior to osmotic shock, thereby exhibiting perfect adaptation (Muzzey et al., 2009). The quantitative measurement of steady-state levels of transcripts described in this study would not capture the kinetic dynamics of pathway adaptation upon a sudden change in cell size. Real-time analysis would be necessary to observe whether cell size causes temporary perturbations in the HOG pathway.

Transcriptional profiling by next-generation sequencing in this thesis project was able to pinpoint pathways that are highly transcriptionally sensitive to cell size. As the transcript abundance is an imperfect proxy for protein abundance (de Godoy et al., 2008), processes affected at the level of translation or post-translational processing would only be identified by proteomic analysis. Transporters on the cell surface and nuclear envelope, if affected by enlarged cell size, could be regulated at levels of translation, post-translational modifications and protein degradation. Since the connection between cell size and physiology is fundamentally underexplored, systematic comparisons of metabolites, membrane lipid and cell wall composition in small and large cells will be necessary to reveal the totality of physiological changes associated with varying cell size.

## **Regulation of *FLO11* by cell size/ploidy and identification of its size-dependent regulator**

My data presented in chapters 2 and 3 suggest that a lack of transcriptional activation, rather than stronger transcriptional repression, is the major cause of reduced expression of *FLO11*. Removal of the potent repressor Sfl1 should enable more efficient binding of Tec1, Ste12 and Flo8. However, deletion of *SFL1* did not alter repression of *FLO11* in polyploids. ChIP results suggest that the *FLO11* promoter is less accessible in polyploids. While physical association between Nrg1 and the *GAT4* promoter is unaffected by ploidy, binding of Nrg1 to the *FLO11* promoter is diminished in polyploids. Hence, the accessibility of the *FLO11* promoter appears to be lower in polyploids, at least when compared to that of *GAT4*. The reduction in binding of Tec1/Ste12 to the *FLO11* promoter could explain this inaccessibility, as Tec1/Ste12 has been shown to recruit the Swi/Snf chromatin remodeling complex (Kim et al., 2004).

Given the complex regulation of *FLO11*, it is plausible that both the filamentous growth MAPK pathway and the cAMP/PKA pathway are inactive in polyploids. In this scenario, removal of repressors in one pathway would be insufficient to restore *FLO11* expression, as seen in my results. It would be informative to study *FLO11* in a ploidy series in which either or both kinase pathways are constitutively active. A ploidy series of a constitutively active *RAS2* mutant could also be informative. As discussed in chapter 2, the enlarged cell size of polyploids could alter signal transduction due to the reduced surface area relative to volume. The constitutively active mutants could help to pinpoint the mechanism by which polyploidy exerts repression on *FLO11*, since the molecular architectures of these signaling pathways have been uncovered. Another unexplored possibility is enhanced inhibition of both kinase pathways by phosphatases in the cytoplasm and nucleoplasm. Polyploidy could actively promote the functions of phosphatases. Alternatively, inhibition by phosphatases in polyploids could increase by a passive

mechanism. MAPKs activated at the cell periphery are expected to encounter more dephosphorylation events before reaching their nuclear targets in polyploids, simply due to the longer distance to travel in a much larger cell.

Besides the pathways mentioned above, it is formally possible that an unidentified regulator/pathway causes down-regulation of *FLO11* in polyploids. A genome-wide screen could be helpful to discover such novel regulators. A library of null deletion mutants in the Sigma 1278b background has been constructed (Dowell et al., 2010), and a systematic approach to create a tetraploid mutant library from a haploid library has been described (Storchova et al., 2006). Although such an approach is practicable, it does not bypass the time- and labor-consuming process of constructing tetraploid strains. In addition, tetraploids are genetically unstable, making a deletion library cumbersome to maintain; mutant strains in the library could easily become aneuploid.

Recently, synthetic RNAi in *S. cerevisiae* has emerged as a viable alternative to null deletions, since components in the RNAi pathway in *S. castellii* have been characterized (Drinnenberg et al., 2009). It is thus technically feasible to design an RNAi library to knock down target transcripts in tetraploids. One advantage of using RNAi is that fresh mutant strains could be conveniently engineered from a WT tetraploid, so specific knock-down mutants could be easily replaced if their genome integrity is of concern. Once constructed, the Sigma 1278b tetraploid mutant library would then be transformed with a plasmid for a genetic screen. The plasmid could express GFP driven by the *FLO11* promoter and RFP by the *ACT1* promoter. Fluorescence microscopy or FACS would then identify mutants displaying higher ratios of GFP to RFP signals than the WT. The library could also be transformed with a plasmid encoding a selectable marker driven by the *FLO11* promoter to identify new regulators via selective growth.

Mutant candidates identified in the screen would then be examined in the context of ploidy, as described in chapter 3. Since much of the physiology of tetraploid yeast is still largely unknown, a tetraploid mutant library in the Sigma 1278b background would serve many purposes for characterization of polyploids.

An alternative and complementary approach to conduct the genome-wide screen would involve use of the *cln3Δ* mutation as a surrogate for polyploidy. The *cln3Δ* haploid could be a suitable proxy for polyploids, since transcriptional activation at *FLO11* is repressed in the *cln3Δ* mutant as in the WT tetraploid. A haploid deletion library in the *cln3Δ* background could be generated by high throughput mating and sporulation. The haploid library would impart several technical advantages over the tetraploid library. It would take less effort to generate, and the haploid mutants would be genetically more stable than tetraploids. Polyploid specific lethal mutants (Storchova et al., 2006) would be viable and represented in the haploid library. Since the *cln3Δ* mutation sufficiently produces a cell size effect on *FLO11* without exacerbating cell wall stress (see discussion in chapter 2), it would also simplify the screen by focusing on factors responding to changes in cell size and thereby avoiding complications caused by elevated cell wall stress.

The genome-wide genetic screens discussed above could be adapted to study regulation of genes besides *FLO11* by cell size. Use of other promoters to drive reporter expression in the screen would facilitate better identification of the mechanism(s) by which cell size is sensed and transmitted as a signal. One major disadvantage of studying *FLO11* is its intrinsic complex regulation. Multiple signaling pathways involving *cis*- and *trans*-regulators control expression of *FLO11*, whose promoter is much longer than the genome-wide average (see chapter 3). Changes in cell size likely affect two or more pathways regulating *FLO11*, making it more difficult to

assess the role of each pathway in transcriptional responses to cell size. Regulation of other genes robustly regulated by cell size, as those identified in chapter 2, may be simpler than that of *FLO11*. These genes could provide a better opportunity for understanding the effect of cell size on cellular physiology at a detailed molecular level.

### **Potential size-sensing signaling mechanisms**

Given the complex cellular architecture and signaling network, changes in cell size could be detected by multiple cellular components. As cell volume changes, the unequal scaling between surface area and volume could affect signaling molecules between the plasma membrane and the cytoplasm. The stoichiometry and biochemical interactions among surface and cytoplasmic components could be altered, thereby affecting signaling and transcription.

In addition to molecules at the interface of cell surface and cytoplasm, the mechanism of cell size-sensing could involve the cytoskeleton or cytoplasmic organelles. Cell size sensing and control, in principle, is an integral aspect of maintaining the cellular architecture. The fact that nuclear size is proportional to cell size in budding and fission yeast (Jorgensen et al., 2007; Neumann and Nurse, 2007) suggests the existence of an elaborate cytoskeletal network connecting the nucleus to the cell periphery. The cytoskeleton thus likely expands as cell size increases. It is unclear if other organelles also enlarge with increasing cell size. Currently, the molecular details of cellular architecture are still largely unclear; whether (and how) a larger cell size affects the functional and signaling properties of various organelles remains to be examined.

Since the relationship between cell size and physiology is fundamentally underexplored, the budding yeast serves as a perfect model organism to investigate functional correlates of cell

size. Experimental tools implemented in this thesis can be developed further and combined with systematic surveys to obtain a comprehensive view of the effects of changes in cell size and pinpoint potential underlying mechanisms of cell size sensing. The principles concerning cell size, ploidy, and physiology discovered in yeast will continuously illuminate our path to understanding the basic cellular biology in other organisms.

## **References**

- Chen, I.A., Roberts, R.W., and Szostak, J.W. (2004). The emergence of competition between model protocells. *Science* 305, 1474-1476.
- Cook, M., and Tyers, M. (2007). Size control goes global. *Curr Opin Biotechnol* 18, 341-350.
- de Godoy, L.M., Olsen, J.V., Cox, J., Nielsen, M.L., Hubner, N.C., Frohlich, F., Walther, T.C., and Mann, M. (2008). Comprehensive mass-spectrometry-based proteome quantification of haploid versus diploid yeast. *Nature*.
- Di Talia, S., Skotheim, J.M., Bean, J.M., Siggia, E.D., and Cross, F.R. (2007). The effects of molecular noise and size control on variability in the budding yeast cell cycle. *Nature* 448, 947-951.
- Dowell, R.D., Ryan, O., Jansen, A., Cheung, D., Agarwala, S., Danford, T., Bernstein, D.A., Rolfe, P.A., Heisler, L.E., Chin, B., *et al.* (2010). Genotype to phenotype: a complex problem. *Science* 328, 469.
- Drinnenberg, I.A., Weinberg, D.E., Xie, K.T., Mower, J.P., Wolfe, K.H., Fink, G.R., and Bartel, D.P. (2009). RNAi in budding yeast. *Science* 326, 544-550.
- Galitski, T., Saldanha, A.J., Styles, C.A., Lander, E.S., and Fink, G.R. (1999). Ploidy regulation of gene expression. *Science* 285, 251-254.
- Hohmann, S. (2009). Control of high osmolarity signalling in the yeast *Saccharomyces cerevisiae*. *FEBS Lett* 583, 4025-4029.
- Huber, M.D., and Gerace, L. (2007). The size-wise nucleus: nuclear volume control in eukaryotes. *J Cell Biol* 179, 583-584.
- Jorgensen, P., Edgington, N.P., Schneider, B.L., Rupes, I., Tyers, M., and Futcher, B. (2007). The size of the nucleus increases as yeast cells grow. *Mol Biol Cell* 18, 3523-3532.
- Jorgensen, P., Nishikawa, J.L., Breikreutz, B.J., and Tyers, M. (2002). Systematic identification of pathways that couple cell growth and division in yeast. *Science* 297, 395-400.
- Kim, T.S., Kim, H.Y., Yoon, J.H., and Kang, H.S. (2004). Recruitment of the Swi/Snf complex by Ste12-Tec1 promotes Flo8-Mss11-mediated activation of STA1 expression. *Mol Cell Biol* 24, 9542-9556.
- Levin, D.E. (2005). Cell wall integrity signaling in *Saccharomyces cerevisiae*. *Microbiol Mol Biol Rev* 69, 262-291.
- Muzzey, D., Gomez-Urbe, C.A., Mettetal, J.T., and van Oudenaarden, A. (2009). A systems-level analysis of perfect adaptation in yeast osmoregulation. *Cell* 138, 160-171.

Neumann, F.R., and Nurse, P. (2007). Nuclear size control in fission yeast. *J Cell Biol* 179, 593-600.

Smits, G.J., Kapteyn, J.C., van den Ende, H., and Klis, F.M. (1999). Cell wall dynamics in yeast. *Curr Opin Microbiol* 2, 348-352.

Storchova, Z., Breneman, A., Cande, J., Dunn, J., Burbank, K., O'Toole, E., and Pellman, D. (2006). Genome-wide genetic analysis of polyploidy in yeast. *Nature* 443, 541-547.



## Appendix

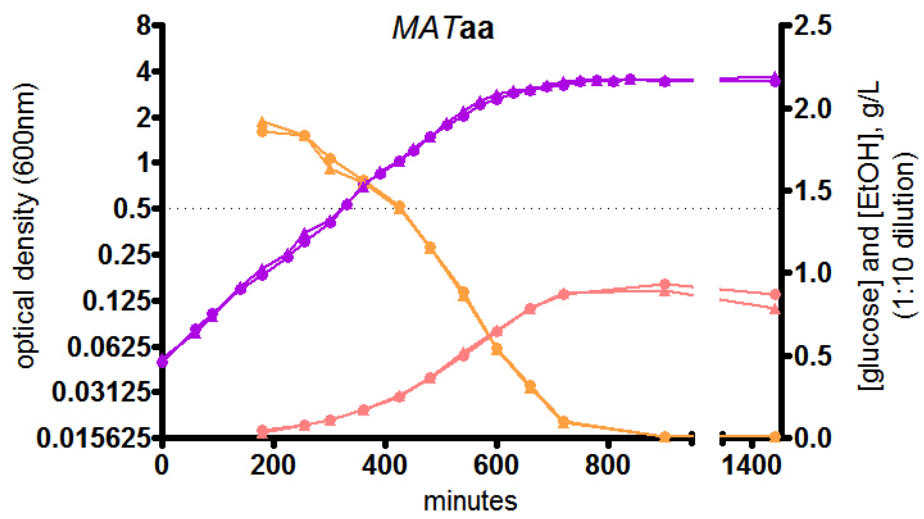
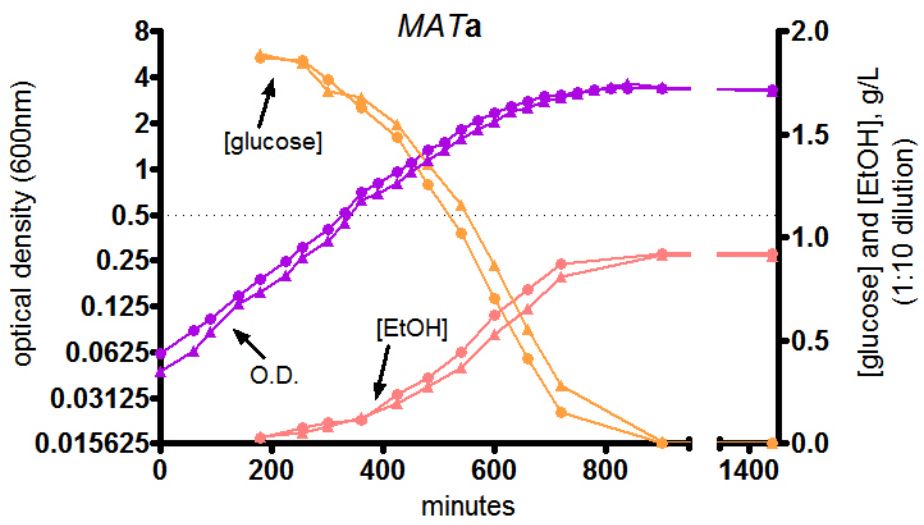
During the course of my study, I characterized growth of Sigma 1278b strains at different ploidy states and mating types. Figures 1 and 2 are results from cultures grown in a standard condition. Figure 3 shows growth of haploid and tetraploid cultures challenged with a DNA damaging agent. These results reveal fundamental properties of the strains and could aid future studies.

Figures 1 and 2 show that strains in the WT ploidy series all grew similarly. As the curves have similar slopes, the rates of change in optical density, glucose consumption and ethanol production are all similar across the series. A small difference, if significant at all, may exist due to mating type differences. The optical densities of *MATa* cultures were a bit lower than other strains during log phase. Consequently, glucose content was higher and ethanol content was lower in the haploid cultures. *MATaa* and *MATaaaa* had high optical densities, low glucose levels and high ethanol contents during log phase. The *MATa/a* cultures seemed equivalent to *MATaa* and *MATaaaa* in terms of optical densities. However, glucose utilization and ethanol production in *MATa/a* cultures appear to resemble *MATa* cultures.

It is interesting that all cultures reached the diauxic shift at about the same time, and the optical densities plateaued at similar levels. Therefore, all cultures appeared metabolically similar despite their different cell densities (table 1). Based on the growth curves, the rate of overall biomass accumulation (approximated by optical density) in the culture is independent of ploidy. Hence, a tetraploid cell is likely metabolically equivalent to multiple haploid cells under this growth condition. Andalis *et al.* discovered that tetraploids fail to arrest cell cycle in stationary phase and lose viability (Andalis et al., 2004). The stationary phase could be a more

suitable condition to reveal large-scale differences in metabolism between haploids and polyploids.

When searching for a mechanism underlying ploidy-regulation of *FLO11*, I once thought about the hypothesis that DNA damage sensing and repair might inhibit *FLO11* expression. Storchova *et al.* had just reported a higher frequency of spontaneous DNA damage and more frequent DNA repair in polyploids (Storchova et al., 2006). A connection between DNA damage repair and *FLO11* expression seemed plausible to explain down-regulation of *FLO11* in polyploids. My preliminary data did not support such a connection, and I did not explore this possibility further. For record keeping, shown in figure 3 are doubling times of haploid and tetraploid strains treated with increasing concentrations of bleomycin. As expected, tetraploids are more sensitive to bleomycin. A noticeable difference in doubling time was seen when bleomycin concentration increased from 1 to 1.5  $\mu\text{g/mL}$ .



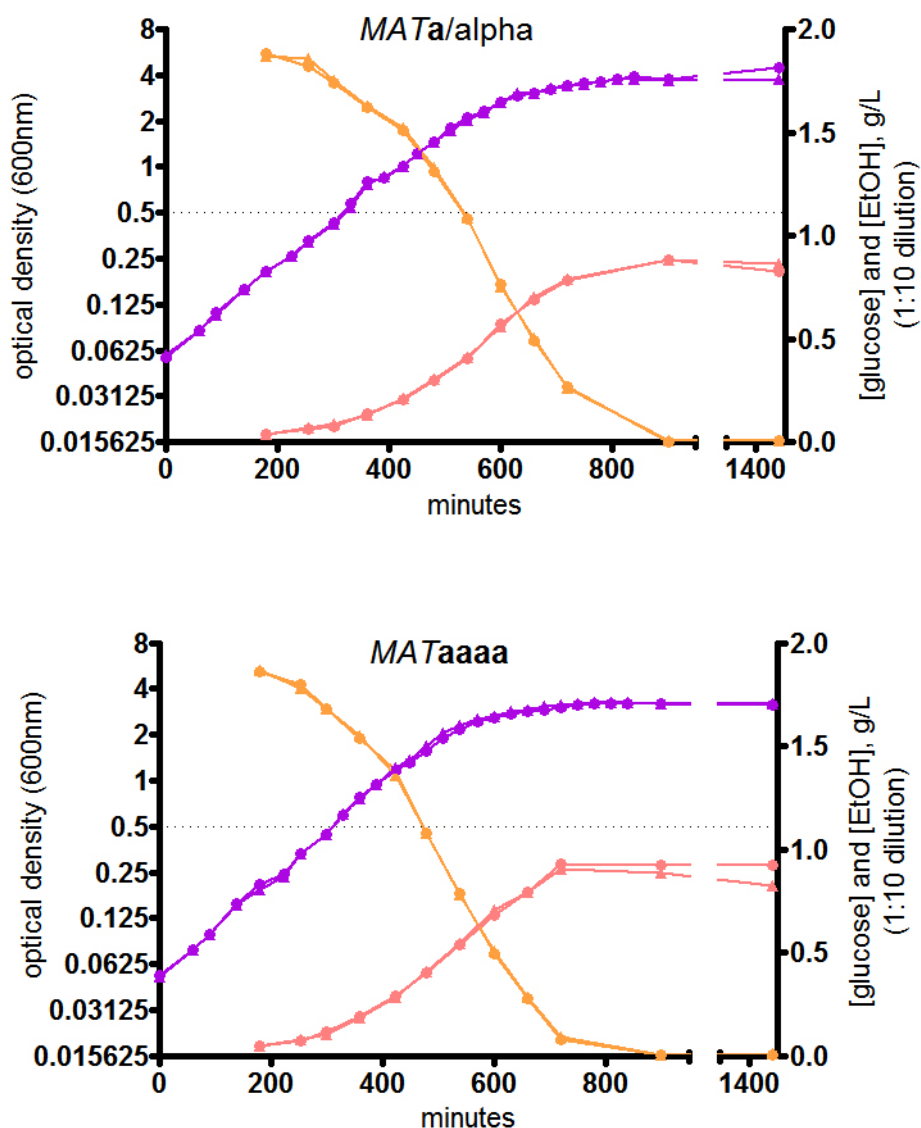


**Figure 1.** Growth characterization of an isogenic WT ploidy series of the Sigma 1278b background. Two cultures were inoculated for each strain, and data from both cultures are shown. Cultures were grown in synthetic complete (SC) medium supplemented with 2% glucose at 30°C. Temperature fluctuation was minimized by growing cultures in water bath shakers instead of air based incubators. Cultures were inoculated at 0.05 O.D.600nm from ~12 hour old pre-cultures that were in exponential growth phase to eliminate lag phase. During the time course, O.D.600nm, glucose concentration and ethanol concentration in the growth medium were tracked at regular intervals. Glucose and ethanol contents were measured on YSI Select 2700 Biochemistry Analyzer. Strain IDs: *MATa* = yCW728, *MATaa* = yCW782, *MATa/alpha* = yCW733, *MATaaaa* = yCW792 #1. Genotype: *ura3-52*, *arg4*, *lys2::kanMX*.

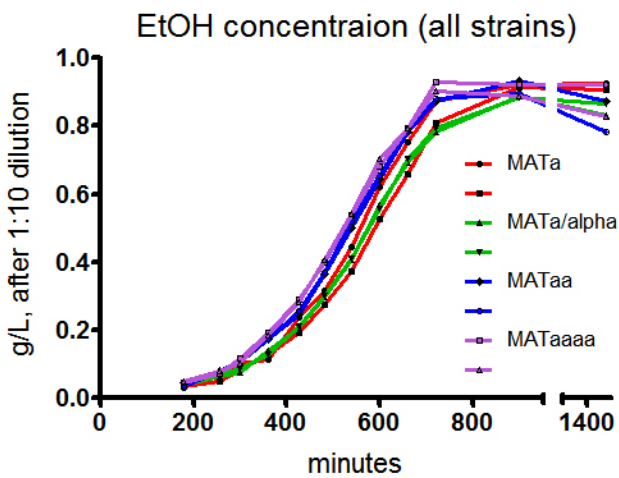
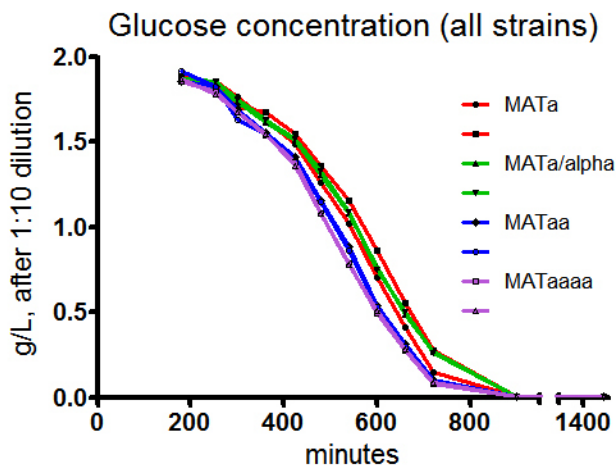
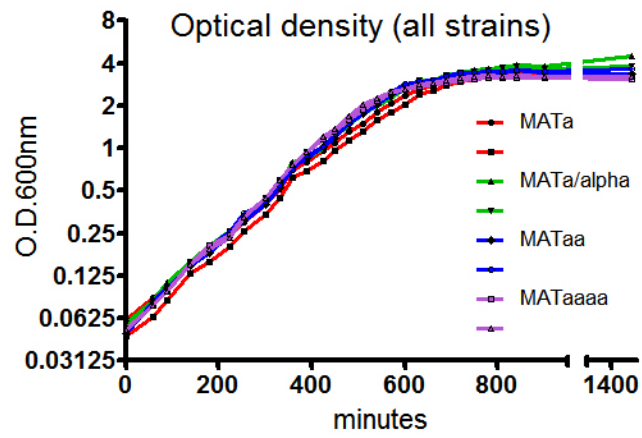


**Figure 2.** Side-by-side comparisons of all strains in each growth-related parameter.

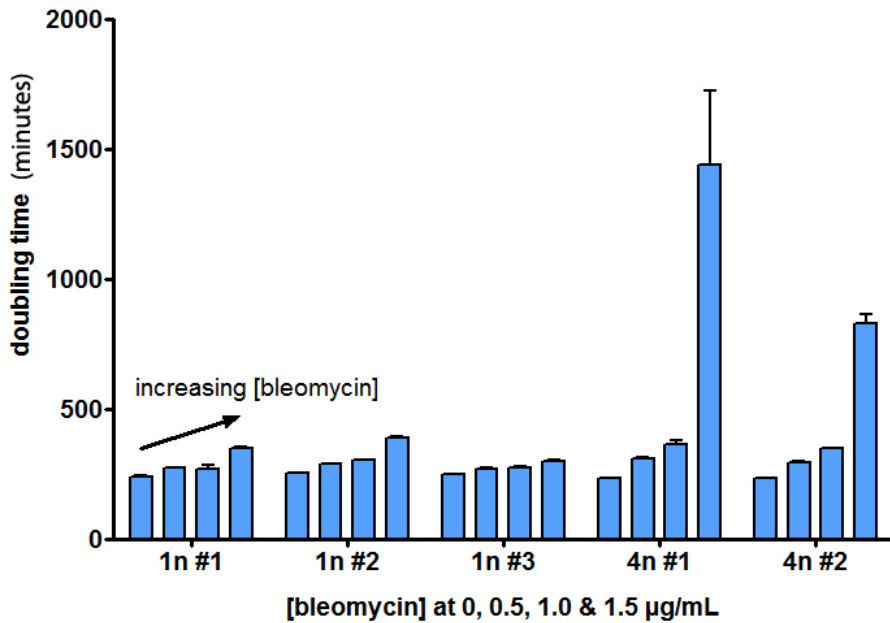


**Figure 3.** Growth of WT Sigma 1278b haploid (*MATa*, L6437) and tetraploid (*MATaaaa*, L6440) treated with increasing concentrations of bleomycin. Cultures were inoculated in SC + 2% glucose and grown at 30°C with periodic agitation in Bioscreen Microbiology Reader. Optical densities were tracked for 48 hours. Doubling times were calculated only from data points within exponential phase.

Strain	O.D.600nm	Cell density (10 <sup>7</sup> /mL)	Cell density per O.D. (10 <sup>7</sup> /mL)
<i>MATa</i>	0.655	1.87	2.85
	0.630	2.09	3.31
	0.595	1.82	3.06
<i>MATa/alpha</i>	0.685	1.08	1.58
	0.640	1.13	1.77
<i>MATaa</i>	0.690	1.48	2.14
	0.680	1.39	2.04
<i>MATaaaa</i>	0.665	0.761	1.14
	0.670	0.763	1.14
	0.680	0.755	1.11

**Table 1.** Correlation between optical and cell densities in a WT isogenic series in the Sigma 1278b strain background. To improve accuracy of optical density measurement, cultures were diluted 5 fold to ensure the spectrophotometric output fell between 0.1 and 0.2 optical units. Due to flocculation, the cell density could not be determined directly, and additional treatments were required. First, NP-40 was added to identical volume of cultures to 0.1% to thoroughly pellet *MATa* and *MATaa* cells that otherwise would adhere loosely to tubes and get removed in subsequent steps. Cell pellets were resuspended in PBS + 3.7% formaldehyde for fixation at 4°C overnight. Fixed cells were washed 3 times in PBS, 1 time in 1.2M sorbitol citrate, resuspended in sorbitol citrate and digested with a mixture of zymolyase and glusulase to alleviate flocculation. Digested cells were washed and resuspended in sorbitol citrate to the original volume prior to cell density counting on an automated cell counter Cellometer.

## References

- Andalis, A.A., Storchova, Z., Styles, C., Galitski, T., Pellman, D., and Fink, G.R. (2004). Defects arising from whole-genome duplications in *Saccharomyces cerevisiae*. *Genetics* 167, 1109-1121.
- Storchova, Z., Breneman, A., Cande, J., Dunn, J., Burbank, K., O'Toole, E., and Pellman, D. (2006). Genome-wide genetic analysis of polyploidy in yeast. *Nature* 443, 541-547.